On Interpolation and Approximation Problems in Numerical Linear Algebra

vorgelegt von Diplom-Mathematiker

Olivier Sète

geboren in Budapest

Von der Fakultät II – Mathematik und Naturwissenschaften –
der Technischen Universität Berlin
zur Erlangung des akademischen Grades
Doktor der Naturwissenschaften
— Dr. rer. nat. —
genehmigte Dissertation.

Promotionsausschuss:

Vorsitzende:	Prof. Dr. Noemi Kurt (TU Berlin)
Gutachter:	Prof. Dr. Jörg Liesen (TU Berlin)
Gutachter:	Prof. Dr. Reinhard Nabben (TU Berlin)
Gutachter:	Prof. Dr. Elias Wegert (TU Bergakademie Freiberg)

Tag der wissenschaftlichen Aussprache: 10. Februar 2016

Berlin 2016

Abstract

This doctoral thesis is on interpolation and approximation problems in the complex plane which are motivated by questions in numerical linear algebra. In the first part of this thesis, we consider the zeros of rational harmonic functions $f(z) = r(z) - \overline{z}$. In this context we sharpen a bound on the number of zeros of such functions, and show that extremal functions, i.e., rational harmonic functions attaining this bound, are always regular. Moreover, we analyze the change of the number of zeros of rational harmonic functions when adding a pole. This generalizes a construction of Rhie (ArXiv Astrophysics e-prints, 2003), who gave the first examples of extremal functions. Her examples, however, have high rotational symmetry. Our analysis yields in particular a construction principle for general non-symmetric extremal functions. We apply this result in the context of gravitational microlensing in astrophysics, to obtain a construction principle for unsymmetric gravitational point lenses for which maximal lensing occurs.

The second part of this thesis is on approximation of analytic functions by series of Faber–Walsh polynomials, which generalize Faber polynomials to compact sets with several components. The Faber–Walsh polynomials are defined through conformal maps of multiply connected domains onto lemniscatic domains, which generalize the Riemann mapping. We first construct two analytic examples of such maps, and give a general construction principle for these maps for certain polynomial pre-images. With these results we derive general properties of the Faber–Walsh polynomials, and relate them to the classical Faber and Chebyshev polynomials. We further present examples of Faber–Walsh polynomials for two real intervals, and also for two nonreal sets consisting of several components.

Contents

Acknowledgments

I wish to express my deep gratitude to my adviser Jörg Liesen for his guidance, support, and encouragement during my PhD studies. I wish to thank both Jörg Liesen and Reinhard Nabben for making me feel very welcome in their research groups. Without doubt the inspiring and open minded working atmosphere there has greatly contributed to this work. I am also grateful to Elias Wegert for his readiness to review this thesis and his interest in this work.

I wish to thank all my colleagues for stimulating mathematical discussions. I am especially grateful to have Robert Luce as collaborator, the many hours we worked together were very rewarding. Further thanks are due to Florian Goßler, who woke my interest in numerical mathematics, and was always ready to discuss mathematical problems.

On a more personal note I wish to thank my family, who has always supported and encouraged me. Finally, I wish to thank Sophie for her support during the wonderful past two years.

1 Introduction

This is a cumulative doctoral thesis in mathematics that contains results on certain rational interpolation and polynomial approximation problems in the complex plane. The results of this thesis have been published in the following research articles:

[44] Robert Luce, Olivier Sète, and Jörg Liesen, *A note on the maximum number of zeros of* $r(z) - \overline{z}$, Comput. Methods Funct. Theory, 15 (2015), pp. 439–448.

[61] Olivier Sète, Robert Luce, and Jörg Liesen, *Perturbing rational harmonic functions by poles*, Comput. Methods Funct. Theory, 15 (2015), pp. 9–35.

[60] Olivier Sète, Robert Luce, and Jörg Liesen, *Creating images by adding masses to gravitational point lenses*, Gen. Relativity Gravitation, 47:42 (2015), pp. 1–8.

[59] Olivier Sète and Jörg Liesen, *On conformal maps from multiply connected domains onto lemniscatic domains*, Electron. Trans. Numer. Anal., 45 (2016), pp. 1–15.

[58] Olivier Sète and Jörg Liesen, *Properties and examples of Faber–Walsh polynomials*, ArXiv e-prints: 1502.07633, (2015), submitted.

Three of these are related to rational interpolation [44, 61, 60] and two to polynomial approximation [59, 58]. The main body of this document contains an introduction to the problems that were studied in the articles, as well as a summary of the main results. Preprint versions of the articles are included in the appendix. The research was motivated by questions arising in numerical linear algebra, which will be discussed in Section 1.3.

1.1 Rational harmonic functions and interpolation problems

The first area of research in this thesis is concerned with the zeros of rational harmonic functions of the form $r(z) - \overline{z}$, where $\overline{z}$ denotes the complex conjugate of $z \in \mathbb{C}$.

The problem we study is derived from the following interpolation problem: Given complex numbers $a_1, \ldots, a_n$, we are interested in the smallest possible degree of a rational function r such that $r(a_j) = \overline{a}_j$. (This problem can be treated within the Loewner framework; see [1].) Alternatively, given r, we ask for the (maximal number of) solutions of $r(z) = \overline{z}$, that is, for the (maximal number of) zeros of $r(z) - \overline{z}$.

The complex-valued function $f(z) = r(z) - \overline{z}$ is *harmonic* since $\Delta f(z) = 4\partial_z \partial_{\overline{z}}(r(z) - \overline{z}) = 0$, but it is *not analytic*. Due to the non-analyticity many

of the standard results from complex function theory cannot be applied, such as the Cauchy integral formula, residue calculus or the classical argument principle. In our work we therefore use results from the theory of harmonic functions, such as Rouché's theorem, the argument principle for harmonic functions, or the Poincaré index of exceptional points.

According to Duren [12], harmonic functions have attracted wide interest only since a landmark paper of Clunie and Sheil-Small from 1984 [9], and since then the subject developed rapidly. Remarkably, many theorems for analytic functions admit a generalization to harmonic functions. One such theorem is the fundamental theorem of algebra.

A *harmonic polynomial* has the form $h(z) = p(z) - \overline{q(z)}$ with two (analytic) polynomials p and q. Although the introduction of terms in $\overline{z}$ may seem harmless, it has a significant impact on the number of zeros. In 1992, Sheil-Small conjectured that a harmonic polynomial $h(z) = p(z) - \overline{q(z)}$ has at most $(\deg(p))^2$ zeros, if $\deg(p) > \deg(q)$. Wilmshurst [76] gave a proof of this generalization of the fundamental theorem of algebra under a more general condition on h. He also showed that this bound cannot be improved in general, by giving an explicit example of a harmonic polynomial with $\deg(q) = \deg(p) - 1$ and $(\deg(p))^2$ zeros. Moreover, Wilmshurst conjectured a smaller bound on the number of zeros of harmonic polynomials with $\deg(q) < \deg(p) - 1$; see [76, Remark 2].

For $\deg(q) = 1$, Khavinson and Świątek [36] established this smaller bound, and Geyer [26] showed that it is sharp for all $\deg(p) > 1$. For $\deg(q) = \deg(p) - 3 > 1$ a counterexample to Wilmshurst's conjecture has recently been given by Lee, Lerario and Lundberg [38], so that the problem of finding a sharp upper bound on the number of zeros of harmonic polynomials is still open for $1 < \deg(q) < \deg(p) - 1$.

The result of Khavinson and Świątek was generalized to rational harmonic functions by Khavinson and Neumann [34] in 2006, who showed that $r(z) - \overline{z}$ has at most $5\deg(r) - 5$ zeros if $\deg(r) \geq 2$. Surprisingly, the sharpness of this bound was proven already in 2003 by the astrophysicist Rhie [55] in the context of gravitational lensing.

The articles [44, 61, 60] are concerned with the zeros of rational harmonic functions $f(z) = r(z) - \overline{z}$. In the article [44], we improve the bound of Khavinson and Neumann, and resolve at the same time an inaccuracy in the original proof. We further show that functions realizing this upper bound have no singular zeros, which are in some sense the "bad" zeros of harmonic functions. In [61], we show that adding a pole to f creates new zeros and we completely characterize this effect. This generalizes Rhie's construction from [55]. In particular, we obtain a construction principle for rational harmonic functions realizing the maximum possible number of zeros. In [60] we describe an application of this method in astrophysics, namely the construction of general unsymmetric gravitational point lenses where maximal lensing occurs. Details are described in Section 2 below.

1.2 Polynomial approximation problems

The second part of this thesis is on the approximation of scalar analytic functions by polynomials on compact sets in the complex plane $\mathbb{C}$.

The question when any analytic function can be approximated by polynomials as well as is desired is settled by Mergelyan's Theorem from 1951 ([24], [63, p. 117], [73, Appendix 1]). It states that if $E \subseteq \mathbb{C}$ is a compact set with connected complement, and if f is continuous on E and analytic in the interior of E, then, for every $\varepsilon > 0$, there *exists* a polynomial p with $\|f - p\|_E < \varepsilon$. Here $\|\cdot\|_E$ denotes the maximum norm on E, i.e., $\|f\|_E = \max_{z\in E} |f(z)|$. As mentioned by Gaier [24], this general theorem is the culmination point of a long sequence of existence results on polynomial approximation. For the approximation of analytic functions, the starting point is Runge's theorem from 1885, where E is the closure of a bounded domain and $\widehat{\mathbb{C}}\backslash E$ is simply connected, and f is analytic on E. Further milestones are a theorem of Walsh from 1926, where E is the closed interior of a Jordan curve and f is continuous on E and analytic at interior points of E, and its generalization by Keldysch from 1945, where E now is the closure of a domain, such that the complement of E is simply connected and contains the point at infinity. See the historical comments in [24, 66, 73] for further details. While Mergelyan's theorem (and its precursors) shows existence of polynomials approximating f, nothing is said about the degree of such polynomials, which may be very high.

Limiting the degree of the approximating polynomials leads to best polynomial approximation problems of the form

$$\min_{p\in\mathcal{P}_k} \|f - p\|_E, \tag{1.1}$$

where $\mathcal{P}_k$ is the set of (complex) polynomials of degree at most k. It is well known that there *exists* a polynomial $p_k^* \in \mathcal{P}_k$ for which the minimum in (1.1) is attained, which is unique provided that E has at least $k+1$ points; see, e.g., [11, 47, 63, 73]. The polynomial p_k^* is called the *polynomial of best approximation* from $\mathcal{P}_k$ to f on E.

Polynomials of best approximation are typically not explicitly available, unless the function f and the set E are very simple. This is due to the fact that the polynomial of best approximation depends non-linearly on the function to be approximated; see, e.g., [54, 69]. The polynomial of best approximation is known, for instance, for $f(z) = z^{k+1}$ and $E = [-1, 1]$ or $E = \{z : |z| \le r\}$. In this case $f - p_k^*$ is the *Chebyshev polynomial* of degree $k+1$ for E, i.e., the monic polynomial of degree $k+1$ with minimal maximum norm on E. On the interval, $f - p_k^*$ the is the (scaled) Chebyshev polynomial of the first kind; see, e.g., [11, Theorem 3.3.4], [22, Theorem 3.2.2], or [54, Theorem 7.3]. On the disk $p_k^*(z) = 0$; see [63, p. 352].

Another line of research, which may be called approximation *practice*, in line with Trefethen [69], is concerned with constructing approximations to

the exact solution of (1.1). One can often obtain such approximations that are efficiently computable, almost optimal in some sense, and usually "good enough" for practical purposes. One prominent example is given in [69, Chapter 16], where $E = [-1, 1]$: Replacing p_k^* by a polynomial interpolating f in Chebyshev points results in a loss of accuracy, compared to the polynomial of best approximation, of at most two digits for degrees up to $k = 10^{66}$.

For complex sets, an important development of approximation practice started in 1903 with Faber's seminal article [20]. For a given simply connected compact set $E \subseteq \mathbb{C}$, Faber constructed polynomials $F_0, F_1, F_2, \ldots$, associated with E, so that any function f which is analytic on E has a unique representation as a *Faber series* $f(z) = \sum_{k=0}^{\infty} a_k F_k(z)$, which converges absolutely and uniformly on E. Both the *Faber polynomials* F_k, and the coefficients a_k are given through the (exterior) Riemann map for E. The expansion into a Faber series generalizes the expansion into a power series (they coincide if E is a disk), and shares many of its properties. In particular, the partial sums $\sum_{k=0}^{n} a_k F_k$ are close to the polynomial of best approximation to f; see [18] for an estimate of the error. We refer to the excellent article of Curtiss [10] for a long list of "classical" applications of Faber polynomials. For examples of Faber polynomials in the context of numerical linear algebra, see for instance [7, 8, 14, 31, 48, 49, 64]. See also [18, 19, 30] for further examples of their use.

In 1956, Walsh generalized the Riemann mapping theorem for the exterior of one simply connected compact set to the exterior of sets consisting of *several* such components [71]. The proof is a pure *existence* proof. Subsequently, he obtained a generalization of the Faber polynomials [72] with this generalized Riemann map. Given the vast number of applications of Faber polynomials, it is surprising that the *Faber–Walsh polynomials* have rarely been studied. This might be due to the fact that previously to [59], no examples of Walsh's conformal map were known in the literature.

The articles [59, 58] are on Walsh's conformal map and Faber–Walsh polynomials. In [59] we discuss general properties of Walsh's conformal map and we derive, for certain polynomial pre-images of simply connected sets, an explicit formula for Walsh's map in terms of the Riemann map for the simply connected set. Further, we explicitly construct two such maps: one for a radial slit domain and one for two equal disks. The former contains the special case of two real intervals of the same length. The article [58] is on Faber–Walsh polynomials. We relate the Faber–Walsh polynomials to the classical Faber and Chebyshev polynomials, and show further that (normalized) Faber–Walsh polynomials are asymptotically optimal in the sense of Eiermann, Niethammer and Varga. In a second part, we compute the Faber–Walsh polynomials for several examples of sets, in particular those from [59], and illustrate numerically their asymptotic optimality. Moreover, we compute the asymptotic convergence factor for each set and arbitrary

complex constraint points. Details are described in Section 3 below.

1.3 Connections to numerical linear algebra

As indicated above, our work in [44, 59, 58, 60, 61] was originally motivated by questions arising in numerical linear algebra, and in particular in the context of Krylov subspace methods.

For a square matrix A and an initial vector v, the kth Krylov subspace of A and v is defined as $K_k(A, v) = \operatorname{span}\{v, Av, \ldots, A^{k-1}v\}$. Many iterative methods for solving linear algebraic systems or eigenvalue problems, or for computing functions of matrices, are based on such Krylov subspaces; see, for instance, [27, 28, 32, 41, 57, 70, 75]. Since each element of $K_k(A, v)$ can be written as $p(A)v$ for some polynomial $p \in \mathcal{P}_{k-1}$, the optimality properties of certain Krylov subspace methods often lead to matrix approximation problems of the form

$$\min_{p \in \mathcal{P}_{k-1}} \|(f(A) - p(A))v\|_2,$$

where f is a function defined on the spectrum of A (in the sense of [25, Vol. I, p. 96] or [32, Definition 1.1]), and $\|\cdot\|_2$ is the 2-norm.

An important example is the Arnoldi algorithm [2]. The Arnoldi algorithm is a variant of the Gram–Schmidt orthogonalization method and generates an orthonormal basis for a Krylov subspace. Let $v \neq 0$ and let d be the smallest integer such that $K_d(A, v)$ is an A-invariant subspace. Then d is the degree of the minimal polynomial of v with respect to A, and in exact arithmetic the Arnoldi algorithm computes orthonormal vectors $v_1, \ldots, v_d$ with $\operatorname{span}\{v_1, \ldots, v_k\} = K_k(A, v)$ for $k = 1, \ldots, d$. Algorithm 1 shows the classical Gram–Schmidt implementation of the Arnoldi algorithm. For practical computations, however, the mathematically equivalent modified Gram–Schmidt implementation should be preferred; see for instance [70, Lecture 8].

As shown by Saad [56, Theorem 5.1], the Arnoldi algorithm generates, at least implicitly, a polynomial that solves the *Arnoldi approximation problem*

$$\min_{p \in \mathcal{P}_{k-1}} \|(A^k - p(A))v\|_2.$$

For each $k \leq d$, the minimum is $\|q_k(A)v\|_2$, where q_k is the characteristic polynomial of the upper Hessenberg matrix $H_k = [h_{ij}] \in \mathbb{C}^{k,k}$, with h_{ij} given as in Algorithm 1.

Greenbaum and Trefethen proposed in [29] to "disentangle [the] matrix essence of the process from the distracting effects of the initial vector," and to consider the *ideal Arnoldi approximation problem*

$$\min_{p \in \mathcal{P}_{k-1}} \|A^k - p(A)\|_2. \tag{1.2}$$

Algorithm 1 Arnoldi algorithm with classical Gram-Schmidt implementation

Input: $A \in \mathbb{C}^{n,n}$, initial vector $v \neq 0$.
Output: Orthonormal vectors $v_1, \ldots, v_d$ with $\operatorname{span}\{v_1, \ldots, v_k\} = K_k(A, v)$ for $k = 1, \ldots, d$.

$v_1 = v/\|v\|$.
for $j = 1, 2, \ldots$
  $\widehat{v}_{j+1} = Av_j - \sum_{i=1}^{j} h_{ij} v_i, \quad h_{ij} = \langle Av_j, v_i \rangle$
  $h_{j+1,j} = \|\widehat{v}_{j+1}\|$. If $h_{j+1,j} = 0$, stop (in this case $d = j$).
  $v_{j+1} = \widehat{v}_{j+1}/h_{j+1,j}$.
end

For a normal matrix, $A = X\Lambda X^H$, with unitary X and diagonal $\Lambda = \operatorname{diag}(\lambda_1, \ldots, \lambda_n)$, the ideal Arnoldi problem (1.2) reduces to the scalar problem

$$\min_{p \in \mathcal{P}_{k-1}} \max_{1 \le j \le n} |\lambda_j^k - p(\lambda_j)|, \tag{1.3}$$

which is of the form (1.1). Hence, the problem (1.2) can be considered a "matrix generalization" of the scalar problem. Accordingly, the polynomial $t^k - p_{k-1}^*(t)$ is called the *kth Chebyshev polynomial of A* [29], where $p_{k-1}^* \in \mathcal{P}_{k-1}$ is the solution of (1.2). Further results on Chebyshev polynomials of matrices can be found in [21, 42, 68].

In (1.3), we consider the minimization of polynomials "normalized at infinity." With a different normalization point, we have the minimization problem

$$\min_{p \in \mathcal{P}_k(z_0)} \|p\|_E, \tag{1.4}$$

where $\mathcal{P}_k(z_0)$ is the set of complex polynomials of degree at most k with value 1 at the *constraint point* $z_0 \in \mathbb{C}$, and E is a compact set, which we assume to have infinitely many points. It is well known that there exists a unique polynomial from $\mathcal{P}_k(z_0)$ for which the minimum in (1.4) is attained; see, e.g., [47]. Following Fischer [22], this polynomial is called the *optimal polynomial* for (1.4). As for the general scalar approximation problem (1.1), optimal polynomials are usually hard to find. In [58] we show that the Faber–Walsh polynomials are asymptotically optimal, i.e., that in an asymptotic sense they are close to the optimal polynomials; see Section 3.4.

The problem (1.4) appears in the analysis of semi-iterative and Krylov subspace methods for solving the linear algebraic system $Ax = b$. There, the compact set E is an inclusion set of the spectrum of A, and the constraint point is $z_0 = 1$ in semi-iterative methods, see [16, 17], and $z_0 = 0$ in Krylov

subspace methods such as CG, MINRES, and GMRES; see [41, Sections 5.6–5.7] for a survey.

Let us next discuss the connection of rational harmonic functions to numerical linear algebra. As mentioned above, the Arnoldi algorithm generates an orthonormal basis $v_1, \ldots, v_k$ of the Krylov subspace $K_k(A, v)$, and each next basis vector is computed via the recurrence

$$h_{j+1,j} v_{j+1} = A v_j - \sum_{i=1}^{j} h_{ij} v_i; \tag{1.5}$$

see Algorithm 1. In general, this full recurrence is needed. If the adjoint A^* of A with respect to the inner product $\langle \cdot, \cdot \rangle$ is a polynomial of degree s in A, that is $A^* = p_s(A)$, then we obtain

$$h_{ij} = \langle A v_j, v_i \rangle = \langle v_j, A^* v_i \rangle = \langle v_j, p_s(A) v_i \rangle = 0 \quad \text{for } i < j - s,$$

since $p_s(A) v_i \in K_{i+s}(A, v) = \operatorname{span}\{v_1, \ldots, v_{i+s}\}$, and since v_j is orthogonal to $v_1, \ldots, v_{j-1}$. In this case, the vector $A v_j$ has to be orthogonalized only against the vectors $v_{j-s}, \ldots, v_j$, and the full recurrence (1.5) reduces to a recurrence with only $s+2$ terms. Conversely, $(s+2)$-term recurrences in the Arnoldi algorithm imply that $A^* = p_s(A)$; see [41, Chapter 4]. Therefore, in the Arnoldi algorithm, a small degree s is equivalent to a short recurrence for the computation of an orthonormal basis of Krylov subspaces. Of course, the length of the recurrence has a significant influence on the computational cost of the method. In practice one is therefore interested in the smallest possible degree s, such that $A^* = p_s(A)$.

There exists a generalization of the Arnoldi algorithm, where $A^* = r(A)$ with a rational function r of low degree leads to short recurrences; see [4, 3]. If A is diagonalizable, then the smallest possible length of a recurrence is given by the smallest possible degree of r with $r(\lambda) = \overline{\lambda}$ for all eigenvalues λ of A; for details see [39] or [41, Section 4.8.2] and the references cited therein. The equation $r(\lambda) = \overline{\lambda}$ can be written as $r(\lambda) - \overline{\lambda} = 0$, where the function $r(z) - \overline{z}$ is a rational harmonic function as described in Section 1.1. In the numerical linear algebra context, the complex numbers $a_1, \ldots, a_n$ in the problem stated there are the eigenvalues of the matrix A. One now asks for the smallest possible degree of r such that $a_1, \ldots, a_n$ are the zeros of $r(z) - \overline{z}$. Alternatively, one is interested in the maximum number of zeros of a rational harmonic function $r(z) - \overline{z}$.

2 Zeros of rational harmonic functions

We summarize the main results from the articles [44, 61, 60], which constitute the first part of this thesis, in Section 2.2. The background for these results is described in Section 2.1.

2.1 Background

We consider functions of the form

$$f(z) = r(z) - \overline{z},$$

where $r = \frac{p}{q}$ is a complex rational function of (McMillan) degree

$$\deg(r) := \max\{\deg(p), \deg(q)\}.$$

Here and in the sequel we always assume that the polynomials p and q are coprime, that is, that they have no common zeros. The function f is not analytic. However, it is a complex-valued harmonic function, and we therefore call f a *rational harmonic function* of degree $\deg(r)$.

We consider the number of zeros of f. Clearly, f has exactly one zero if r is a constant. If $\deg(r) = 1$, so that r is a Möbius transformation, a direct calculation shows that f has either 0, 1, 2 or infinitely many zeros. In the latter case, the solutions are all points of a line or circle in $\mathbb{C}$. Note that the point at infinity cannot be a zero of f; see [34, p. 1078].

For $\deg(r) \geq 2$ the following important theorem of Khavinson and Neumann [34] gives a bound on the number of (distinct) zeros of f.

Theorem 2.1 ([34, Theorem 1])**.** *A rational harmonic function $f(z) = r(z) - \overline{z}$ of degree $n \geq 2$ has at most $5(n-1)$ zeros.*

Functions attaining this bound are of particular interest [5, 6], and have special properties, as we shall see.

Definition 2.2. Let $f(z) = r(z) - \overline{z}$ be a rational harmonic function of degree $\deg(r) \geq 2$. If f has the maximum number of $5\deg(r) - 5$ zeros, we say that f is *extremal*. In this case we also say that r is *extremal*.

The first examples of extremal functions were given by Rhie [55]. Her construction starts with the rational function

$$r_0(z) = \frac{z^{n-1}}{z^n - a^n}, \tag{2.1}$$

where a is a fixed real parameter satisfying

$$0 < a < r_{\mathrm{cr}} := \left(\frac{n-2}{n}\right)^{\frac{1}{2}} \left(\frac{2}{n-2}\right)^{\frac{1}{n}}.$$

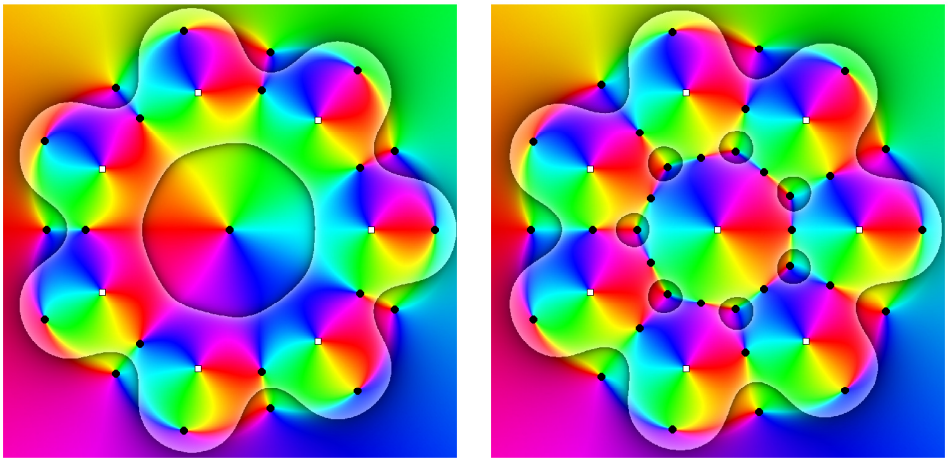

(a) Phase portrait of $r_0(z) - \overline{z}$ (b) Phase portrait of $r_\varepsilon(z) - \overline{z}$

Figure 1: Phase portraits of $r_0(z) - \overline{z}$ and $r_\varepsilon(z) - \overline{z}$ with $n = 7$ and $\varepsilon = 0.15$. Black disks indicate zeros and white squares show poles.

The quantity r_{cr} is known as the *critical radius*; see [5]. It is well-known that $f_0(z) = r_0(z) - \overline{z}$ has $3n+1$ zeros if $n \geq 3$; see [45]. Thus f_0 is extremal for $n = 3$, and one can check by hand that it is also extremal for $n = 2$ (and $0 < a < 1$). By adding a pole at the origin, Rhie obtained the function

$$f_\varepsilon(z) = r_\varepsilon(z) - \overline{z} = (1-\varepsilon)\frac{z^{n-1}}{z^n - a^n} + \frac{\varepsilon}{z} - \overline{z} \tag{2.2}$$

of degree $n+1$ which has $5n$ zeros for sufficiently small $\varepsilon > 0$, and is therefore extremal. The function f_ε has $2n$ zeros close to the origin, where the pole was added, and $3n$ zeros that are located close to the $3n$ other zeros of f_0; see Figure 1 (cf. [61, Fig. 1]) for an illustration.

In the article [43], which is not included in this thesis, we give a rigorous analysis of Rhie's original construction and derive sharp bounds on the parameters (a and ε) in (2.2), so that the function is extremal. We also study a related construction of Bayer and Dyer [5, 6], who consider (2.2) without the factor $1 - \varepsilon$, and we show that both functions are equivalent in some sense.

To further study rational harmonic functions $f(z) = r(z) - \overline{z}$ and to generalize Rhie's construction, we need to take a closer look at the zeros of f, which behave quite differently from the zeros of analytic functions. In particular, the usual notion of multiplicity of a zero does not apply, since zeros cannot be factored out, as the following example illustrates: Each $z_0 \in \mathbb{R}$ is a zero of the function $f(z) = z - \overline{z}$, but there exists no harmonic function g with $f(z) = (z - z_0)g(z)$ or $f(z) = \overline{(z - z_0)}g(z)$. Even if f has only a finite number of zeros, such decompositions do in general not exist;

see [61, p. 11].

We therefore consider the *Poincaré index* of a zero or pole of f (called *multiplicity* in [62]), which generalizes the multiplicity of a zero or pole of an analytic function; see Section 2 in [61] for details.

2.2 Main results

We summarize the main results obtained in the articles [44, 61] and [60].

The first part of the article [44] makes two contributions related to Theorem 2.1 by Khavinson and Neumann. First, we resolve an inaccuracy in the original proof of Theorem 2.1; see [44, Section 1] for details. Second, we sharpen the bound on the number of zeros by taking into account the individual degrees of the numerator and denominator polynomials.

Recall that a zero z_0 of a rational harmonic function $f(z) = r(z) - \overline{z}$ is called *sense-preserving* if $|r'(z_0)| > 1$, *sense-reversing* if $|r'(z_0)| < 1$, and *singular* if $|r'(z_0)| = 1$; see [61]. If f has no singular zeros, then f and r are called *regular*.

Theorem 2.3 ([44, Theorem 1.1])**.** *A rational harmonic function $f(z) = r(z) - \overline{z}$ of degree $n \geq 2$ has at most $3(n-1)$ sense-preserving zeros, and at most $2(n-1)$ sense-reversing or singular zeros. Moreover, if $r = \frac{p}{q}$ with $\deg(p) > \deg(q)$, then f has at most $5(n-1)-1$ zeros.*

Our proof of Theorem 2.3 employs similar techniques as the original proof of Theorem 2.1. However, it makes more systematic use of the *co-conjugates* $\overline{T} \circ r \circ T^{-1}$ of a rational function r, where T is a Möbius transformation. Essentially, co-conjugates preserve the number of zeros of $r(z) - \overline{z}$, as well as their type (sense-preserving, sense-reversing, or singular); see [44, Proposition 2.1].

In the second part of [44], we show that extremal rational harmonic functions are always regular.

Theorem 2.4 ([44, Theorem 3.1])**.** *Let $r = \frac{p}{q}$ be a rational function of degree $n \geq 2$ and set $f(z) = r(z) - \overline{z}$. If*

1. *f has $5(n-1)$ zeros, or*
2. *$\deg(p) > \deg(q)$ and f has $5(n-1)-1$ zeros,*

then f is regular.

To fully appreciate Theorem 2.4, recall that singular zeros are the "bad" zeros in the theory of harmonic functions. There, many results are formulated with the assumption that the harmonic function has no singular zeros, or even that it is sense-preserving (in which case both sense-reversing and singular zeros are excluded); see, for example, [12, 13, 67]. Even for rational harmonic functions $r(z) - \overline{z}$, singular zeros are not well understood, and they present one of the technical difficulties encountered in [61].

In the article [61], we investigate the effect of adding a pole to a rational harmonic function on the number of its zeros. This work is motivated by Rhie's example described in Section 2.1. Recall that adding a simple pole to the function $f_0(z) = r_0(z) - \overline{z}$ with r_0 from (2.1) results in the creation of $2n$ zeros close to the location of the pole (Figure 1). The analysis of Rhie's construction and of the variant of Bayer and Dyer takes advantage of the rotational symmetry of r_0; see also [43] for a rigorous proof and a comparison of both approaches.

We show that this "zero creating effect" is *not* specific to the function r_0, but rather generic for rational harmonic functions, under suitable conditions on the point z_0.

Theorem 2.5 ([61, Theorem 3.1])**.** *Let $f(z) = r(z) - \overline{z}$ be a regular rational harmonic function with $\deg(r) \geq 2$ satisfying $\lim_{z\to\infty} f(z) = \infty$. Let further $z_0 \in \mathbb{C}$ and the integer $N \geq 3$ satisfy*

$$f(z_0) = 0, \quad r'(z_0) = \ldots = r^{(N-2)}(z_0) = 0, \quad \text{and} \quad r^{(N-1)}(z_0) \neq 0.$$

Then, for sufficiently small $\varepsilon > 0$, the closed disk $D := \{z \in \mathbb{C} : |z - z_0| \leq (\frac{N}{N-1})^{\frac{1}{2}}\varepsilon\}$ contains no further zeros of f, and the function

$$F(z) = f(z) + \frac{\varepsilon}{z - z_0}$$

has at least $2N$ zeros in D, and the same number of zeros as f in $\mathbb{C}\backslash D$.

The above is a simplified version of the main theorem from [61]. In its original form, the theorem has weaker assumptions, and provides more details on the location of the zeros of F. For a discussion of the rather mild assumptions of the theorem see [61, Remark 3.2]. Theorem 2.5 covers in particular the example of Bayer and Dyer for an extremal function.

Theorem 2.5 can be used to *construct* extremal rational harmonic functions of higher degree from lower degree extremal functions, as we explain next. Suppose that $f(z) = r(z) - \overline{z}$ is an extremal rational harmonic function as in Theorem 2.5 with a zero z_0 at which $r'(z_0) = 0$. Then $F(z) = r(z) + \frac{\varepsilon}{z-z_0} - \overline{z}$ has at least $2N - 1 \geq 5$ more zeros than f by Theorem 2.5, that is F has at least $5\deg(r)$ zeros, while its degree is $\deg(r) + 1$. This shows that F is extremal. Let us consider an example. Let $r(z) = \frac{2z-(1+i)}{z^2-e^{i\pi/3}}$ and z_0 be the zero of r' with larger real part. Figure 2 shows on the left the phase portrait of the function $f(z) = r(z) - \overline{z} - (r(z_0) - \overline{z}_0)$, which is of degree two and has five zeros, so that it is extremal. The assumptions of Theorem 2.5 are satisfied at the zero z_0 indicated in the phase portrait. The right phase portrait shows the function $F(z) = f(z) + \frac{\varepsilon}{z-z_0}$ with $\varepsilon = 0.05$, which has ten zeros and thus is also extremal. Further examples of such a construction are given in [61, Section 4.4].

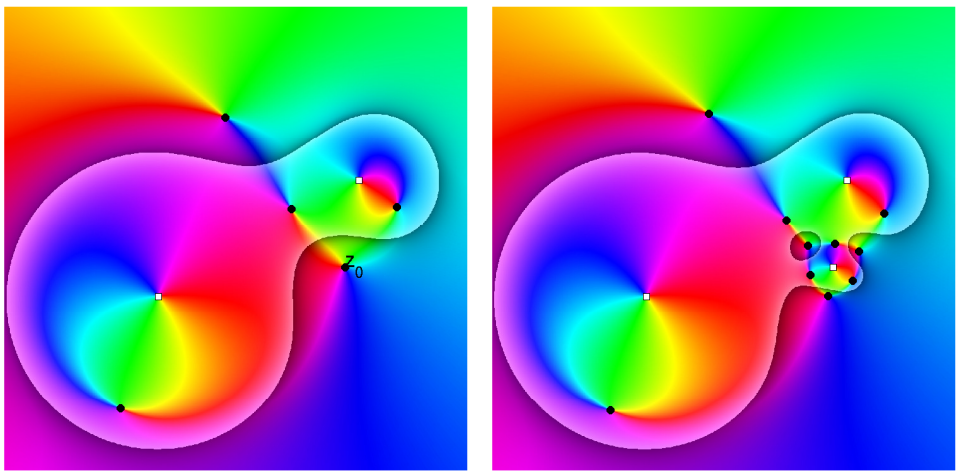

Figure 2: Phase portraits of an extremal function of degree two (left), and of a perturbation (right); see the discussion below Theorem 2.5. Black disks indicate zeros and white squares show poles.

One may wonder about the effect of adding a simple pole to a rational harmonic function at a point z_0 that does not satisfy the assumptions in Theorem 2.5. A complete discussion of all possibilities is given in the next theorem.

Theorem 2.6 ([61, Theorem 3.14])**.** *Let $f(z) = r(z) - \overline{z}$ with $\deg(r) \geq 2$ be regular and satisfy $\lim_{z\to\infty} f(z) = \infty$, and let $z_0 \in \mathbb{C}$. For sufficiently small $\varepsilon > 0$, if*

$$F(z) = f(z) + \tfrac{\varepsilon}{z-z_0}$$

is regular, then the following holds:

1. *If z_0 is a pole of f, then F and f have the same number of zeros.*
2. *If $0 < |f(z_0)| < \infty$, then there exists a disk D around z_0 such that f has no zeros or poles in D, and F has at least one zero in D.*
3. *If $f(z_0) = 0$, and $|r'(z_0)| > 1$, then there exists a disk D around z_0 such that f has no zeros or poles in $D\backslash\{z_0\}$, and F has at least two zeros in D.*
4. *If $f(z_0) = 0$, and $0 < |r'(z_0)| < 1$, then there exists a disk D around z_0 such that f has no zeros or poles in $D\backslash\{z_0\}$, and F has at least four zeros in D.*

Moreover, in 2.–4., F and f have the same number of zeros outside D.

It is possible to also indicate the type (sense-preserving, sense-reversing) of the zeros of F; see [61, Theorem 3.14] for the full statement. Examples for each case are given in [61, Section 4]. There, we also consider extensions of

Theorems 2.5 and 2.6, in particular to complex residues and poles of higher orders.

Both Theorem 2.5 and Theorem 2.6 give a *lower bound* on the number of zeros that are created by adding a pole to a rational harmonic function. Extensive numerical experiments suggest that *exactly* the stated number of zeros is created, provided that ε is sufficiently small. A rigorous study is subject to further work.

In the article [60] we applied our results from [61] to gravitational microlensing in astrophysics. In gravitational microlensing we consider a distant light source (e.g., a star or quasar) and an observer (e.g., the Hubble space telescope), and n point masses (e.g., stars, galaxies, or black holes) located in the *lens plane* between the light source and the observer. These point masses bend the light from the light source through gravitation. As a result, the observer may see multiple images of the single light source. Mathematically, gravitational microlensing can be modeled by the *lens equation*

$$\zeta = z - \gamma\overline{z} - \sum_{j=1}^{n} \frac{m_j}{\overline{z} - \overline{z}_j}, \tag{2.3}$$

where $z_1, \ldots, z_n \in \mathbb{C}$ are the positions of the point masses $m_1, \ldots, m_n > 0$ in the lens plane, ζ is the position of the light source (projected onto the lens plane), and $\gamma \in \mathbb{C}$ is the (constant) external shear. The external shear models the gravitational pull from the surroundings of the lens. The solutions of the lens equation (2.3) are the observed images of the light source ζ. Since (2.3) can be written as

$$r(z) - \overline{z} = 0, \quad \text{with} \quad r(z) = \overline{\gamma} z + \sum_{j=1}^{n} \frac{m_j}{z - z_j} + \overline{\zeta},$$

the observed images are the zeros of a rational harmonic function. For a more detailed exposition on gravitational microlensing see the introductory overview article [35]; see also [51, 52, 53, 65, 74].

Note that in the context of gravitational microlensing models, the additive perturbations $\frac{\varepsilon}{z-z_0}$ considered in [61] can be interpreted as adding a mass $\varepsilon > 0$ at the position z_0 to the gravitational lens. Therefore, our mathematical results from [61] have several implications for gravitational microlensing. First, they give a complete description of the image creating effect of adding a small mass to an existing gravitational point lens, and are applicable to point lens models with or without external shear. Roughly speaking, if a small mass is added to a gravitational lens at the position z_{n+1} in the lens plane, "new" images appear close to z_{n+1}, while all other images alter only slightly their position. The number of new images depends on the properties of the underlying rational function at the point z_{n+1}, which

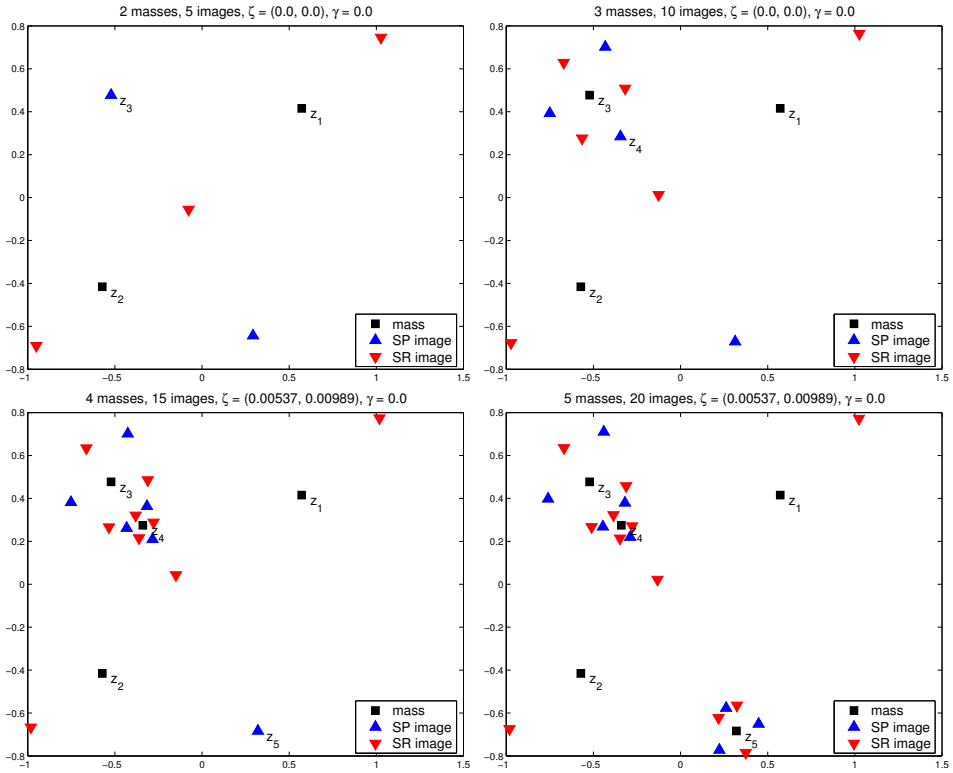

Figure 3: Numerical example for the image-creating effect of adding small masses at certain images of a maximal lens.

we can fully classify according to Theorem 2.5 and Theorem 2.6; see [60, Theorem 2.1] for the formulation in astrophysical terms.

As a second application of our results from [61], we obtain generally applicable conditions that allow the construction of maximal lenses with $n+1$ point masses from maximal lenses with n point masses. With these we construct several examples of maximal lensing models that do not share the highly symmetric appearance of Rhie's construction. Figure 3 (cf. [60, Fig. 2]) shows an example, where we start with a maximal point lens with two point masses (top left), and successively construct maximal lenses with three, four and five masses; see [60, Section 3] for details. Since in the astrophysical setting (2.3) the formulation usually is $z - \overline{r(z)} - \zeta = 0$, i.e., the rational function is conjugated, the roles of sense-preserving and sense-reversing points are interchanged. Thus, in the figure, a sense-preserving image (SP image) indicates that $|r'(z)| < 1$, and a sense-reversing image (SR image) indicates that $|r'(z)| > 1$ at the given zero.

In summary, in [44, 61, 60], we studied the zeros of rational harmonic functions and functions having the maximal possible number of zeros. We analyzed the known upper bound on the number of zeros and showed that

extremal functions are always regular. Moreover, we analyzed the effect of adding a pole to a rational harmonic function on the number of its zeros, and completely characterized this zero creating effect. We further applied these findings to gravitational point lenses in the article [60], which the editors of General Relativity and Gravitation distinguished as "Editor's Choice" article.

3 Lemniscatic maps and the Faber–Walsh polynomials

We summarize the main contributions made in the articles [59] and [58]. The background for the respective articles is described in Sections 3.1 and 3.3.

3.1 Background on lemniscatic maps

Let us begin with Walsh's generalization of the Riemann mapping theorem. In the sequel a domain always is an open and connected set in the extended complex plane $\widehat{\mathbb{C}} = \mathbb{C} \cup \{\infty\}$.

A *lemniscatic domain* is a domain of the form

$$\mathcal{L} = \{w \in \widehat{\mathbb{C}} : |U(w)| > \mu\}, \quad U(w) = \prod_{j=1}^{n} (w - a_j)^{m_j}, \tag{3.1}$$

where $a_1, \ldots, a_n$ are distinct points in $\mathbb{C}$, $m_1, \ldots, m_n, \mu$ are positive real numbers, and $\sum_{j=1}^{n} m_j = 1$. The function U is analytic but in general multi-valued. Its absolute value however is single-valued. For $n = 1$ a lemniscatic domain is the exterior of a disk with radius μ and center a_1.

Lemniscatic domains are *canonical domains* for nondegenerate domains of connectivity n that contain the point at infinity, as the next theorem shows.

Theorem 3.1 ([71, Theorems 3 and 4])**.** *Let $E := \cup_{j=1}^{n} E_j$, where $E_1, \ldots, E_n$ are mutually exterior simply connected compact subsets of $\mathbb{C}$ (none a single point). Then there exist a unique lemniscatic domain $\mathcal{L}$ of the form* (3.1) *with $\mu > 0$ equal to the logarithmic capacity of E, and a unique bijective conformal map*

$$\Phi : \mathcal{K} := \widehat{\mathbb{C}} \backslash E \to \mathcal{L}$$

normalized by

$$\Phi(z) = z + \mathcal{O}\left(\frac{1}{z}\right), \quad z \text{ near infinity.}$$

The function Φ is called the lemniscatic map *of $\mathcal{K}$ (or of E). Its inverse is consistently denoted by $\psi = \Phi^{-1}$.*

Theorem 3.1 is a generalization of the Riemann mapping theorem. In fact, for $n = 1$ both theorems are equivalent. There is more. Lemniscatic maps share many properties with the Riemann map. For instance, the logarithmic capacity of E is an explicit parameter of the lemniscatic domain, and Green's function with pole at infinity for $\mathcal{K}$ is given by $g_{\mathcal{K}}(z) = \log|U(\Phi(z))| - \log(\mu)$; see (3.5) below.

Several authors gave alternative *existence* proofs of Walsh's result; see the Introduction of [59] for an overview. Apart from these existence proofs, lemniscatic maps have rarely been studied, and we are not aware of any example in the published literature. The only algorithm for the computation of lemniscatic maps (prior to [50]) is an iteration method from Landau [37] that requires knowledge of the harmonic measure of parts of the boundary. It may be for this reason that lemniscatic maps have not found many applications until now.

3.2 Main results on lemniscatic maps

We summarize the main results from [59].

We begin with a result that shows that certain symmetry properties of the domain $\mathcal{K}$ imply corresponding properties of its lemniscatic map and lemniscatic domain. Similar results are well-known for the Riemann map (i.e., the case $n = 1$). Here, we consider rotational symmetry, that is when $\mathcal{K} = e^{i\theta}\mathcal{K} = \{e^{i\theta}z : z \in \mathcal{K}\}$ holds, as well as symmetry with respect to the real and imaginary axis, expressed by $\mathcal{K} = \mathcal{K}^* = \{\overline{z} : z \in \mathcal{K}\}$ and $\mathcal{K} = -\mathcal{K}^*$, respectively.

Lemma 3.2 ([59, Lemma 2.2])**.** *In the notation of Theorem 3.1 we have:*

1. *If $\mathcal{K} = e^{i\theta}\mathcal{K}$, then $\Phi(z) = e^{-i\theta}\Phi(e^{i\theta}z)$ and $\mathcal{L} = e^{i\theta}\mathcal{L}$.*
2. *If $\mathcal{K} = \mathcal{K}^*$, then $\overline{\Phi(\bar{z})} = \Phi(z)$ and $\mathcal{L} = \mathcal{L}^*$.*
3. *If $\mathcal{K} = -\mathcal{K}^*$, then $-\overline{\Phi(-\bar{z})} = \Phi(z)$ and $\mathcal{L} = -\mathcal{L}^*$.*

In each case $\psi = \Phi^{-1}$ has the same symmetry properties as Φ.

The main part of the article [59] is devoted to the *construction* of lemniscatic maps. If the compact set E is a polynomial pre-image of a simply connected compact set Ω for which the exterior Riemann map is known, then the lemniscatic map for E can be explicitly constructed. This is the content of the following theorem.

Theorem 3.3 ([59, Theorem 3.1])**.** *Let $\Omega = \Omega^* \subseteq \mathbb{C}$ be a simply connected compact set (not a single point) with exterior Riemann map*

$$\widetilde{\Phi} : \widehat{\mathbb{C}}\backslash\Omega \to \{w \in \widehat{\mathbb{C}} : |w| > 1\}, \quad \text{with } \widetilde{\Phi}(\infty) = \infty \text{ and } \widetilde{\Phi}'(\infty) > 0.$$

Let $P(z) = \alpha z^n + \alpha_0$ with $\alpha_0 \in \mathbb{R}$ to the left of Ω, $\alpha > 0$, and $n \geq 2$. Then $E := P^{-1}(\Omega)$ is the disjoint union of n simply connected compact sets, and

$$\Phi : \widehat{\mathbb{C}}\backslash E \to \mathcal{L} = \{w \in \widehat{\mathbb{C}} : |U(w)| > \mu\},$$
$$\Phi(z) = z\Big(\frac{\mu^n}{z^n}[\widetilde{\Phi}(P(z)) - \widetilde{\Phi}(P(0))]\Big)^{\frac{1}{n}},$$

is the lemniscatic map of E, where we take the principal branch of the nth root, and where

$$\mu := (\alpha\widetilde{\Phi}'(\infty))^{-\frac{1}{n}} > 0 \quad \textit{and} \quad U(w) := (w^n + \mu^n \widetilde{\Phi}(P(0)))^{\frac{1}{n}}.$$

The theorem is proven by the explicit construction of the lemniscatic map as a composition of conformal maps. We apply this general theorem to a radial slit domain.

Corollary 3.4 ([59, Corollary 3.3])**.** *Let $E = \cup_{j=1}^{n} e^{i2\pi j/n}[C, D]$ with $0 < C < D$. Then*

$$\Phi(z) = z\left(\frac{1}{2} + \frac{\sqrt{D}^n\sqrt{C}^n}{2}\frac{1}{z^n} \pm \frac{1}{2z^n}\sqrt{(z^n - C^n)(z^n - D^n)}\right)^{\frac{1}{n}} \tag{3.2}$$

is the lemniscatic map of E with corresponding lemniscatic domain

$$\mathcal{L} = \left\{ w \in \widehat{\mathbb{C}} : |U(w)| = \left| w^n - \frac{(\sqrt{D}^n + \sqrt{C}^n)^2}{4} \right|^{\frac{1}{n}} > \left(\frac{D^n - C^n}{4}\right)^{\frac{1}{n}} \right\}.$$

The inverse of Φ is given by

$$\Phi^{-1}(w) = w\left(1 + \frac{(\sqrt{D}^n - \sqrt{C}^n)^2}{4}\frac{1}{w^n - \frac{(\sqrt{D}^n + \sqrt{C}^n)^2}{4}}\right)^{\frac{1}{n}},$$

where we take the principal branch of the nth root.

In particular, for $n = 2$, we obtain the lemniscatic map of two intervals, $E = [-D, -C] \cup [C, D]$, which we will use in Theorem 3.5 below and in the article [58]. Figure 4 illustrates Corollary 3.4 for $C = 0.15$, $D = 1$ and $n = 5$.

A second lemniscatic map is constructed explicitly for the exterior of two equal disks. Without loss of generality (cf. [59, Lemma 2.3]), we can assume that $E = D_r(z_0) \cup D_r(-z_0)$ with $z_0 > 0$, where $D_r(z_0)$ denotes the closed disk with center z_0 and radius r. Although this set is a polynomial pre-image as in Theorem 3.3, the Riemann map of the corresponding set Ω seems not to be available explicitly. Therefore, we construct the map directly as composition of auxiliary conformal maps, involving in particular the lemniscatic map of $[-D, -C] \cup [C, D]$ just introduced.

Theorem 3.5 ([59, Theorem 4.2])**.** *Let $r, z_0 \in \mathbb{R}$ with $0 < r < z_0$, and $E = D_r(z_0) \cup D_r(-z_0)$. Let T be the Möbius transformation*

$$T(z) = \frac{\alpha + z}{\alpha - z}, \quad \alpha = \sqrt{z_0^2 - r^2} > 0,$$

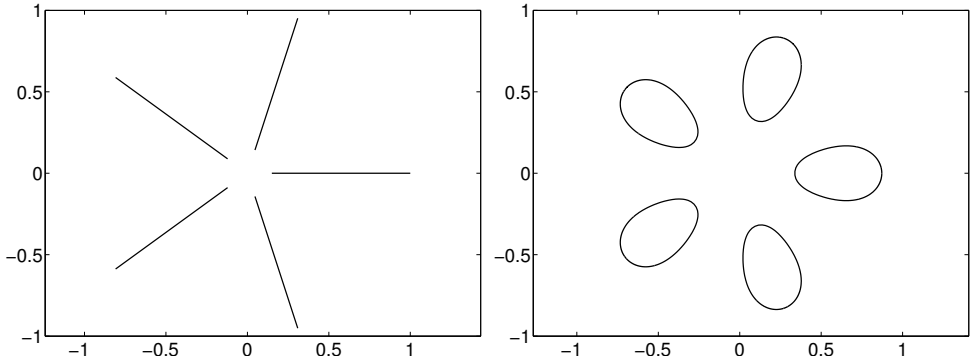

Figure 4: Illustration of Corollary 3.4: Radial slit domain (left) and corresponding lemniscatic domain (right).

which maps $\widehat{\mathbb{C}}\backslash E$ *onto an annulus. Let* f *be the conformal map from [59, Lemma 4.1] with parameter* $\rho = T(-z_0 + r)$*, which maps this annulus to the complex plane with slits. Further let* Φ_1 *be the lemniscatic map from* (3.2) *for* $n = 2$*, with*

$$C = \frac{2K\alpha}{\pi}(1-L)^2, \quad D = \frac{2K\alpha}{\pi}(1+L)^2,$$

where K *and* L *are constants depending on* f*. Then*

$$\Phi(z) = \Phi_1(f'(-1) \cdot (T^{-1} \circ f \circ T)(z))$$

is the lemniscatic map of E *with corresponding lemniscatic domain*

$$\mathcal{L} = \left\{ w \in \widehat{\mathbb{C}} : \left| w^2 - \left(\frac{2K\alpha}{\pi}(1+L^2) \right)^2 \right|^{\frac{1}{2}} > \sqrt{2L(1+L^2)} \frac{2K\alpha}{\pi} \right\}.$$

In particular, E *has the logarithmic capacity* $\sqrt{2L(1+L^2)}\frac{2K\alpha}{\pi}$*.*

Figure 5 (cf. [59, Figure 6]) shows the two disks (left) and corresponding lemniscatic domain (right) in Theorem 3.5, with $z_0 = 1$ and $r = 0.5, 0.7$ and 0.9.

In summary, we explicitly constructed two lemniscatic maps in [59], and Theorem 3.3 gives a construction principle for the lemniscatic map of certain polynomial pre-images of simply connected sets.

A method for the numerical computation of lemniscatic maps for a large class of sets has been proposed in [50], which is joint work with Nasser and Liesen. The method takes as input a discretization of the boundary, which is assumed to consist of Jordan curves. Its output are the parameters of the lemniscatic domain and the boundary values of the lemniscatic map at the discretization points of the boundary. For an n-times connected domain, the method solves n boundary integral equations with the Neumann kernel

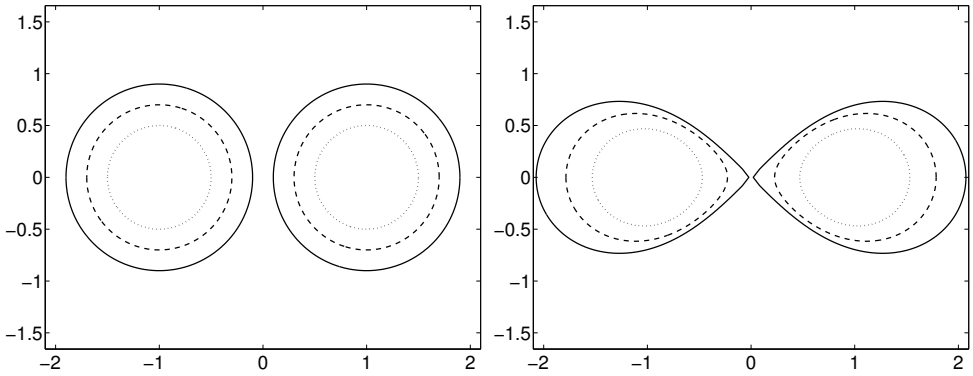

Figure 5: Illustration of Theorem 3.5.

(with an overall cost of $\mathcal{O}(n^2 n_d \log(n_d))$), and a system of $(n+1)n_d$ nonlinear equations, where n_d is the number of discretization points of each boundary component. The numerical experiments in [50] show that the method is fast and accurate, and also works for domains with piecewise smooth boundaries, close to touching boundaries, and for domains of high connectivity.

As an application of this method for computing lemniscatic maps, we have obtained a fast and accurate method for the numerical computation of the logarithmic capacity of compact sets [40]. The two articles [50, 40] are not included in this thesis.

3.3 Background on Faber–Walsh polynomials

Before we describe the contributions made in the article [58], we recall the definition of Faber–Walsh polynomials from [72]. Its two main ingredients are lemniscatic maps and the generalization of Laurent series to lemniscatic domains. The Laurent series of a function that is analytic outside a disk with center a_1 builds on the polynomials $(w - a_1)^k$, whose zeros are at the center of the disk. The following lemma describes how to generalize the polynomial $(w - a_1)^k$ for the disk to a polynomial $u_k(w)$ for a lemniscatic domain $\mathcal{L}$, in order to obtain a generalized Laurent series convergent in $\mathcal{L}$. In a nutshell, the zeros of $u_k(w)$ must be at the centers $a_1, \ldots, a_n$ of $\mathcal{L}$, and the multiplicity of each zero a_j must fit its "importance" for $\mathcal{L}$, given by the exponent m_j.

Lemma 3.6 ([72, Lemma 2])**.** *Let $\mathcal{L}$ be a lemniscatic domain as in* (3.1)*.*

1. *There exists a sequence $(\alpha_j)_{j=1}^{\infty}$, chosen from the centers $a_1, \ldots, a_n$, such that*

$$|N_{k,j} - km_j| \leq A, \quad \text{for } j = 1, 2, \ldots, n, \quad k = 1, 2, \ldots, \tag{3.3}$$

where $N_{k,j}$ denotes the number of times a_j appears in the sequence $\alpha_1, \ldots, \alpha_k$, and where A is a positive constant.

2. *Any such sequence has the following property: For any closed set* $S \subseteq \widehat{\mathbb{C}}$ *not containing any of the points* $a_1, \ldots, a_n$ *there exist constants* $A_1, A_2 > 0$ *such that*

$$A_1 < \frac{|u_k(w)|}{|U(w)|^k} < A_2, \quad \text{for } k = 0, 1, 2, \ldots \text{ and any } w \in S, \quad (3.4)$$

where $u_k(w) := \prod_{j=1}^{k}(w - \alpha_j)$.

For $n = 1$ the lemniscatic domain is the exterior of a disk, and we have $\alpha_j = a_1$ for all j and $u_k(w) = (w - a_1)^k$. For $n \geq 2$, the sequence $(\alpha_j)_{j=1}^{\infty}$ is *not unique*, but can be chosen constructively from $a_1, \ldots, a_n$; see [72]. Note that a smaller constant A in (3.3) implies better bounds in (3.4).

Before stating Walsh's main theorem on Faber–Walsh polynomials, let us say a word on the level curves of Green's function. In the notation of Theorem 3.1, the Green's function with pole at infinity for the lemniscatic domain $\mathcal{L}$ and for $\mathcal{K} = \widehat{\mathbb{C}} \backslash E$ are

$$g_{\mathcal{L}}(w) = \log|U(w)| - \log(\mu) \quad \text{and} \quad g_{\mathcal{K}}(z) = g_{\mathcal{L}}(\Phi(z)), \quad (3.5)$$

respectively. We will consistently denote their level curves for $\sigma > 1$ by

$$\Gamma_\sigma = \{z \in \mathcal{K} : g_{\mathcal{K}}(z) = \log(\sigma)\} \quad \text{and} \quad \Lambda_\sigma = \{w \in \mathcal{L} : g_{\mathcal{L}}(w) = \log(\sigma)\}.$$

Note that $\Lambda_\sigma = \Phi(\Gamma_\sigma)$. In what follows, ext and int denote the exterior and interior of a curve (or union of curves). We can now state Walsh's main result from [72].

Theorem 3.7 ([72, Theorem 3])**.** *Let the notation be as in Theorem 3.1, and let* $(\alpha_j)_{j=1}^{\infty}$ *and the corresponding polynomials* $u_k(w)$ *be as in Lemma 3.6.*

1. *For any* $z \in \Gamma_\sigma$ *and* $w \in \operatorname{ext}(\Lambda_\sigma)$ *we have*

$$\frac{\psi'(w)}{\psi(w) - z} = \sum_{k=0}^{\infty} \frac{b_k(z)}{u_{k+1}(w)},$$

where

$$b_k(z) = \frac{1}{2\pi i} \int_{\Lambda_\lambda} u_k(\tau) \frac{\psi'(\tau)}{\psi(\tau) - z}\, d\tau = \frac{1}{2\pi i} \int_{\Gamma_\lambda} \frac{u_k(\Phi(\zeta))}{\zeta - z}\, d\zeta \quad (3.6)$$

for any $\lambda > \sigma$. *The function* b_k *is a monic polynomial of degree* k, *which is called the* kth Faber–Walsh polynomial *for* E *and* $(\alpha_j)_{j=1}^{\infty}$.

2. *Let* f *be analytic on* E, *and let* $\rho > 1$ *be the largest number such that* f *is analytic and single-valued in* $\operatorname{int}(\Gamma_\rho)$. *Then* f *has a unique representation as a* Faber–Walsh series

$$f(z) = \sum_{k=0}^{\infty} a_k b_k(z), \quad (3.7)$$

which converges absolutely in $\operatorname{int}(\Gamma_\rho)$ *and maximally on* E*. The coefficients are given by*

$$a_k = \frac{1}{2\pi i} \int_{\Lambda_\lambda} \frac{f(\psi(\tau))}{u_{k+1}(\tau)}\, d\tau, \quad 1 < \lambda < \rho.$$

Let us comment on the theorem. When the set E is simply connected, the Faber–Walsh polynomials are the (possibly scaled) Faber polynomials F_k. More precisely, $b_k(z) = F_k(z)$ if the (exterior) Riemann map $\widetilde{\Phi}$ is normalized by $\widetilde{\Phi}'(\infty) = 1$, so that the Faber polynomials are monic (as, for instance, in [18, 46, 63]), and $b_k(z) = \mu^k F_k(z)$ if $\widetilde{\Phi}$ maps onto the exterior of the unit disk and $\widetilde{\Phi}'(\infty) = \mu^{-1} > 0$; see, for instance, [10, 24, 66].

The maximal convergence of the series (3.7) to f on E is equivalent to

$$\limsup_{N\to\infty} \|f - \sum_{k=0}^{N} a_k b_k\|_E^{1/N} = \frac{1}{\rho}.$$

It implies uniform convergence on any compact subset in $\operatorname{int}(\Gamma_\rho)$. For an entire function f, we have $\rho = \infty$ and $\operatorname{int}(\Gamma_\rho) = \mathbb{C}$.

3.4 Main results on Faber–Walsh polynomials

We summarize the main results obtained in [58].

First, general properties of the Faber–Walsh polynomials are studied, and we start with a different representation.

Corollary 3.8 ([58, Corollary 3.1])**.** *In the notation of Theorem 3.7, the* k*th Faber–Walsh polynomial* $b_k(z)$ *is the polynomial part of the Laurent series at infinity of* $u_k(\Phi(z))$*.*

We use this characterization and Theorem 3.3 to relate the Faber polynomials of a simply connected compact set Ω to the Faber–Walsh polynomials of a polynomial pre-image of Ω. This gives a "transplantation" result for Faber–Walsh polynomials, which is an analogue of a similar result for Chebyshev polynomials shown in [23, 33].

Theorem 3.9 ([58, Theorem 3.3])**.** *In the notation of Theorem 3.3, denote the* $n \geq 2$ *distinct roots of the polynomial* $(U(w))^n$ *by* $a_1, \ldots, a_n$*. Then, the* (kn)*th Faber–Walsh polynomials for* E *and* $(a_1, a_2, \ldots, a_n, a_1, a_2, \ldots, a_n, \ldots)$ *satisfy*

$$b_{kn}(z) = \frac{1}{(\alpha\widetilde{\Phi}'(\infty))^k} F_k(P(z))$$

for all $k \geq 0$*, where* F_k *is the* k*th Faber polynomial for* Ω*.*

For polynomials of degree one the situation is different from Theorem 3.9, since P then is a linear transformation and thus preserves the number of components of a set. In this case, we obtain the following stronger result.

Proposition 3.10 ([58, Proposition 3.4])**.** *Let the notation be as in Theorem 3.7, and let $P(z) = az + b$ with $a \neq 0$. Then the Faber–Walsh polynomials $\widetilde{b}_k$ for $P(E)$ and $(P(\alpha_j))_{j=1}^{\infty}$ satisfy $b_k(z) = \frac{1}{a^k}\widetilde{b}_k(P(z))$ for all $k \geq 0$.*

Next, we show that Faber–Walsh polynomials are *asymptotically optimal*. This concept is related to the polynomial approximation problem (1.4); see the discussion in Section 1.3. To measure how close a sequence of polynomials will be to the sequence of optimal polynomials, Eiermann, Niethammer and Varga [16, 17] introduced the following concepts. Let $E \subseteq \mathbb{C}$ be a compact set and $z_0 \in \mathbb{C}$. The *asymptotic convergence factor* for polynomials from $\mathcal{P}_k(z_0)$ associated with E is

$$R_{z_0}(E) = \limsup_{k\to\infty} \Big(\min_{p\in\mathcal{P}_k(z_0)} \|p\|_E \Big)^{1/k},$$

see Section 1.3 for the definiton of $\mathcal{P}_k(z_0)$, and a sequence of polynomials $p_k \in \mathcal{P}_k(z_0)$ is called *asymptotically optimal* on E with respect to z_0, if

$$\lim_{k\to\infty} \|p_k\|_E^{1/k} = R_{z_0}(E).$$

For sets E as in Theorem 3.1, the asymptotic convergence factor can be characterized with the Green's function (3.5) as

$$R_{z_0}(E) = \exp(-g_{\mathcal{K}}(z_0)) = \frac{\mu}{|U(\Phi(z_0))|} \quad \text{for any } z_0 \in \mathbb{C}\backslash E; \tag{3.8}$$

see [15, Equation (3.3)]. With the numerical method for the computation of the lemniscatic map from [50], we thus can compute the asymptotic convergence factor for a large class of complex sets E and any $z_0 \in \mathbb{C}\backslash E$. We give several examples below.

With the characterization (3.8), we show that normalized Faber–Walsh polynomials are asymptotically optimal.

Proposition 3.11 ([58, Proposition 3.7])**.** *In the notation of Theorem 3.7, let $z_0 \in \mathbb{C}\backslash E$. Then the normalized Faber–Walsh polynomials $b_k/b_k(z_0)$ are asymptotically optimal on E with respect to z_0, i.e.,*

$$\lim_{k\to\infty} \left(\frac{\|b_k\|_E}{|b_k(z_0)|} \right)^{1/k} = R_{z_0}(E).$$

After establishing these general results on Faber–Walsh polynomials, we consider the Faber–Walsh polynomials for several special sets. We begin with two intervals and, in particular, with two equal intervals

$$E = [-D, -C] \cup [C, D], \quad 0 < C < D. \tag{3.9}$$

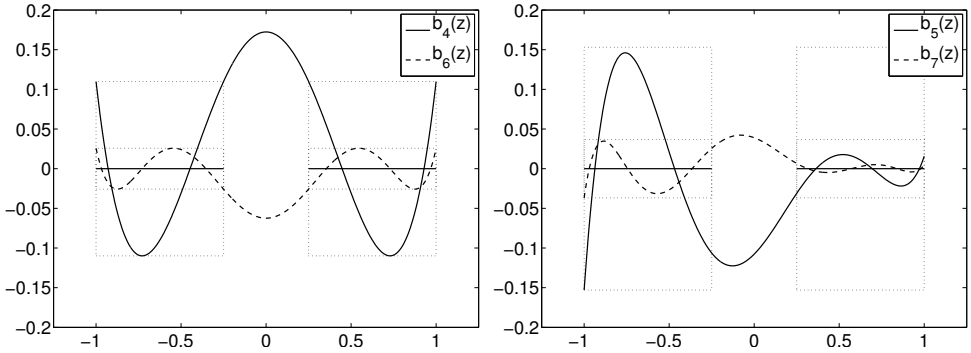

Figure 6: Faber–Walsh polynomials b_k for $E = [-1, -\frac{1}{4}] \cup [\frac{1}{4}, 1]$.

The lemniscatic map of this set is known explicitly from Corollary 3.4 (with $n = 2$). We can thus explicitly compute the Faber–Walsh polynomials by a recursion; see [58, Proposition 2.4]. Figure 6 (cf. [58, Figure 1]) shows a few computed Faber–Walsh polynomials. We observe that the polynomials b_k of even degrees $k = 4, 6$ have $k + 2$ extremal points on E. This suggests that they are the Chebyshev polynomials for E, which in fact is true.

Theorem 3.12 ([58, Theorem 4.2])**.** *Let $E = [-D, -C] \cup [C, D]$ with $0 < C < D$. Then the Faber–Walsh polynomials b_{2k} for E and the sequence $\left(\frac{D+C}{2}, -\frac{D+C}{2}, \frac{D+C}{2}, -\frac{D+C}{2}, \ldots\right)$ are the Chebyshev polynomials for E, i.e.,*

$$b_{2k}(z) = T_{2k}(z; E), \quad k \geq 0.$$

The theorem also holds for two arbitrary real intervals of equal length, and for the radial slit domain from Corollary 3.4; see Theorem 4.2 and the following discussion in [58]. The proof of Theorem 3.12 uses Theorem 3.9 and the relation of Faber and Chebyshev polynomials on a single interval. As a consequence of Theorem 3.12, the normalized Faber–Walsh polynomials $b_{2k}/b_{2k}(z_0)$ with real constraint point $z_0 \in \mathbb{R} \backslash E$ are the optimal polynomials; see [58, Corollary 4.3]. This does not extend to odd degrees, as we further show in [58]. We numerically compute the Faber–Walsh polynomials $b_{k,j}$ for the sets

$$E_j = [-1, -2^{-j}] \cup [2^{-j}, 1], \quad j = 1, 2, 3, 4, \tag{3.10}$$

and the sequence $(\frac{D+C}{2}, -\frac{D+C}{2}, \frac{D+C}{2}, -\frac{D+C}{2}, \ldots)$. Figure 7 (left; cf. [58, Figure 2]) shows the values $\|b_{k,j}\|/|b_{k,j}(0)|$ of the normalized Faber–Walsh polynomials for the degrees $k = 1, \ldots, 30$. A comparison with the values $R_0(E_j)^k$ in Figure 7 (right) shows that the rate at which the norms converge to zero almost exactly matches the rate predicted by the asymptotic analysis (Proposition 3.11), already for small values of k. The "zigzags" in the curves on the left are due to the fact that the polynomial $b_k/b_k(0)$ is optimal for

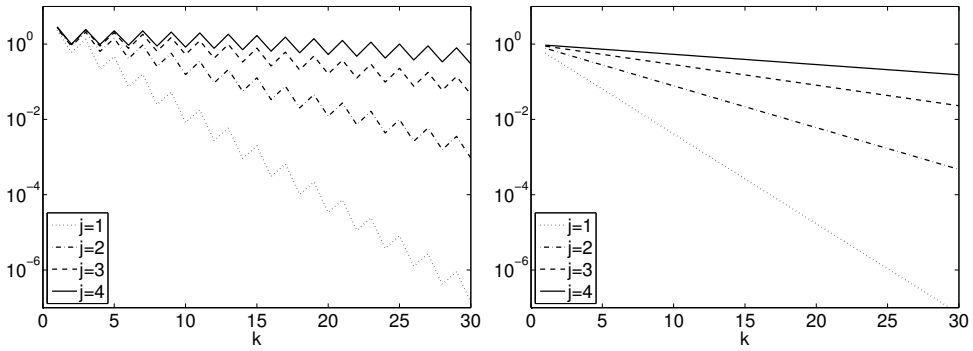

Figure 7: The values $\frac{\|b_{k,j}\|_{E_j}}{|b_{k,j}(0)|}$ (left) and $R_0(E_j)^k$ (right) for the sets E_j from (3.10).

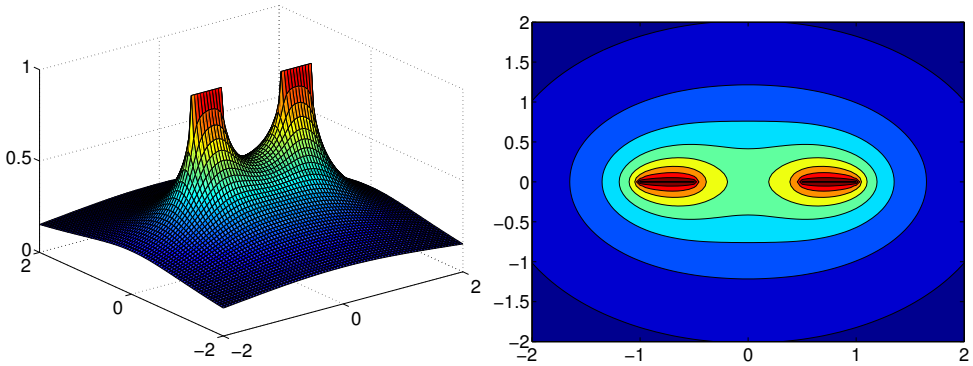

Figure 8: Asymptotic convergence factor $R_{z_0}([-1,-\frac{1}{2}]\cup[\frac{1}{2},1])$ as a function of $z_0 \in \mathbb{C}$.

even degrees, while for odd degrees it is not. We also observe that the convergence to zero slows down as j increases, which is related to the growing values $R_0(E_j)$.

From (3.8) and Corollary 3.4 we obtain the asymptotic convergence factor for E from (3.9) and any $z_0 \in \mathbb{C}\backslash E$ as

$$R_{z_0}(E) = \frac{\mu}{|U(\Phi(z_0))|} = \frac{1}{\sqrt{\frac{2}{D^2-C^2}|z_0^2 - \frac{D^2+C^2}{2} \pm \sqrt{(z_0^2-C^2)(z_0^2-D^2)}|}},$$

where the sign of the square root is chosen so as to maximize the denominator. This simple expression of $R_{z_0}(E)$ in terms of elementary functions seems to be new in the literature. Figure 8 (cf. [58, Figure 3]) shows $R_{z_0}([-1,-\frac{1}{2}]\cup[\frac{1}{2},1])$ as a function of $z_0 \in \mathbb{C}$.

For two arbitrary real intervals

$$E = [A,B]\cup[C,D], \quad A<B<C<D,$$

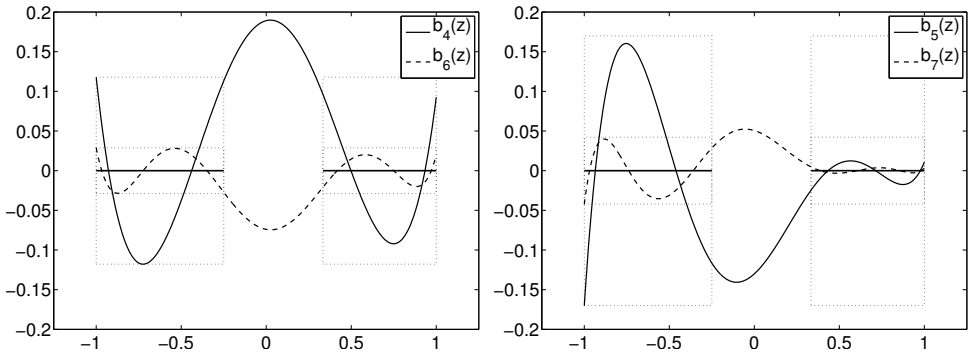

Figure 9: Faber–Walsh polynomials b_k for $E = [-1, -\frac{1}{4}] \cup [\frac{1}{3}, 1]$.

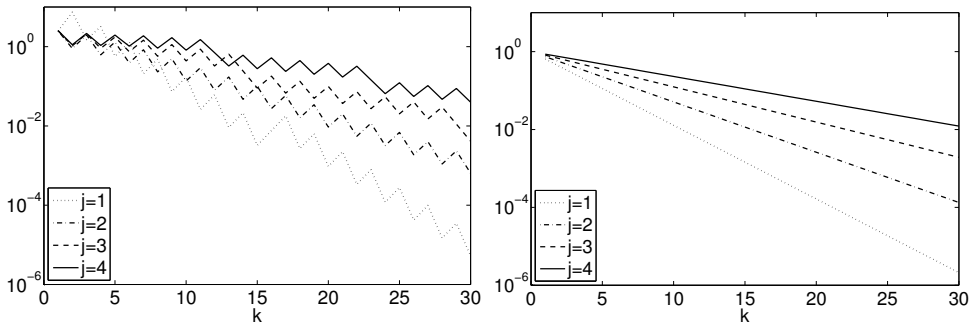

Figure 10: The values $\frac{\|b_{k,j}\|_{E_j}}{|b_{k,j}(0)|}$ (left) and $R_0(E_j)^k$ (right) for the sets E_j from (3.11).

the lemniscatic map is not known analytically. We numerically obtain the lemniscatic map and lemniscatic domain with the method from [50] after a preliminary conformal map; see Section 4.2 in [58] for details. We then can numerically compute the Faber–Walsh polynomials; see Figure 9 (cf. [58, Figure 6]). In contrast to the case of two equal intervals, the Faber–Walsh polynomials in Figure 9 do not have the equioscillation property and thus are in general not the Chebyshev polynomials for E. We further compute the Faber–Walsh polynomials $b_{k,j}$ for the sets

$$E_j = [-1, -2^{-j}] \cup [3^{-1}, 1], \quad j = 1, 2, 3, 4. \tag{3.11}$$

Figure 10 (left; cf. [58, Figure 7]) shows the norms of the normalized Faber–Walsh polynomials, $\|b_{k,j}\|_E/|b_{k,j}(0)|$, and the values $R_0(E_j)^k$ (right). As before, the convergence speed to zero matches almost exactly the rate predicted by the asymptotic analysis, already for small k. The norms also have a few irregular jumps, which occur precisely when in the sequence $(\alpha_j)_{j=1}^{\infty}$ (see Lemma 3.6) one of the centers of the lemniscatic domain is chosen twice in a row. We computed the asymptotic convergence factors $R_0(E_j)$ using (3.8)

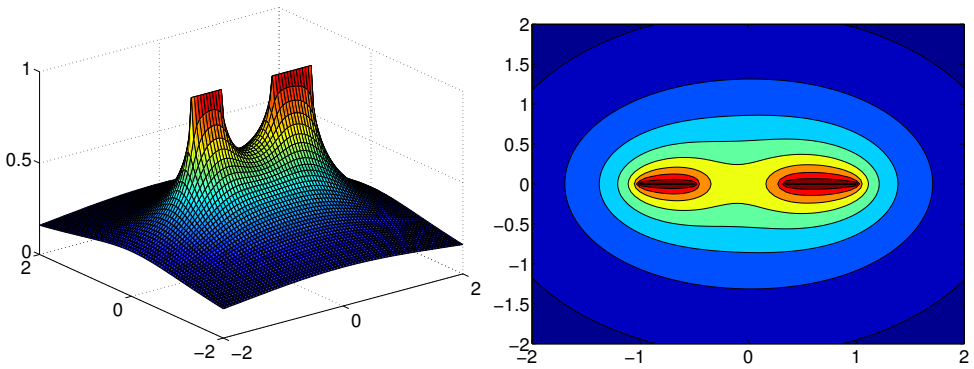

Figure 11: Asymptotic convergence factor $R_{z_0}([-1,-\frac{1}{2}]\cup[\frac{1}{3},1])$ as a function of $z_0 \in \mathbb{C}$.

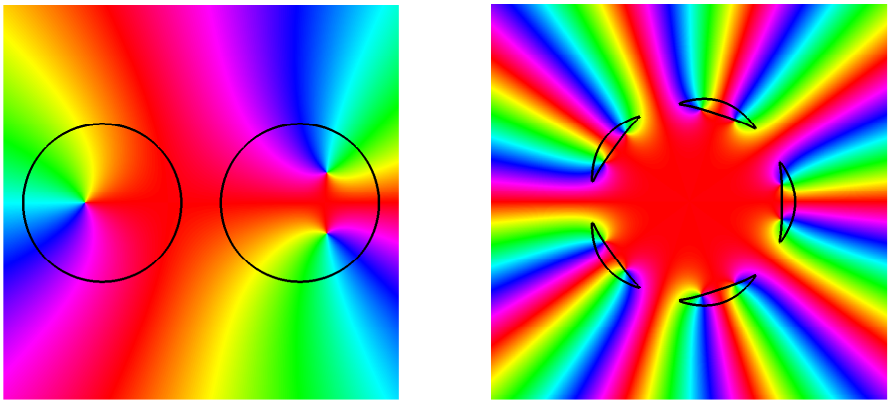

Figure 12: Phase portraits of Faber–Walsh polynomials; see the end of Section 3.4 for details.

and the numerically computed lemniscatic map. Figure 11 (cf. [58, Figure 8]) shows $R_{z_0}(E_1)$ with variable $z_0 \in \mathbb{C}$.

In the last section of [58] we explore the Faber–Walsh polynomials on two complex sets, using the previously established theory. Since the results are similar to those obtained for two intervals, we give here a brief summary and refer to [58, Section 5] for details. The first sets consists of the two equal disks from Theorem 3.5, the second is a polynomial pre-image of a simply connected set Ω (see [58, Figure 13(a)]), for which the Riemann map is known analytically. The boundaries of the two sets are indicated by the black contours in Figure 12. The figure also shows phase portraits of Faber–Walsh polynomials, which we compute numerically with (3.6). The lemniscatic maps for the two sets are known from Theorem 3.3 and Theorem 3.5.

Moreover, we study the norms of the normalized Faber–Walsh polynomials for these two complex sets, with results similar to the case of two

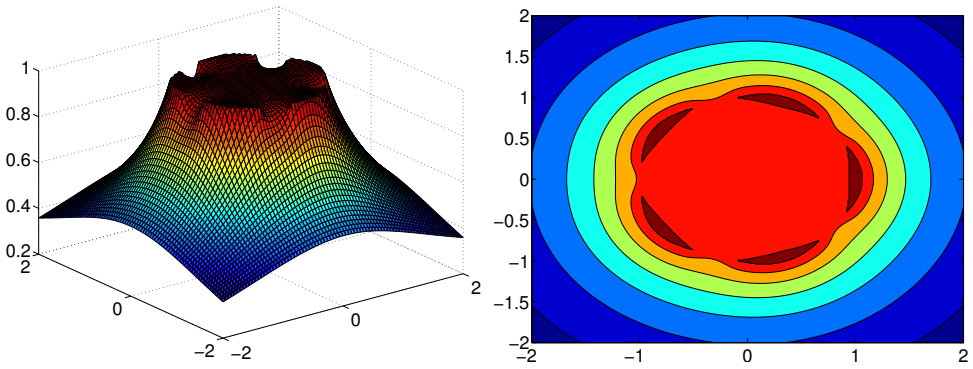

Figure 13: Asymptotic convergence factor $R_{z_0}(E)$ as a function of $z_0 \in \mathbb{C}$ for E as in Figure 12 (right).

intervals. In this context we also compute the asymptotic convergence factor $R_{z_0}(E)$ as a function of $z_0 \in \mathbb{C}$, shown for the second set in Figure 13 (cf. [58, Figure 15]).

In summary, we derived in [58] general properties of Faber–Walsh polynomials, in particular their relation to the classical Faber polynomials as well as their asymptotic optimality. Moreover, for several sets, we computed the Faber–Walsh polynomials, the asymptotic convergence factor, as well as the norms of the normalized Faber–Walsh polynomials. In the case of two equal intervals, we further showed that the Faber–Walsh polynomials of even degree are the Chebyshev polynomials.

4 Summary and outlook

In this thesis we studied questions in complex analysis that were motivated by questions from the theory of Krylov subspace methods in numerical linear algebra. These studies rely on a variety of tools, which range from classical function theory (conformal mappings and polynomial approximation) to the theory of (non-analytic) complex-valued harmonic functions.

In the first area of research we studied the zeros of rational harmonic functions ([44, 61, 60]). We sharpened the known upper bound on the maximal possible number of zeros of these functions, and showed that extremal functions are always regular. Moreover, we investigated the change of the number of zeros which occurs when adding a simple pole to a rational harmonic function. As described in Section 2.2, we were able to completely characterize this "zero creating" effect, depending on the properties of the rational harmonic function at the perturbation point. As an application of this general perturbation result, we obtained a construction principle for general (unsymmetric) extremal functions, that do not share the highly symmetric appearance of the previously known examples (see (2.2) in Section 2.1).

We further applied our mathematical results to gravitational microlensing, where gravitational point lenses are modeled by rational harmonic functions, whose zeros are relevant physical quantities, namely observed images (see Section 2.2). In this context, adding a pole corresponds to adding a mass to the gravitational lens. Our mathematical results from [61] give therefore a complete characterization of the number of created images, when adding a mass to a gravitational point lens. Further, we derived a construction principle for unsymmetric point lenses where maximal lensing occurs (i.e., of extremal functions). In the same context we wrote the article [43], which studies the previously known examples of extremal functions (gravitational lenses with maximal lensing), but is not part of this thesis. Both [43] and [60] are published in General Relativity and Gravitation, and received the "Editor's Choice" distinction from its editors.

In the second area of research, we studied Faber–Walsh polynomials and the conformal maps through which they are defined. We investigated the lemniscatic maps in [59], focusing on constructive aspects. We gave a construction principle for this map for certain polynomial pre-images, as well as two analytic examples of lemniscatic maps. In [58] we derived new theoretical results for the Faber–Walsh polynomials, and demonstrated their numerical computability for several sets, using either the explicitly available lemniscatic maps from [59] or the numerical method from [50] for their computation. Further, our numerical experiments indicate that the normalized Faber–Walsh polynomials, which are asymptotically optimal, are close to the optimal polynomials already for small degrees.

Finally, we collect a few open questions and further research topics related to the research in this thesis.

1. Theorem 2.5 and Theorem 2.6 assert that *at least* a certain number of zeros is created when adding a pole. Is it the *exact* number? Extensive numerical experiments suggest this, but so far this question has resisted all attempts of proof.

2. In [43] we derived sharp bounds on ε so that in Rhie's construction (2.2) the maximal number of zeros is created. It would be interesting to quantify when ε is "sufficiently small" in Theorems 2.5 and 2.6, so that the stated number of zeros is created. Note that if ε is too large, more than the stated number of zeros may be created; see the example in [61, Section 4.2].

3. A more detailed study of the singular zeros of rational harmonic functions is of interest. Although the regular functions are dense in the set of all rational harmonic functions ([34, p. 1081]), singular zeros do appear, in particular in the gravitational microlensing model.

4. Truncation of the Faber–Walsh series (3.7) yields a polynomial approximating the analytic function f on a compact set with several components, similar to truncated Faber series on simply connected compact sets, or to truncated Chebyshev series on an interval. How good is this approximation? By Theorem 3.7 it converges maximally to f, but a *quantitative bound* on $\|f - \sum_{k=0}^{N} a_k b_k\|_E$ has still to be established.

5. Find bounds on the norm of the projection which truncates the Faber–Walsh series, analogously to the cases of Faber series [18] and Chebyshev series [69].

6. In [50] we have derived a fast and accurate method for the numerical computation of lemniscatic maps. Subject to further work is a practical and numerically stable method for the computation of the Faber–Walsh series (3.7), as well as its implementation.

References

[1] A. Antoulas and B. Anderson, *On the scalar rational interpolation problem.*, IMA J. Math. Control Inf., 3 (1986), pp. 61–88.

[2] W. E. Arnoldi, *The principle of minimized iteration in the solution of the matrix eigenvalue problem*, Quart. Appl. Math., 9 (1951), pp. 17–29.

[3] T. Barth and T. Manteuffel, *Conjugate gradient algorithms using multiple recursions*, in Linear and nonlinear conjugate gradient-related methods (Seattle, WA, 1995), SIAM, Philadelphia, PA, 1996, pp. 107–123.

[4] ——, *Multiple recursion conjugate gradient algorithms. I. Sufficient conditions*, SIAM J. Matrix Anal. Appl., 21 (2000), pp. 768–796.

[5] J. Bayer and C. C. Dyer, *Maximal lensing: mass constraints on point lens configurations*, Gen. Relativity Gravitation, 39 (2007), pp. 1413–1418.

[6] ——, *Erratum: Maximal lensing: mass constraints on point lens configurations*, Gen. Relativity Gravitation, 41 (2009), p. 669.

[7] B. Beckermann and M. Crouzeix, *Faber polynomials of matrices for non-convex sets*, Jaen J. Approx., 6 (2014), pp. 219–231.

[8] B. Beckermann and L. Reichel, *Error estimates and evaluation of matrix functions via the Faber transform*, SIAM J. Numer. Anal., 47 (2009), pp. 3849–3883.

[9] J. Clunie and T. Sheil-Small, *Harmonic univalent functions*, Ann. Acad. Sci. Fenn. Ser. A I Math., 9 (1984), pp. 3–25.

[10] J. H. Curtiss, *Faber polynomials and the Faber series*, Amer. Math. Monthly, 78 (1971), pp. 577–596.

[11] P. J. Davis, *Interpolation and approximation*, Blaisdell Publishing Co. Ginn and Co. New York-Toronto-London, 1963.

[12] P. Duren, *Harmonic mappings in the plane*, vol. 156 of Cambridge Tracts in Mathematics, Cambridge University Press, Cambridge, 2004.

[13] P. Duren, W. Hengartner, and R. S. Laugesen, *The argument principle for harmonic functions*, Amer. Math. Monthly, 103 (1996), pp. 411–415.

[14] M. Eiermann, *On semiiterative methods generated by Faber polynomials*, Numer. Math., 56 (1989), pp. 139–156.

[15] M. Eiermann, X. Li, and R. S. Varga, *On hybrid semi-iterative methods*, SIAM J. Numer. Anal., 26 (1989), pp. 152–168.

[16] M. Eiermann and W. Niethammer, *On the construction of semi-iterative methods*, SIAM J. Numer. Anal., 20 (1983), pp. 1153–1160.

[17] M. Eiermann, W. Niethammer, and R. S. Varga, *A study of semi-iterative methods for nonsymmetric systems of linear equations*, Numer. Math., 47 (1985), pp. 505–533.

[18] S. W. Ellacott, *Computation of Faber series with application to numerical polynomial approximation in the complex plane*, Math. Comp., 40 (1983), pp. 575–587.

[19] ——, *A survey of Faber methods in numerical approximation*, Comput. Math. Appl. Part B, 12 (1986), pp. 1103–1107.

[20] G. Faber, *Über polynomische Entwickelungen*, Math. Ann., 57 (1903), pp. 389–408.

[21] V. Faber, J. Liesen, and P. Tichý, *On Chebyshev polynomials of matrices*, SIAM J. Matrix Anal. Appl., 31 (2009/10), pp. 2205–2221.

[22] B. Fischer, *Polynomial based iteration methods for symmetric linear systems*, Wiley-Teubner Series Advances in Numerical Mathematics, John Wiley & Sons, Ltd., Chichester; B. G. Teubner, Stuttgart, 1996.

[23] B. Fischer and F. Peherstorfer, *Chebyshev approximation via polynomial mappings and the convergence behaviour of Krylov subspace methods*, Electron. Trans. Numer. Anal., 12 (2001), pp. 205–215 (electronic).

[24] D. Gaier, *Vorlesungen über Approximation im Komplexen*, Birkhäuser Verlag, Basel, 1980.

[25] F. R. Gantmacher, *The theory of matrices. Vols. 1, 2*, Translated by K. A. Hirsch, Chelsea Publishing Co., New York, 1959.

[26] L. Geyer, *Sharp bounds for the valence of certain harmonic polynomials*, Proc. Amer. Math. Soc., 136 (2008), pp. 549–555.

[27] G. H. Golub and C. F. Van Loan, *Matrix computations*, Johns Hopkins Studies in the Mathematical Sciences, Johns Hopkins University Press, Baltimore, MD, fourth ed., 2013.

[28] A. Greenbaum, *Iterative methods for solving linear systems*, vol. 17 of Frontiers in Applied Mathematics, Society for Industrial and Applied Mathematics (SIAM), Philadelphia, PA, 1997.

[29] A. Greenbaum and L. N. Trefethen, *GMRES/CR and Arnoldi/Lanczos as matrix approximation problems*, SIAM J. Sci. Comput., 15 (1994), pp. 359–368.

[30] M. Hasson, *Expansion of analytic functions of an operator in series of Faber polynomials*, Bull. Austral. Math. Soc., 56 (1997), pp. 303–318.

[31] V. Heuveline and M. Sadkane, *Arnoldi-Faber method for large non-Hermitian eigenvalue problems*, Electron. Trans. Numer. Anal., 5 (1997), pp. 62–76 (electronic).

[32] N. J. Higham, *Functions of matrices. Theory and computation*, Society for Industrial and Applied Mathematics (SIAM), Philadelphia, PA, 2008.

[33] S. O. Kamo and P. A. Borodin, *Chebyshev polynomials for Julia sets*, Vestnik Moskov. Univ. Ser. I Mat. Mekh., (1994), pp. 65–67.

[34] D. Khavinson and G. Neumann, *On the number of zeros of certain rational harmonic functions*, Proc. Amer. Math. Soc., 134 (2006), pp. 1077–1085.

[35] ——, *From the fundamental theorem of algebra to astrophysics: a "harmonious" path*, Notices Amer. Math. Soc., 55 (2008), pp. 666–675.

[36] D. Khavinson and G. Świątek, *On the number of zeros of certain harmonic polynomials*, Proc. Amer. Math. Soc., 131 (2003), pp. 409–414.

[37] H. J. Landau, *On canonical conformal maps of multiply connected domains*, Trans. Amer. Math. Soc., 99 (1961), pp. 1–20.

[38] S.-Y. Lee, A. Lerario, and E. Lundberg, *Remarks on Wilmshurst's theorem*, Indiana Univ. Math. J., 64 (2015), pp. 1153–1167.

[39] J. Liesen, *When is the adjoint of a matrix a low degree rational function in the matrix?*, SIAM J. Matrix Anal. Appl., 29 (2007), pp. 1171–1180.

[40] J. Liesen, O. Sète, and M. M. S. Nasser, *Computing the logarithmic capacity of compact sets via conformal mapping*, ArXiv e-prints: 1507.05793, (2015).

[41] J. Liesen and Z. Strakoš, *Krylov subspace methods. Principles and analysis*, Numerical Mathematics and Scientific Computation, Oxford University Press, Oxford, 2013.

[42] J. Liesen and P. Tichý, *On best approximations of polynomials in matrices in the matrix 2-norm*, SIAM J. Matrix Anal. Appl., 31 (2009), pp. 853–863.

[43] R. Luce, O. Sète, and J. Liesen, *Sharp parameter bounds for certain maximal point lenses*, Gen. Relativity Gravitation, 46 (2014), p. 46:1736.

[44] ——, *A note on the maximum number of zeros of $r(z) - \overline{z}$*, Comput. Methods Funct. Theory, 15 (2015), pp. 439–448.

[45] S. Mao, A. O. Petters, and H. J. Witt, *Properties of point mass lenses on a regular polygon and the problem of maximum number of images*, in The Eighth Marcel Grossmann Meeting, Part A, B (Jerusalem, 1997), World Sci. Publ., River Edge, NJ, 1999, pp. 1494–1496.

[46] A. I. Markushevich, *Theory of functions of a complex variable. Vol. III*, Revised English edition, translated and edited by Richard A. Silverman, Prentice-Hall, Inc., Englewood Cliffs, N.J., 1967.

[47] G. Meinardus, *Approximation of functions: Theory and numerical methods*, Expanded translation of the German edition. Springer Tracts in Natural Philosophy, Vol. 13, Springer-Verlag New York, Inc., New York, 1967.

[48] I. Moret and P. Novati, *The computation of functions of matrices by truncated Faber series*, Numer. Funct. Anal. Optim., 22 (2001), pp. 697–719.

[49] ——, *An interpolatory approximation of the matrix exponential based on Faber polynomials*, J. Comput. Appl. Math., 131 (2001), pp. 361–380.

[50] M. M. S. Nasser, J. Liesen, and O. Sète, *Numerical computation of the conformal map onto lemniscatic domains*, Comput. Methods Funct. Theory, (2016), pp. 1–27.

[51] A. O. Petters, *Gravity's action on light*, Notices Amer. Math. Soc., 57 (2010), pp. 1392–1409.

[52] A. O. Petters, H. Levine, and J. Wambsganss, *Singularity theory and gravitational lensing*, vol. 21 of Progress in Mathematical Physics, Birkhäuser Boston, Inc., Boston, MA, 2001.

[53] A. O. Petters and M. C. Werner, *Mathematics of gravitational lensing: multiple imaging and magnification*, Gen. Relativity Gravitation, 42 (2010), pp. 2011–2046.

[54] M. J. D. Powell, *Approximation theory and methods*, Cambridge University Press, Cambridge-New York, 1981.

[55] S. H. Rhie, *n-point gravitational lenses with 5(n-1) images*, ArXiv e-prints: astro-ph/0305166v1, (2003).

[56] Y. Saad, *Projection methods for solving large sparse eigenvalue problems*, in Matrix Pencils, B. Kågström and A. Ruhe, eds., vol. 973 of Lecture Notes in Mathematics, Springer Berlin Heidelberg, 1983, pp. 121–144.

[57] ——, *Iterative methods for sparse linear systems*, Society for Industrial and Applied Mathematics, Philadelphia, PA, second ed., 2003.

[58] O. Sète and J. Liesen, *Properties and examples of Faber–Walsh polynomials*, ArXiv e-prints: 1502.07633, (2015).

[59] ——, *On conformal maps from multiply connected domains onto lemniscatic domains*, Electron. Trans. Numer. Anal., 45 (2016), pp. 1–15.

[60] O. Sète, R. Luce, and J. Liesen, *Creating images by adding masses to gravitational point lenses*, Gen. Relativity Gravitation, 47, Art. 42 (2015), pp. 1–8.

[61] ——, *Perturbing rational harmonic functions by poles*, Comput. Methods

Funct. Theory, 15 (2015), pp. 9–35.

[62] T. Sheil-Small, *Complex polynomials*, vol. 75 of Cambridge Studies in Advanced Mathematics, Cambridge University Press, Cambridge, 2002.

[63] V. I. Smirnov and N. A. Lebedev, *Functions of a complex variable: Constructive theory*, Translated from the Russian by Scripta Technica Ltd, The M.I.T. Press, Cambridge, Mass., 1968.

[64] G. Starke and R. S. Varga, *A hybrid Arnoldi-Faber iterative method for nonsymmetric systems of linear equations*, Numer. Math., 64 (1993), pp. 213–240.

[65] N. Straumann, *Complex formulation of lensing theory and applications*, Helv. Phys. Acta, 70 (1997), pp. 894–908.

[66] P. K. Suetin, *Series of Faber polynomials*, vol. 1 of Analytical Methods and Special Functions, Gordon and Breach Science Publishers, Amsterdam, 1998.

[67] T. J. Suffridge and J. W. Thompson, *Local behavior of harmonic mappings*, Complex Variables Theory Appl., 41 (2000), pp. 63–80.

[68] K.-C. Toh and L. N. Trefethen, *The Chebyshev polynomials of a matrix*, SIAM J. Matrix Anal. Appl., 20 (1999), pp. 400–419.

[69] L. N. Trefethen, *Approximation theory and approximation practice*, Society for Industrial and Applied Mathematics (SIAM), Philadelphia, PA, 2013.

[70] L. N. Trefethen and D. Bau, III, *Numerical linear algebra*, Society for Industrial and Applied Mathematics (SIAM), Philadelphia, PA, 1997.

[71] J. L. Walsh, *On the conformal mapping of multiply connected regions*, Trans. Amer. Math. Soc., 82 (1956), pp. 128–146.

[72] ——, *A generalization of Faber's polynomials*, Math. Ann., 136 (1958), pp. 23–33.

[73] ——, *Interpolation and approximation by rational functions in the complex domain*, Fifth edition. American Mathematical Society Colloquium Publications, Vol. XX, American Mathematical Society, Providence, R.I., 1969.

[74] J. Wambsganss, *Gravitational lensing in astronomy*, Living Rev. Relativity, 1 (1998). URL (cited on August 12, 2015): http://www.livingreviews.org/lrr-1998-12.

[75] D. S. Watkins, *The matrix eigenvalue problem. GR and Krylov subspace methods*, Society for Industrial and Applied Mathematics (SIAM), Philadelphia, PA, 2007.

[76] A. S. Wilmshurst, *The valence of harmonic polynomials*, Proc. Amer. Math. Soc., 126 (1998), pp. 2077–2081.

A Note on the Maximum Number of Zeros of $r(z) - \overline{z}$*

Robert Luce† Olivier Sète† Jörg Liesen†

Abstract

An important theorem of Khavinson & Neumann (Proc. Amer. Math. Soc. 134(4), 2006) states that the complex harmonic function $r(z) - \overline{z}$, where r is a rational function of degree $n \geq 2$, has at most $5(n-1)$ zeros. In this note we resolve a slight inaccuracy in their proof and in addition we show that for certain functions of the form $r(z) - \overline{z}$ no more than $5(n-1) - 1$ zeros can occur. Moreover, we show that $r(z) - \overline{z}$ is regular, if it has the maximal number of zeros.

1 Introduction

Let $r = \frac{p}{q}$ be a complex rational function of degree

$$n = \deg(r) := \max\{\deg(p), \deg(q)\}.$$

Here and in the sequel the polynomials p and q are always assumed to be coprime. We then say that the rational harmonic function

$$f(z) := r(z) - \overline{z} \tag{1}$$

is of degree n, too. Such functions have an interesting application in *gravitational microlensing*; see the introductory overview article of Khavinson & Neumann [6]. They also play a role in the matrix theory problem of expressing certain adjoints of diagonalizable matrices as rational functions of the matrix [7].

An important theorem of Khavinson & Neumann [5, Theorem 1] states that a rational harmonic function (1) of degree $n \geq 2$ has at most $5(n-1)$ zeros. In this note we give an alternative proof of their result (the differences to the original proof are discussed in Remark 2.8). Moreover, we show that

*A final version of this preprint manuscript appeared as follows: R. Luce, O. Sète and J. Liesen. A Note on the Maximum Number of Zeros of $r(z) - \overline{z}$. *Comput. Methods Funct. Theory* (2015) 15(3), pp. 439–448.

†TU Berlin, Institute of Mathematics, MA 4-5, Straße des 17. Juni 136, 10623 Berlin, Germany (`{luce,sete,liesen}@math.tu-berlin.de`)

a slightly better bound can be given if one takes into account the individual degrees of the numerator and denominator polynomials. In order to state our main result, we recall that a zero z_0 of f is called *sense-preserving* if $|r'(z_0)| > 1$, *sense-reversing* if $|r'(z_0)| < 1$, and *singular* if $|r'(z_0)| = 1$; see [10].

Theorem 1.1. *A rational harmonic function $f(z) = r(z) - \overline{z}$ of degree $n \geq 2$ has at most $3(n-1)$ sense-preserving zeros, and at most $2(n-1)$ sense-reversing or singular zeros. Moreover, if $r = \frac{p}{q}$ with $\deg(p) > \deg(q)$, then f has at most $5(n-1)-1$ zeros.*

The first part of this theorem was already stated in [5, Theorem 1 and Proposition 1] (see also [1, Appendix B], where several extensions to this bound are presented). Our proof in the next section employs similar techniques as the one in [5], but it avoids a subtle inaccuracy in the argument, which we will explain next.

If $f(z) = r(z) - \overline{z}$ has no singular zero, then f as well as r are called *regular*. In the proof of the Main Lemma in [5], part (2), it is implicitly assumed that if $f(z) = r(z) - \overline{z}$ is regular, then the function

$$F(w) = \frac{1}{r(\frac{1}{w})} - \overline{w}$$

is regular as well. However, this implication is in general not correct. For example, consider the rational harmonic function $f(z) = z + \frac{1}{z} - \overline{z}$. Clearly, 0 is not a zero of f, so that we have

$$f(z) = 0 \;\Leftrightarrow\; z^2 + 1 = |z|^2,$$

and hence f has (only) the two zeros $\pm\frac{i}{\sqrt{2}}$. Since $|r'(\pm\frac{i}{\sqrt{2}})| = 3 > 1$, the function f is regular. Now consider

$$F(w) = \frac{1}{r(\frac{1}{w})} - \overline{w} = \frac{w}{1+w^2} - \overline{w} =: R(w) - \overline{w}. \tag{2}$$

Then $F(0) = 0$, and $|R'(0)| = 1$ shows that 0 is a singular zero of F.

In Section 2 we give a new proof of Theorem 1.1. In Section 3 we further show that $r(z) - \overline{z}$ has no singular zeros, if it has the maximal number of zeros as stated in Theorem 1.1.

2 Proof of Theorem 1.1

In order to prove Theorem 1.1 we need some preliminary results. First note that the function R defined in (2) can be written as

$$R(w) = \overline{T} \circ r \circ T^{-1}(w), \tag{3}$$

where $w = T(z) = \frac{1}{z}$ is a Möbius transformation. More generally, we say that for a rational function $r(z)$ and any given Möbius transformation $T(z)$, a function $R(w)$ of the form (3) is a *co-conjugate* of $r(z)$. Here $\overline{T}(z)$ denotes the Möbius transformation obtained from $T(z)$ by conjugating all the coefficients. Co-conjugates maintain the number and sense of zeros of $r(z) - \overline{z}$, as we show next.

Proposition 2.1. *Let $r(z)$ be rational and of degree $n \geq 1$, and let $T(z) = \frac{az+b}{cz+d}$ be a Möbius transformation. Then $R(w) = \overline{T} \circ r \circ T^{-1}(w)$ is a rational function of degree n and we have:*

1. *$r(z) = \overline{z}$ if and only if $R(w) = \overline{w}$, for all $z \in \mathbb{C}$ with $w = T(z) \neq \infty$. In that case, if $r(z) = \overline{z}$, we have $|r'(z)| = |R'(w)|$.*
2. *Writing $r = \frac{p}{q}$ with $p(z) = \sum_{k=0}^{n} p_k z^k$ and $q(z) = \sum_{k=0}^{n} q_k z^k$, R has the representation*

$$R(w) = \frac{\sum_{k=0}^{n} (\overline{a} p_k + \overline{b} q_k)(dw - b)^k (a - cw)^{n-k}}{\sum_{k=0}^{n} (\overline{c} p_k + \overline{d} q_k)(dw - b)^k (a - cw)^{n-k}}. \tag{4}$$

Proof. The degree of R can be seen from the degree formula $\deg(r \circ s) = \deg(r) \deg(s)$ for non-constant rational functions; see [3, p. 32]. The first claim can be seen from the computations

$$r(z) = \overline{z} \Leftrightarrow (\overline{T} \circ r)(z) = \overline{T}(\overline{z}) = \overline{T(z)} \Leftrightarrow R(w) = \overline{w},$$

and

$$R'(w) = \overline{T}'(r(z)) r'(z) (T^{-1})'(w) = \overline{T}'(\overline{z}) r'(z) \tfrac{1}{T'(z)} = \tfrac{\overline{T'(z)}}{T'(z)} r'(z).$$

For the second claim, note that $T^{-1}(w) = \frac{dw-b}{a-cw}$, so that we have

$$r(T^{-1}(w)) = \frac{\sum_{k=0}^{n} p_k (dw - b)^k (a - cw)^{n-k}}{\sum_{k=0}^{n} q_k (dw - b)^k (a - cw)^{n-k}},$$

from which we see that $R(w) = \overline{T}(r(T^{-1}(w)))$ has the form (4). □

In our proof of Theorem 1.1 we also need the winding of a complex function along a curve, and indices of zeros and poles of harmonic functions (sometimes called order, or multiplicity). Here we only give the most relevant definitions. A compact summary of these concepts is given in [10, Section 2], see also [2] and [11, p. 29] (where the winding is called "degree").

Let Γ be a rectifiable curve with parametrization $\gamma : [a, b] \to \Gamma$. Let $f : \Gamma \to \mathbb{C}$ be a continuous function with no zeros on Γ. Let $\arg f(z)$ denote a continuous branch of the argument of f on Γ. The *winding* (or *rotation*) *of $f(z)$ on the curve* Γ is defined as

$$V(f; \Gamma) := \tfrac{1}{2\pi} (\arg f(\gamma(b)) - \arg f(\gamma(a)))$$

The winding is independent of the choice of the branch of $\arg f(z)$. Let z_0 be a zero or pole of $f(z) = r(z) - \overline{z}$. Denote by Γ a circle around z_0 not containing any further zeros or poles of f. Then the *Poincaré index* of f at z_0 is defined as

$$\operatorname{ind}(z_0; f) := V(f; \Gamma).$$

The Poincaré index is independent of the choice of Γ.

Moreover, we will use the following results in our proof.

Proposition 2.2 ([10, Proposition 2.7])**.** *Let $f(z) = r(z) - \overline{z}$ be a rational harmonic function with $\deg(r) \geq 2$. The indices of f at z_0 can be summarized as follows:*

1. *If z_0 is a sense-preserving zero of f, then $\operatorname{ind}(z_0; f) = 1$.*
2. *If z_0 is a sense-reversing zero of f, then $\operatorname{ind}(z_0; f) = -1$.*
3. *If z_0 is a pole of r of order m, then $\operatorname{ind}(z_0; f) = -m$.*

Proposition 2.3 ([5, Proposition 1])**.** *A rational harmonic function $f(z) = r(z) - \overline{z}$ of degree $n \geq 2$ has at most $2(n-1)$ sense-reversing or singular zeros.*

Lemma 2.4 ([5, Lemma])**.** *If r is rational and of degree at least 2, then the set of complex numbers c for which $r - c$ is regular, is open and dense in $\mathbb{C}$.*

A useful application of the preceeding "density lemma" emerges when combined with the continuity of the non-singular zeros of harmonic functions. In the following we call f sense-preserving on an open subset U, if $|r'(z)| > 1$ for all $z \in U$ (similarly for sense-reversing).

Lemma 2.5. *Let $f(z) = r(z) - \overline{z}$ with $\deg(r) \geq 2$. Then for every sufficiently small $\varepsilon > 0$ there exists $\delta > 0$ such such that for $|c| < \delta$ holds: For every sense-preserving zero z_0 of f, the perturbed function $f - c$ has exactly one zero z_0' in $\{z : |z - z_0| < \varepsilon\}$, which is again sense-preserving. The same applies to sense-reversing zeros.*

In particular the function $f - c$ has at least as many sense-preserving (and sense-reversing) zeros as f.

Proof. Let $\Omega_+ = \{z : |r'(z)| > 1\}$ be the set where f is sense-preserving. Denote the sense-preserving zeros of f by $z_1, \ldots, z_{n_+}$. Let $\varepsilon > 0$ be sufficiently small such that

1. all disks $\{z : |z - z_j| \leq \varepsilon\}$ are mutually disjoint and contained in Ω_+,
2. f has no zero or pole in each $\{z : 0 < |z - z_j| \leq \varepsilon\}$. (This is possible, since the zeros and poles of f are isolated.)

Fix $j \in \{1, \ldots, n_+\}$. Set $\gamma_j = \{z : |z - z_j| = \varepsilon\}$ and let $\delta_j = \min_{z \in \gamma_j} |f(z)| > 0$. Then, for any $|c| < \delta_j$ we have

$$|f - (f - c)| = |c| < \delta_j \leq |f| + |f - c| \quad \text{on } \gamma_j.$$

Rouché's theorem shows $V(f-c;\gamma_j) = V(f;\gamma_j) = +1$, so $f-c$ (again sense-preserving on Ω_+) has exactly one sense-preserving zero interior to γ_j (Proposition 2.2 combined with the argument principle [4]). The same applies to sense-reversing zeros (by considering the set $\Omega_- = \{z : |r'(z)| < 1\}$). Taking δ as the minimum of all δ_j completes the proof. □

Proof of Theorem 1.1. Let us denote

$$r = \tfrac{p}{q}, \quad p(z) = \sum_{k=0}^{n} p_k z^k, \quad q(z) = \sum_{k=0}^{n} q_k z^k,$$

and let n_+, n_0, n_- be the number of sense-preserving, singular, sense-reversing zeros of f, respectively. Sometimes we make the dependence on f explicit by writing $n_+(f)$ etc.

By Proposition 2.3, $n_{-,0} := n_- + n_0 \le 2(n-1)$. It therefore remains to show that $n_+ \le 3(n-1)$ and to show that f has at most $5(n-1)-1$ zeros when $\deg(p) > \deg(q)$. We divide the proof in four steps.

Step 1: Let r be regular with $\deg(p) \le \deg(q) = n$, so the number of singular zeros is $n_0 = 0$. Let γ be a circle containing all zeros and poles of f. In this case, since r is bounded for $z \to \infty$, we have

$$|\overline{z} - f(z)| = |r(z)| \le C < |\overline{z}| + |f(z)|, \quad z \in \gamma,$$

provided that γ is sufficiently large. Rouché's theorem [10, Theorem 2.3] implies $V(f;\gamma) = V(\overline{z};\gamma) = -1$. Applying the argument principle for complex-valued harmonic functions yields

$$-1 = V(f;\gamma) = \sum_{z_j : f(z_j)=0} \operatorname{ind}(z_j; f) + \sum_{z_j : q(z_j)=0} \operatorname{ind}(z_j; f) = n_+ - n_- - n,$$

where we used Proposition 2.2. In particular, the sum of the orders of the poles of f is equal to $\deg(q) = n$. By Proposition 2.3 we have $n_- \le 2(n-1)$. Thus,

$$n_+ = n - 1 + n_- \le n - 1 + 2(n-1) = 3(n-1).$$

Step 2: Let $\deg(p) \le \deg(q) = n$. If r is regular, we are done by Step 1, so assume that r is not regular. By Lemma 2.4 there exists a sequence $c_k \in \mathbb{C}$ such that $r_k(z) := r(z) - c_k$ are regular and $c_k \to 0$. Then r_k satisfies the conditions of Step 1 and, setting $f_k(z) := r_k(z) - \overline{z}$, we have $n_+(f_k) \le 3(n-1)$ by Step 1. For sufficiently small $|c_k|$, Lemma 2.5 shows that the function $f_k = f - c_k$ has at least as many sense-preserving zeros as f, that is, $n_+(f) \le n_+(f_k) \le 3(n-1)$.

Step 3: Let $n = \deg(p) > \deg(q)$ and $p(0) \ne 0$. In this case we have $p_n \ne 0$, $p_0 \ne 0$ and $q_n = 0$. Let $w = T(z) = \frac{1}{z}$, then

$$R(w) = \overline{T} \circ r \circ T^{-1}(w) = \tfrac{1}{r(\frac{1}{w})} = \frac{\sum_{k=0}^{n} q_k w^{n-k}}{\sum_{k=0}^{n} p_k w^{n-k}},$$

which can be seen from (4). Since $p_0 \neq 0$, we see that $F(w) = R(w) - \overline{w}$ satisfies the conditions in Step 2. Thus, $n_+(F) \leq 3(n-1)$ and $n_{-,0}(F) \leq 2(n-1)$.

Since $f(0) = \frac{p(0)}{q(0)} \neq 0$, every zero z_j of f gives rise to a zero $w_j = T(z_j)$ of F, and every zero $0 \neq w_j$ of F corresponds to a zero $z_j = \frac{1}{w_j}$ of f; see Proposition 2.1. Since the senses of the zeros are preserved under the co-conjugation with T, we find

$$n_+(f) \leq n_+(F) \leq 3(n-1) \quad \text{and} \quad n_{-,0}(f) \leq n_{-,0}(F) \leq 2(n-1).$$

Notice that $F(0) = 0$, since $q_n = 0$. This zero of F has no corresponding zero of f, so that f has at most $5(n-1)-1$ zeros.

Step 4: Let $n = \deg(p) > \deg(q)$ and $p(0) = 0$. In that case we have $p_n \neq 0$, $q_n = 0$ and $p_0 = 0$. Let $b \in \mathbb{C}$ satisfy $r(b) \neq \overline{b}$. With the Möbius transformation $T(z) = z - b$ we consider

$$R(w) = \overline{T} \circ r \circ T^{-1}(w) = \frac{\sum_{k=0}^{n}(p_k + -\overline{b}q_k)(w+b)^k}{\sum_{k=0}^{n} q_k(w+b)^k};$$

see Proposition 2.1. The coefficient of w^n in the numerator of R is $p_n - \overline{b}q_n = p_n \neq 0$, and in the denominator it is $q_n = 0$. Further, the constant term of the numerator of R is

$$\sum_{k=0}^{n}(p_k - \overline{b}q_k)b^k = p(b) - \overline{b}q(b) \neq 0,$$

since $r(b) \neq \overline{b}$. Thus $F(w) := R(w) - \overline{w}$ satisfies the conditions in Step 3, so that

$$n_{-,0}(F) \leq 2(n-1) \quad \text{and} \quad n_+(F) \leq 3(n-1),$$

and F has at most $5(n-1)-1$ zeros.

Proposition 2.1 implies that $r(z) = \overline{z}$ if and only if $R(w) = \overline{w}$, where $w = T(z)$. Thus f and F have the same number of zeros, and all corresponding zeros have the same sense (or are singular). Hence $n_{-,0}(f) = n_{-,0}(F) \leq 2(n-1)$ and $n_+(f) = n_+(F) \leq 3(n-1)$, and the total number of zeros of f is bounded by $5(n-1)-1$. □

Remark 2.6. Let $f(z) = \frac{p(z)}{q(z)} - \overline{z}$ with $\deg(p) > \deg(q)$, so that f has at most $5(n-1)-1$ zeros. Then the point ∞ in $\hat{\mathbb{C}}$ can be regarded as the "missing solution" to $r(z) = \overline{z}$. However, the point infinity can *not* be a zero of the function $r(z) - \overline{z}$, see [5, p. 1078].

Remark 2.7. In Step 3 in the above proof, one can infer the type of the zero $w = 0$ of F. In this step $p_n \neq 0$ and $q_n = 0$. We compute

$$R'(w) = \frac{-r'(\frac{1}{w})\frac{-1}{w^2}}{r(\frac{1}{w})^2} = r'(z)\frac{z^2}{r(z)^2} = \frac{(p'(z)q(z) - p(z)q'(z))z^2}{p(z)^2}.$$

Note that z^{2n} is the highest power of z that may occur in both numerator and denominator. The coefficient of z^{2n} in the denominator is p_n^2, and in the numerator it is

$$np_nq_{n-1} - p_nq_{n-1}(n-1) = p_nq_{n-1},$$

which yields

$$R'(0) = \lim_{w\to 0} R'(w) = \lim_{z\to\infty} \tfrac{(p'(z)q(z)-p(z)q'(z))z^2}{p(z)^2} = \tfrac{q_{n-1}}{p_n}.$$

This shows that $w = 0$ may be a sense-preserving, sense-reversing or singular zero of F.

Remark 2.8. Let us briefly discuss how our proof of Theorem 1.1 differs from the original proof of Khavinson & Neumann in [5]. A major ingredient in both proofs is Proposition 2.3, due to Khavinson & Neumann, which bounds the number of sense-reversing and singular zeros. Because of this result it only remains to bound the number of sense-preserving zeros. Here the two main technical challenges are (i) dealing with singular zeros, and (ii) the slightly different behavior of rational functions $f(z) = \frac{p(z)}{q(z)} - \overline{z}$ with $\deg(p) \le \deg(q)$ and $\deg(p) > \deg(q)$. The main difference between the two proofs is the order in which (i) and (ii) are handled. While Khavinson & Neumann first resolve (ii) under the assumption that all zeros are regular, and then apply the density lemma (Lemma 2.4) to resolve (i), our proof first treats the case $\deg(p) \le \deg(q)$, using the density lemma (steps 1 and 2), and then transfers the result to the other case using Proposition 2.1 (steps 3 and 4). By this order we avoid a transformation of variables which may introduce singular zeros at a stage of the proof where this case is not covered.

The bounds in Theorem 1.1 are sharp. If $f(z) = r(z) - \overline{z}$ of degree $n \ge 2$ attains the maximal number of $5(n-1)$ zeros, we call f and r *extremal*. Examples of extremal functions were constructed by Rhie [9]. She considered the function

$$f(z) = \tfrac{z^{n-1}}{z^n - a^n} - \overline{z} \tag{5}$$

which is extremal for degree $n = 2, 3$ for a special value of $a \in (0, 1)$, and the function

$$f(z) = (1-\varepsilon)\tfrac{z^{n-1}}{z^n-a^n} + \tfrac{\varepsilon}{z} - \overline{z} = \tfrac{z^n - \varepsilon a^n}{z^{n+1} - a^n z}, \tag{6}$$

of degree $n+1$ which is extremal for $n \ge 3$, provided that ε is sufficiently small. See [8] for a rigorous analysis of admissible parameters a and ε such that these functions are indeed extremal. Note that the rational function in (6) is a convex combination of the rational function in (5) and a pole located at a zero of (5). This general construction principle for extremal functions has been studied in detail in [10].

A phase portrait (see [13, 12] and [10, Section 4]) of an extremal function of the form (6) with $n = 4$, and $\varepsilon = 0.04$ is shown in Figure 1 (left).

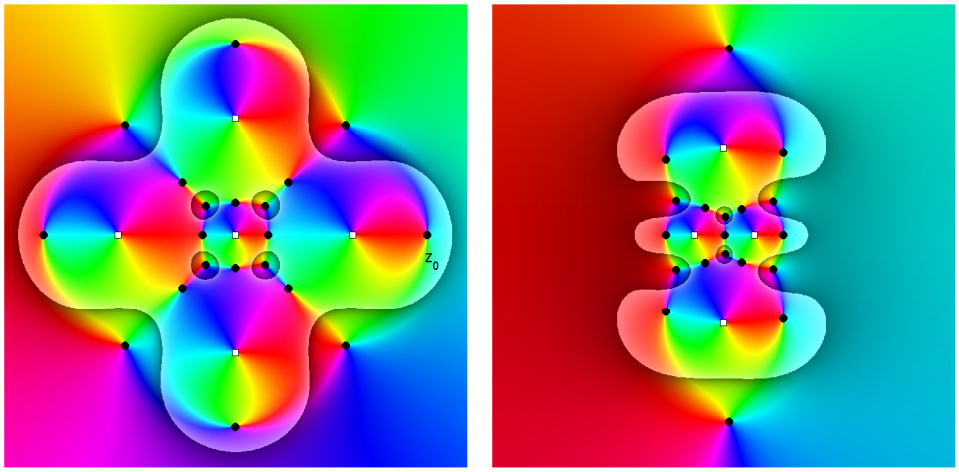

Figure 1: Phase portrais of (6) (left), and of (7) (right). Each image shows a part of the domain of the corresponding function. By indentifying the unit circle with the standard HSV color wheel, each point in the domain is colored according to the phase $e^{i \arg f(z)}$ of the function value at that point (see [12]). The brightened regions indicate the parts of the domain where the function is sense-preserving. Black disks denote zeros, white squares poles. Both functions are of degree five, and have 20 and 19 zeros, respectively, which is the maximum possible number in each case.

We show that for rational functions with $\deg(p) > \deg(q)$ the new bound from Theorem 1.1 is also sharp. Let r be the any of the extremal rational functions from (5) and (6). Let z_0 be any zero of $f(z) = r(z) - \overline{z}$ and consider the co-conjugate of r with $w = T(z) = \frac{1}{z - z_0}$:

$$R(w) = \overline{T} \circ r \circ T^{-1}(w) = \frac{1}{r(\frac{1}{w} + z_0) - \overline{z}_0}.$$

From Proposition 2.1 it is easy to see that the numerator of R has degree $\deg(r)$ and the denominator has degree (at most) $\deg(r) - 1$. Further the zeros of

$$F(w) = R(w) - \overline{w} \tag{7}$$

are exactly the images of the zeros ($\neq z_0$) of $f(z) = r(z) - \overline{z}$, so that F has $5(\deg(R) - 1) - 1$ zeros. Figure 1 (right) illustrates this construction for $n = 4$, where z_0 is the rightmost zero of f in the left phase portrait.

3 Extremal Rational Harmonic Functions are Regular

In this section we will show that functions $f(z) = r(z) - \overline{z}$ that attain the maximum number of zeros as stated in Theorem 1.1 are, surprisingly,

guaranteed to be regular.

Theorem 3.1. *Let $r = \frac{p}{q}$ be a rational function of degree $n \geq 2$ and set $f(z) = r(z) - \overline{z}$. If*
(i) f has $5(n-1)$ zeros, or
(ii) $\deg(p) > \deg(q)$ and f has $5(n-1)-1$ zeros,
then none of the zeros are singular.

Proof. (i) Let $\Omega_+ := \{z : |r'(z)| > 1\}$ be the set where f is sense-preserving. Denote by n_+ the number of zeros of f in Ω_+ and by $n_{-,0}$ the number of zeros of f in $\{z : |r'(z)| \leq 1\}$. Since f has $5(n-1)$ zeros, Theorem 1.1 implies

$$n_+ = 3(n-1), \quad n_{-,0} = 2(n-1).$$

Suppose f has a singular zero z_0. Let $z_1, \ldots, z_{n_+}$ be the $n_+ = 3(n-1)$ zeros of f in Ω_+. Let $\varepsilon > 0$ be such that the disks $\{z : |z - z_j| \leq \varepsilon\}$ do not intersect for $0 \leq j \leq n_+$, and are contained in Ω_+ for $1 \leq j \leq n_+$. By Lemma 2.5 applied to f on Ω_+ there exists $\delta > 0$ such that for all $|c| < \delta$ the function $f - c$ has exactly one zero in each ε-disk $D_\varepsilon(z_j) = \{z : |z - z_j| < \varepsilon\}$, $1 \leq j \leq n_+$.

Now, since $f(z_0) = 0$ and f is continuous near z_0, there exists $0 < \eta \leq \varepsilon$ such that $|f(z)| < \delta$ in $D_\eta(z_0) = \{z : |z - z_0| < \eta\}$. Further, there exists $\zeta \in D_\eta(z_0) \cap \Omega_+$. Indeed, assume the contrary, then $|r'(z)| \leq 1$ in $D_\eta(z_0)$ and $|r'(z_0)| = 1$, which implies that r' is constant by the maximum modulus theorem, a contradiction to $\deg(r) \geq 2$.

Finally, consider the function $F(z) := f(z) - f(\zeta)$. Since $|f(\zeta)| < \delta$, F has exactly one zero in each disk $D_\varepsilon(z_j)$, $1 \leq j \leq n_+$, and further $F(\zeta) = 0$. Thus F has $n_+ + 1 = 3(n-1) + 1$ distinct sense-preserving zeros in Ω_+, in contradiction to Theorem 1.1. Therefore f has no singular zeros.

(ii) We reduce this case to the previous one. Let $b \in \mathbb{C}$ such that $r(b) \neq \overline{b}$, and define the Möbius transformation $w = T(z) = \frac{1}{z-b}$. Consider the co-conjugate $R = \overline{T} \circ r \circ T^{-1}$ and $F(w) = R(w) - \overline{w}$. By Proposition 2.1, all $5(n-1)-1$ zeros of f transform to zeros of F with $|r'(z)| = |R'(w)|$, so that the senses are preserved. Note that none of the zeros of f is mapped to 0 under T. However, (4) and $n = \deg(p) > \deg(q)$ imply $R(0) = \frac{q_n}{p_n} = 0$, so that we have $F(0) = 0$. Thus F has a total number of $5(n-1)$ zeros, none of which is singular by the first part. Hence none of the zeros of f are singular. □

Ackowledgements We would like to thank Dmitry Khavinson for pointing out reference [1] to us. We are grateful to the anonymous referee for the careful reading of the manuscript, and many valuable remarks.

Robert Luce's work is supported by Deutsche Forschungsgemeinschaft, Cluster of Excellence "UniCat".

References

[1] Jin H. An and N. Wyn Evans. The Chang-Refsdal lens revisited. *Monthly Notices of the Royal Astronomical Society*, 369(1):317–334, 2006.

[2] Mark Benevich Balk. *Polyanalytic Functions*. Mathematical Research. 63. Berlin: Akademie-Verlag. 197 p. , 1991.

[3] Alan F. Beardon. *Iteration of rational functions*, volume 132 of *Graduate Texts in Mathematics*. Springer-Verlag, New York, 1991.

[4] Peter Duren, Walter Hengartner, and Richard S. Laugesen. The argument principle for harmonic functions. *Amer. Math. Monthly*, 103(5):411–415, 1996.

[5] Dmitry Khavinson and Genevra Neumann. On the number of zeros of certain rational harmonic functions. *Proc. Amer. Math. Soc.*, 134(4):1077–1085, 2006.

[6] Dmitry Khavinson and Genevra Neumann. From the fundamental theorem of algebra to astrophysics: a "harmonious" path. *Notices Amer. Math. Soc.*, 55(6):666–675, 2008.

[7] Jörg Liesen. When is the adjoint of a matrix a low degree rational function in the matrix? *SIAM J. Matrix Anal. Appl.*, 29(4):1171–1180, 2007.

[8] Robert Luce, Olivier Sète, and Jörg Liesen. Sharp parameter bounds for certain maximal point lenses. *Gen. Relativity Gravitation*, 46(5):46:1736, 2014.

[9] S. H. Rhie. n-point Gravitational Lenses with 5(n-1) Images. *ArXiv Astrophysics e-prints*, May 2003.

[10] Olivier Sète, Robert Luce, and Jörg Liesen. Perturbing rational harmonic functions by poles. *Comput. Methods Funct. Theory*, pages 1–27, 2014.

[11] T. Sheil-Small. *Complex polynomials*, volume 75 of *Cambridge Studies in Advanced Mathematics*. Cambridge University Press, Cambridge, 2002.

[12] Elias Wegert. *Visual complex functions*. Birkhäuser/Springer Basel AG, Basel, 2012.

[13] Elias Wegert and Gunter Semmler. Phase plots of complex functions: a journey in illustration. *Notices Am. Math. Soc.*, 58(6):768–780, 2011.

Perturbing rational harmonic functions by poles*

Olivier Sète† Robert Luce† Jörg Liesen†

Abstract

We study how adding certain poles to rational harmonic functions of the form $R(z) - \overline{z}$, with $R(z)$ rational and of degree $d \geq 2$, affects the number of zeros of the resulting functions. Our results are motivated by and generalize a construction of Rhie derived in the context of gravitational microlensing (arXiv:astro-ph/0305166). Of particular interest is the construction and the behavior of rational functions $R(z)$ that are *extremal* in the sense that $R(z) - \overline{z}$ has the maximal possible number of $5(d-1)$ zeros.

1 Introduction

This work is concerned with the zeros of functions in the complex variable z of the form $R(z) - \overline{z}$, where $R(z)$ is a rational function. The analysis of such rational harmonic functions has received considerable attention in recent years. As nicely explained in the expository article of Khavinson and Neumann [12], they have important applications in gravitational microlensing; see also the survey [18]. In addition they are related to the matrix theory problem of expressing certain adjoints of a diagonalizable matrix as a rational function in the matrix [15].

In the sequel, whenever we write a rational function $R(z) = \frac{p(z)}{q(z)}$, we assume that the polynomials $p(z)$ and $q(z)$ are coprime, i.e., that they have no common zero. Then the *degree* of $R(z)$, denoted by $\deg(R)$, is defined as the maximum of the degrees of $p(z)$ and $q(z)$.

It is easy to see that $R(z) - \overline{z}$ has exactly one zero if $\deg(R) = 0$, and either $0, 1, 2$ or infinitely many zeros (given by all points of a line or a circle in the complex plane) if $\deg(R) = 1$. More interesting is the case $\deg(R) = d \geq 2$, which we consider in this paper. An important result of Khavinson and Neumann states that in this case $R(z) - \overline{z}$ may have at most $5(d-1)$ zeros [11]. Prior to the work of Khavinson and Neumann the

*A final version of this preprint manuscript appeared as follows: O. Sète, R. Luce and J. Liesen. Perturbing rational harmonic functions by poles. *Comput. Methods Funct. Theory* (2015) 15(1), pp. 9–35.

†TU Berlin, Institute of Mathematics, MA 4-5, Straße des 17. Juni 136, 10623 Berlin, Germany (`{sete,luce,liesen}@math.tu-berlin.de`)

astrophysicist Sun Hong Rhie (1955–2013) had constructed, in the context of gravitational lensing, examples of functions $R(z)-\overline{z}$ with exactly $5(d-1)$ zeros for every $d \geq 2$ [19]. Hence the bound of Khavinson and Neumann is sharp for every $d \geq 2$.

Motivated by the result of Khavinson and Neumann we call a rational function $R(z)$ of degree $d \geq 2$ *extremal*, when the function $R(z) - \overline{z}$ has the maximal possible number of $5(d-1)$ zeros. Examples of such extremal rational functions in the published literature are rare. For $d = 2$ an example is given in [11]. The only other published example we are aware of is given by the construction of Rhie [19] and in the closely related works [2, 3]; see also [16]. Rhie's construction served as a motivation for our work, and some of our results can be considered a generalization of her original idea.

To briefly explain this idea, consider the rational harmonic function

$$R_0(z) - \overline{z}, \quad \text{where} \quad R_0(z) = \tfrac{z^{d-1}}{z^d - r^d}$$

and $r > 0$ is a real parameter. For $d = 2$ a straightforward computation shows that $R_0(z)-\overline{z}$ has 5 zeros if $r < 1$, and fewer zeros for $r \geq 1$. Moreover, it was shown in [17] that for $d \geq 3$ the function $R_0(z) - \overline{z}$ has $3d + 1$ zeros if $r < \left(\frac{d-2}{d}\right)^{\frac{1}{2}} \left(\frac{2}{d-2}\right)^{\frac{1}{d}}$, and fewer zeros for larger values of r. Thus, $R_0(z)$ is extremal only for $d = 2$ or $d = 3$ (and when r is small enough). Rhie suggested in [19] to perturb $R_0(z) - \overline{z}$ by adding a pole at one of its zeros, namely at the point $z = 0$. More precisely, she showed that for a particular value $r > 0$ and sufficiently small $\varepsilon > 0$ the rational harmonic function

$$R_\varepsilon(z) - \overline{z}, \quad \text{where} \quad R_\varepsilon(z) = (1-\varepsilon)R_0(z) + \tfrac{\varepsilon}{z}, \tag{1}$$

has $5d$ zeros, so that $R_\varepsilon(z)$ (of degree $d + 1$) is indeed extremal. An elementary proof and sharp bounds on the parameters r and ε that guarantee extremality of $R_\varepsilon(z)$ are given in [16].

A numerical example for Rhie's construction is shown in Figure 1, where we use phase portraits for visualization [23, 22]; see also Section 4 below. Here $d = \deg(R_0) = 7$, and $r > 0$ is chosen sufficiently small. Figure 1(a) shows that $R_0(z)-\overline{z}$ has $3d+1 = 22$ zeros and 7 poles. We choose $\varepsilon = 0.15$, which is sufficiently small in order to obtain an extremal function $R_\varepsilon(z)$, i.e. a function $R_\varepsilon(z) - \overline{z}$ with $5d = 35$ zeros; see Figure 1(b). Two essential observations are to be made when comparing Figures 1(a) and 1(b):

(1) The zero of $R_0(z) - \overline{z}$ at the perturbation point $z = 0$ becomes a pole of the perturbed function, but all other zeros of $R_0(z) - \overline{z}$ "survive" the perturbation in the sense that perturbed versions of them are still zeros of $R_\varepsilon(z) - \overline{z}$.

(2) In a neighborhood of the perturbation point $z = 0$ the function $R_\varepsilon(z) - \overline{z}$ has $2d$ additional zeros, which are located on two circles of radius approximately $\sqrt{\varepsilon}$ around $z = 0$. (In Figure 1(b) the two circles are visually almost indistinguishable.)

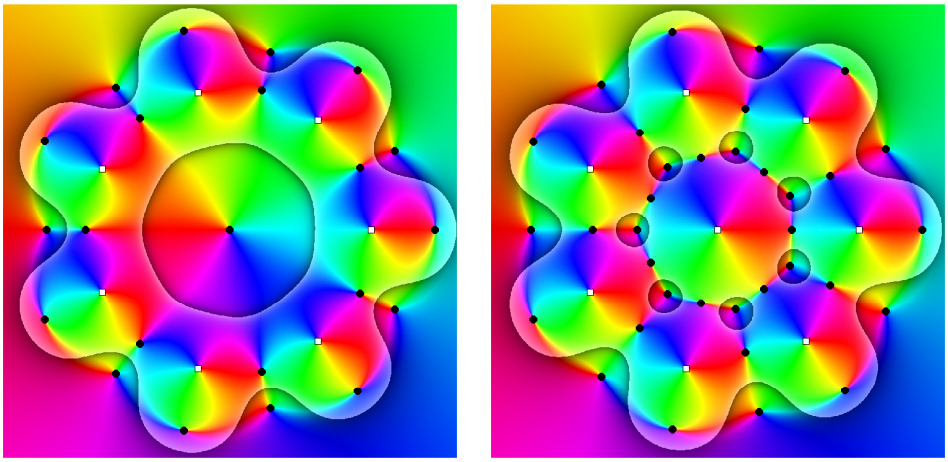

(a) Phase portrait of $R_0(z) - \overline{z}$ (b) Phase portrait of $R_\varepsilon(z) - \overline{z}$

Figure 1: Phase portraits of $R_0(z) - \overline{z}$ and $R_\varepsilon(z) - \overline{z}$. Black disks indicate zeros and white squares show poles.

While the function $R_\varepsilon(z)$ considered by Rhie arises from a convex combination of $R_0(z)$ with the pole $\frac{1}{z}$, it was shown in [16] that qualitatively the same "zero creating effect" can be observed for a purely additive perturbation with $\frac{1}{z}$, resulting in the function $R_0(z) + \frac{\varepsilon}{z} - \overline{z}$. The analyses of this effect draw heavily from the rotational symmetry of $R_0(z)$. Hence it is tempting to regard this effect as a special property of $R_0(z)$.

The main goal of this paper is to prove, however, that *the effect is generic to any rational harmonic function* $R(z) - \overline{z}$, provided that it satisfies certain conditions at the perturbation point. In more details, we show that if $z_0 \in \mathbb{C}$ is a zero of $R(z) - \overline{z}$ and if $n - 1$ is the order of the first non-vanishing derivative of $R(z)$ at z_0, then $R(z) - \overline{z}$ can be perturbed by a pole at z_0 such that the perturbed rational harmonic function has (at least) $2n$ additional zeros in a neighborhood of z_0, while the other zeros of $R(z) - \overline{z}$ "survive" the perturbation. The precise statement of this result is given in Theorem 3.1 below. In order to fully characterize this zero creating effect, perturbations with poles at arbitrary points $z_0 \in \mathbb{C}$ are studied in Theorem 3.14.

Adding poles to rational harmonic functions of the form $R(z) - \overline{z}$ in order to create new zeros has been used, for example, in [2, 4]. However, a complete mathematical characterization of this effect as in this work has not been given before.

We would also like to point out that the conceptually similar problem of constructing extremal harmonic *polynomials* $p(z) - \overline{z} = 0$ appears to be more challenging. A class of examples that realizes the maximal number of zeros $3\deg(p) - 2$ (see [13]) is given by Geyer [8]. Recent progress concerning Wilmshurst's conjecture [24] on the maximal number of zeros for general

harmonic polynomials $p(z) - \overline{q(z)}$ has been reported in [14].

The paper is organized as follows. In Section 2 we review tools from harmonic function theory that we need in our proofs. The major part of Section 3 consists of the proof of Theorem 3.1. We first show that sufficiently many zeros are created in a neighborhood of the perturbation point (Section 3.1), and we then show that the effect of the perturbation is local in the sense that the remaining zeros "survive" the perturbation (Section 3.2). In Section 4 we give several numerical illustrations. In Section 5 we state conclusions and some open questions in the context of our result.

2 Mathematical background

In this section we review the required mathematical background including the winding of continuous functions, the Poincaré index of exceptional points and an argument principle that will allow to "count" zeros of $R(z) - \overline{z}$ in Section 3.

The functions of the form $f(z) = R(z) - \overline{z}$ we consider in this paper are obviously not analytic. They are *harmonic* because for $z = x + iy$ they are twice continuously differentiable with respect to the real variables x and y, and additionally $\frac{\partial^2 f}{\partial x^2} + \frac{\partial^2 f}{\partial y^2} = 0$. In contrast to [6] we make no assumption whether a harmonic function is (locally) bijective or not. Since f is harmonic, it has locally a representation of the form $f = h + \overline{g}$, where h and g are analytic functions. Both h and g are unique up to additive constants; see [7].

Roughly speaking, a harmonic function $h+\overline{g}$ is called sense-preserving if the analytic part h is dominant, and sense-reversing if the co-analytic part $\overline{g}$ dominates. Since the exact definition simplifies for the harmonic functions of our interest, $f(z) = R(z)-\overline{z}$, we give the definition for this case only and refer to [7] and [21] for the general case.

Definition 2.1. Let $f(z) = R(z) - \overline{z}$ and $z_0 \in \mathbb{C}$.

1. If $|R'(z_0)| > 1$, then $f(z)$ is called *sense-preserving* at z_0.
2. If $|R'(z_0)| < 1$, then $f(z)$ is called *sense-reversing* at z_0.
3. If $|R'(z_0)| = 1$, then z_0 is called a *singular point of* $f(z)$.

In either case, if additionally $f(z_0) = 0$, then z_0 is respectively called a *sense-preserving*, *sense-reversing* or *singular zero* of $f(z)$. A zero z_0 of $f(z)$ that is not singular is called *regular*. If all zeros of $f(z)$ are regular, then the functions $f(z)$ and $R(z)$ are called *regular*.

We now turn our attention to the zeros of harmonic functions and their "multiplicity". It is clear that zeros of harmonic functions can, in general, not be "factored out". For example, each $z_0 \in \mathbb{R}$ is a zero of the harmonic function $z - \overline{z}$, but there exists no harmonic function $g(z)$ with $z - \overline{z} = (z-z_0)g(z)$ or $z-\overline{z} = \overline{(z-z_0)}g(z)$. Even if all the zeros are isolated, as it is

the case for harmonic polynomials of the form $p(z)-\overline{z}$ with $\deg(p) > 1$, such decompositions typically do not exist, as the number of zeros may exceed the degree of the polynomial [8, 13]. In order to still "count" zeros, we will use the concept of the Poincaré index, which will be defined below; see Definition 2.4.

In order to define the Poincaré index, we need the following definition of the winding of a continuous function [1]; see also [22, p. 101] and [20, p. 29] (where the winding is called "degree"). Let Γ be a rectifiable curve with parametrization $\gamma : [a, b] \to \Gamma$. Let $f : \Gamma \to \mathbb{C}$ be a continuous function with no zeros on Γ. Let $\Theta(z)$ denote a continuous branch of $\arg f(z)$ on Γ. The *winding* (or *rotation*) *of* $f(z)$ *on the curve* Γ is defined as

$$V(f;\Gamma) := \tfrac{1}{2\pi}(\Theta(\gamma(b)) - \Theta(\gamma(a))) = \tfrac{1}{2\pi}\Delta_\Gamma \arg f(z).$$

The winding is independent of the choice of the branch of $\arg f(z)$. The next proposition collects elementary properties of the winding.

Proposition 2.2 (see [1, p. 37] or [20, p. 29])**.** *Let* Γ *be a rectifiable curve, and let* $f(z)$ *and* $g(z)$ *be continuous and nonzero functions on* Γ*.*

1. *If* Γ *is a closed curve, then* $V(f;\Gamma)$ *is an integer.*
2. *If* Γ *is a closed curve and if there exists a continuous and single-valued branch of the argument on* $f(\Gamma)$*, then* $V(f;\Gamma) = 0$*.*
3. *We have* $V(fg;\Gamma) = V(f;\Gamma) + V(g;\Gamma)$*.*
4. *If* $f(z) = c \neq 0$ *is constant on* Γ*, then* $V(f;\Gamma) = 0$*.*

The next result is a version of Rouché's theorem that is somewhat stronger than the classical one; see [1, p. 37]. Its formulation for analytic functions is due to Glicksberg [9]; see also [5]. We give a short proof for our more general setting.

Theorem 2.3 (Rouché's theorem)**.** *Let* Γ *be a rectifiable closed curve, and let* $f(z)$ *and* $g(z)$ *be two continuous functions on* Γ*. If*

$$|f(z) + g(z)| < |f(z)| + |g(z)|, \quad z \in \Gamma, \tag{2}$$

then $f(z)$ *and* $g(z)$ *have the same winding on* Γ*, i.e.* $V(f;\Gamma) = V(g;\Gamma)$*.*

Proof. Note first that (2) implies that $f(z)$ and $g(z)$ are nonzero on Γ. For $z \in \Gamma$, the inequality (2) yields $|\frac{f(z)}{g(z)} + 1| < |\frac{f(z)}{g(z)}| + 1$, hence $\frac{f(z)}{g(z)} \in \mathbb{C}\backslash[0, \infty[$. Thus $V(\frac{f}{g};\Gamma) = 0$ since there is a continuous single-valued argument function on $\mathbb{C}\backslash[0, \infty[$. Using Proposition 2.2 we find $V(f;\Gamma) = V(g\frac{f}{g};\Gamma) = V(g;\Gamma) + V(\frac{f}{g};\Gamma) = V(g;\Gamma)$. □

Definition 2.4. Let the function $f(z)$ be continuous and different from zero in a punctured neighborhood D of the point z_0. If $f(z)$ is either zero, not continuous, or not defined at z_0, then the point z_0 is called an *isolated exceptional point* of $f(z)$. The *Poincaré index* of the (isolated) exceptional point z_0 of the function $f(z)$ is defined as

$$\operatorname{ind}(z_0; f) := V(f; \gamma) = \tfrac{1}{2\pi}\Delta_\gamma \arg f(z) \in \mathbb{Z},$$

where γ is an arbitrary closed Jordan curve in D surrounding z_0.

The Poincaré index is independent of the choice of γ; see [1], where exceptional points are called *critical points*. In [20, p. 44] the Poincaré index is called the "multiplicity of f at z_0". It is a generalization of the multiplicity of a zero and pole of a meromorphic function, as is shown in the next example.

Example 2.5. *Let $f(z)$ be a meromorphic function. The only isolated exceptional points of $f(z)$ are its zeros and poles. Suppose $f(z) = (z-z_0)^m g(z)$ holds in some neighborhood of z_0, where $g(z)$ is analytic and nonzero in this neighborhood, and $m \in \mathbb{Z}$. Then, for a sufficiently small circle γ around z_0 lying in this neighborhood, Proposition 2.2 yields*

$$\operatorname{ind}(z_0; f) = V(f; \gamma) = V((z - z_0)^m g(z); \gamma) = mV(z - z_0; \gamma) + V(g; \gamma) = m.$$

Thus, for a zero of $f(z)$ ($m > 0$) the Poincaré index is the multiplicity of the zero, and for a pole ($m < 0$) it is (minus) the order of the pole.

With the Poincaré index, an argument principle for continuous functions with a finite number of exceptional points can be proven; see [1, p. 39] for the version below, or [20, p. 44].

Theorem 2.6. *Let Γ be a closed Jordan curve. Let $f(z)$ be continuous on and interior to Γ, except possibly for finitely many exceptional points $z_1, z_2, \ldots, z_k$ in the interior of Γ. Then*

$$\tfrac{1}{2\pi}\Delta_\Gamma \arg f(z) = V(f; \Gamma) = \operatorname{ind}(z_1; f) + \operatorname{ind}(z_2; f) + \ldots + \operatorname{ind}(z_k; f).$$

This "abstract argument principle" includes as special cases the argument principle for meromorphic functions (see Example 2.5), and the argument principles for harmonic functions [7] and for harmonic functions with poles [21, Theorems 2.2 and 2.3].

We end this section with a discussion of the exceptional points and their Poincaré indices of $f(z) = R(z) - \overline{z}$, where $\deg(R) \geq 2$. The exceptional points of $f(z)$ are its zeros and its poles. The function $f(z)$ has a pole of order m at z_0, if z_0 is a pole of order m of $R(z)$. The assumption $\deg(R) \geq 2$ implies that $f(z)$ has at most $5(\deg(R) - 1)$ zeros (cf. the Introduction).

Hence all exceptional points of $f(z)$ are isolated and thus have a Poincaré index.

The Poincaré index of a regular zero of a general harmonic function can be read off the power series of its analytic and co-analytic parts. This characterization was implicitly obtained in [7]. Under certain conditions the Poincaré index of a pole can be determined in a similar way [21]. Using [7, p. 412], Lemma 2.2 and the argument principle in [21], we obtain the following characterization for rational harmonic functions of the form $f(z) = R(z) - \overline{z}$.

Proposition 2.7. *Let $f(z) = R(z) - \overline{z}$ with $\deg(R) \geq 2$.*

1. *A sense-preserving zero of $f(z)$ has Poincaré index $+1$ and a sense-reversing zero of $f(z)$ has Poincaré index -1.*
2. *If z_0 is a pole of $R(z)$ of order m, then $f(z)$ is sense-preserving in a neighborhood of z_0 and has Poincaré index $-m$ at z_0.*

3 Creating zeros by adding poles

In Theorem 3.1, the main result of this paper, we generalize Rhie's construction as outlined in the Introduction. In short, the effect of an additive perturbation with a pole at a point z_0 where $R(z) - \overline{z}$ has a sense-reversing zero at which some derivatives of $R(z)$ vanish, can be roughly summarized as follows: New zeros appear "close to z_0", and existing zeros of $R(z) - \overline{z}$ "away from z_0" do not disappear.

We denote by $D(z, r)$ and $\overline{D}(z, r)$ the open and the closed disks around $z \in \mathbb{C}$ with radius $r > 0$, respectively. The open and closed annuli of radii $r > 0$ and $s > 0$ around $z \in \mathbb{C}$ are denoted by $A(z, r, s)$ and $\overline{A}(z, r, s)$, respectively.

Theorem 3.1. *Let $f(z) = R(z) - \overline{z}$ with $\deg(R) \geq 2$ satisfy $\lim_{z\to\infty} f(z) = \infty$. Further, let $z_0 \in \mathbb{C}$ and the integer $n \geq 3$ satisfy*

$$f(z_0) = 0, \quad R'(z_0) = \ldots = R^{(n-2)}(z_0) = 0, \quad \text{and} \quad R^{(n-1)}(z_0) \neq 0, \quad (3)$$

and set $\eta := (\frac{n}{n-1})^{\frac{1}{2}}$. Then, for sufficiently small $\varepsilon > 0$, the disk $\overline{D}(z_0, \eta\sqrt{\varepsilon})$ contains no further zero of $f(z)$ and the function

$$F(z) := f(z) + \tfrac{\varepsilon}{z - z_0}$$

satisfies the following:

(i) $F(z)$ has at least n zeros in $A(z_0, \eta^{-1}\sqrt{\varepsilon}, \sqrt{\varepsilon})$, at least n zeros in $A(z_0, \sqrt{\varepsilon}, \eta\sqrt{\varepsilon})$, and no zeros in $\overline{D}(z_0, \eta^{-1}\sqrt{\varepsilon})$. If $F(z)$ is regular, then at least n of its zeros in $A(z_0, \eta^{-1}\sqrt{\varepsilon}, \sqrt{\varepsilon})$ are sense-preserving and at least n of its zeros in $A(z_0, \sqrt{\varepsilon}, \eta\sqrt{\varepsilon})$ are sense-reversing.

(ii) Denote the regular zeros of $f(z)$ outside $\overline{D}(z_0, \eta\sqrt{\varepsilon})$ by $z_1, \ldots, z_N$. Then there exist mutually disjoint disks $\overline{D}(z_k, r)$ such that $F(z)$ has exactly one zero in each $D(z_k, r)$, and the index of this zero is $\operatorname{ind}(z_k; f)$.

(iii) If $f(z)$ is regular, then $f(z)$ and $F(z)$ have the same number of zeros outside $\overline{D}(z_0, \eta\sqrt{\varepsilon})$.

The proof of this result will be given in two parts, spanning the Sections 3.1 and 3.2. First we will give several remarks on the technical conditions on $f(z)$ and $F(z)$ we impose in this theorem.

Remark 3.2.
1. The condition that $\lim_{z\to\infty} f(z) = \infty$ is rather nonrestrictive. First note that if $f(z)$ has a limit for $z \to \infty$, this limit is ∞. Further, $f(z)$ has no limit for $z \to \infty$ only when $R(z) = a_1 z + \frac{p(z)}{q(z)}$, with $|a_1| = 1$ and $\deg(p) \leq \deg(q)$. For all other $R(z)$, the limit $\lim_{z\to\infty} f(z)$ exists.
2. As shown in [11, p. 1081], the set of regular rational functions is dense in the space of all rational functions with respect to the supremum norm on the Riemann sphere. Hence, restricting $f(z)$ to be regular in *(iii)* is a very mild condition.
3. However, the effects of a perturbation on a non-regular function $f(z)$ can be quite unpleasant: Zeros of $f(z)$ far away from z_0 can vanish or additional zeros may appear. This is why the regularity assumptions in *(ii)* and *(iii)* are necessary.

In particular, Theorem 3.1 can be used to explain the maximality of Rhie's construction for a gravitational point lens, which we briefly discussed in the introduction. This is the content of the following Corollary; see also Section 4.1 and Figure 1.

Corollary 3.3. *Under the assumptions of Theorem 3.1, suppose that $f(z) = R(z) - \overline{z}$ is regular and has $3n + 1$ zeros, and that* $\deg(R) = n$. *Then, for sufficiently small $\varepsilon > 0$, the function $R(z) + \frac{\varepsilon}{z - z_0}$ is extremal.*

Proof. By Theorem 3.1 the function $F(z) = R(z) + \frac{\varepsilon}{z-z_0} - \overline{z}$ with sufficiently small $\varepsilon > 0$ has at least $2n$ zeros inside $A(z_0, \eta^{-1}\sqrt{\varepsilon}, \eta\sqrt{\varepsilon})$ (cf. item *(i)*) and exactly $3n$ zeros outside $\overline{D}(z_0, \eta\sqrt{\varepsilon})$ (cf. item *(iii)*). Since $F(z)$ may have at most $5n$ zeros, it in fact has exactly $5n$ zeros, so that $R(z) + \frac{\varepsilon}{z-z_0}$ is extremal. □

In the following Section 3.1 we prove part *(i)* of Theorem 3.1. The proof of parts *(ii)* and *(iii)* are the content of Section 3.2. Finally, in Section 3.3, we analyze the effect of a perturbation with a pole at points z_0 that do not satisfy the assumptions of Theorem 3.1.

3.1 Behavior near z_0 (Proof of *(i)* in Theorem 3.1)

The idea of our proof is the following: We approximate $F(z)$ by a truncation of the Laurent series of the analytic part of $F(z)$, and we show that this approximation has $2n$ zeros near z_0 that carry over to zeros of $F(z)$, provided ε is sufficiently small.

Let

$$R(z) = \sum_{k=0}^{\infty} \frac{R^{(k)}(z_0)}{k!}(z - z_0)^k$$

be the series expansion of $R(z)$ at z_0 (convergent in some suitable disk around z_0). For the moment, consider any $\varepsilon > 0$. We will specify below when ε is "sufficiently small". Using (3) we can write

$$\begin{aligned} F(z) &= R(z) + \tfrac{\varepsilon}{z-z_0} - \overline{z} \\ &= \tfrac{R^{(n-1)}(z_0)}{(n-1)!}(z - z_0)^{n-1} + \sum_{k=n}^{\infty} \tfrac{R^{(k)}(z_0)}{k!}(z - z_0)^k + \tfrac{\varepsilon}{z-z_0} - \overline{z - z_0}. \end{aligned}$$

We substitute $w := z - z_0$, so that z_0 is mapped to 0. To simplify notation, we write again $F(w)$ instead of introducing a new notation $\widetilde{F}(w) := F(z)$. In the following we assume that the same substitution has been applied to $R(z)$ and $f(z)$ in order to obtain $R(w)$ and $f(w)$. We set $c := \frac{R^{(n-1)}(0)}{(n-1)!} \neq 0$ and hence obtain

$$F(w) = cw^{n-1} + \sum_{k=n}^{\infty} \frac{R^{(k)}(0)}{k!} w^k + \frac{\varepsilon}{w} - \overline{w}. \tag{4}$$

Consider the function

$$G(w) := cw^{n-1} + \frac{\varepsilon}{w} - \overline{w}, \tag{5}$$

obtained from $F(w)$ by truncation of the series expansion of $R(w)$. The zeros of $G(w)$ are the solutions of the equation

$$cw^n - |w|^2 + \varepsilon = 0. \tag{6}$$

In the following, we will assume without loss of generality that $c > 0$. Indeed, the solutions of (6) with general $c \neq 0$ have the form $e^{-i\frac{\arg(c)}{n}} w$, where w solves $|c|w^n - |w|^2 + \varepsilon = 0$.

The next three lemmata characterize the zeros of $G(w)$. First, we will derive conditions on ε such that $G(w)$ admits a maximal number of zeros (Lemma 3.4). Then, in Lemma 3.5, we derive bounds on the moduli of certain such zeros that will be needed later. The sense of these zeros is determined in Lemma 3.6.

Lemma 3.4. *Let $n \geq 3$, $c > 0$ and $0 < \varepsilon < \varepsilon_* := \frac{n-2}{n}\left(\frac{2}{nc}\right)^{\frac{2}{n-2}}$. Then (6) has exactly $3n$ solutions $\rho_1 e^{i\frac{(2k+1)\pi}{n}}$, $\rho_2 e^{i\frac{2k\pi}{n}}$, $\rho_3 e^{i\frac{2k\pi}{n}}$, $1 \leq k \leq n$, where $\rho_1 < \sqrt{\varepsilon} < \rho_2 < \left(\frac{2}{nc}\right)^{\frac{1}{n-2}} < \rho_3$.*

Proof. Write $w = \rho e^{i\varphi}$ with $\rho > 0$ and $\varphi \in \mathbb{R}$. Equation (6) is equivalent to

$$c\rho^n e^{in\varphi} - \rho^2 + \varepsilon = 0, \quad \text{or} \quad e^{in\varphi} = \tfrac{\rho^2-\varepsilon}{c\rho^n}. \tag{7}$$

Thus $e^{in\varphi}$ is real and we distinguish the two cases $e^{in\varphi} = \pm 1$.

If $e^{in\varphi} = -1$, then $\rho^2 < \varepsilon$, $\varphi = \frac{(2k+1)\pi}{n}$ for some $k \in \mathbb{Z}$, and equation (7) becomes $c\rho^n + \rho^2 - \varepsilon = 0$. By Descartes' rule of signs (see [10, p. 442]), this equation has exactly one positive root, say $\rho_1 < \sqrt{\varepsilon}$.

If $e^{in\varphi} = +1$, then $\rho^2 > \varepsilon$, $\varphi = \frac{2k\pi}{n}$ for some $k \in \mathbb{Z}$, and (7) yields

$$f_+(\rho) := c\rho^n - \rho^2 + \varepsilon = 0.$$

By Descartes' rule of signs $f_+(\rho)$ has 0 or 2 positive roots, counting multiplicities. We derive a necessary and sufficient condition on ε such that $f_+(\rho)$ has two (distinct) positive roots. Since $f_+'(\rho) = nc\rho^{n-1} - 2\rho = \rho(nc\rho^{n-2} - 2)$, the only positive critical point of $f_+(\rho)$ is $\rho = (\frac{2}{nc})^{\frac{1}{n-2}}$. From $f_+(0) = \varepsilon > 0$ and $\lim_{\rho\to\infty} f_+(\rho) = \infty$, we see that $f_+(\rho)$ has two distinct positive roots if and only if $f_+\big((\frac{2}{nc})^{\frac{1}{n-2}}\big) < 0$, which is equivalent to $\varepsilon < \varepsilon_*$. Hence, $f_+(\rho)$ has two distinct positive roots $\sqrt{\varepsilon} < \rho_2 < (\frac{2}{nc})^{\frac{1}{n-2}} < \rho_3$ if and only if $\varepsilon < \varepsilon_*$. □

Lemma 3.5. *In the notation of Lemma 3.4, if*

$$0 < \varepsilon < \min\big\{\varepsilon_*,\ (\tfrac{1}{nc})^{\frac{2}{n-2}}(\tfrac{n}{n-1})^{\frac{n}{n-2}},\ (\tfrac{1}{c(n-1)})^{\frac{2}{n-2}}(\tfrac{n-1}{n})^{\frac{n}{n-2}}\big\}, \tag{8}$$

then $G(w)$ has $3n$ zeros, and we have

$$\eta^{-1}\sqrt{\varepsilon} < \rho_1 < \sqrt{\varepsilon} < \rho_2 < \eta\sqrt{\varepsilon}, \quad \textit{where } \eta := (\tfrac{n}{n-1})^{\frac{1}{2}}.$$

Proof. Recall that ρ_1 is the positive root of $f_-(\rho) := c\rho^n + \rho^2 - \varepsilon$. Note that $f_-(\sqrt{\varepsilon}) > 0$. We then have $(\frac{n-1}{n})^{\frac{1}{2}}\sqrt{\varepsilon} < \rho_1 < \sqrt{\varepsilon}$, if

$$f_-\Big((\tfrac{n-1}{n})^{\frac{1}{2}}\sqrt{\varepsilon}\Big) = c(\tfrac{n-1}{n})^{\frac{n}{2}}\varepsilon^{\frac{n}{2}} + \tfrac{n-1}{n}\varepsilon - \varepsilon = c(\tfrac{n-1}{n})^{\frac{n}{2}}\varepsilon^{\frac{n}{2}} - \tfrac{1}{n}\varepsilon < 0,$$

which holds if and only if $\varepsilon < (\frac{1}{nc})^{\frac{2}{n-2}}(\frac{n}{n-1})^{\frac{n}{n-2}}$. To derive the bound for ρ_2, the smaller positive root of $f_+(\rho) := c\rho^n - \rho^2 + \varepsilon$, note first that $f_+(\sqrt{\varepsilon}) = c\sqrt{\varepsilon}^n > 0$. We then have $\sqrt{\varepsilon} < \rho_2 < (\frac{n}{n-1})^{\frac{1}{2}}\sqrt{\varepsilon}$, if

$$f_+\big((\tfrac{n}{n-1})^{\frac{1}{2}}\sqrt{\varepsilon}\big) = c(\tfrac{n}{n-1})^{\frac{n}{2}}\varepsilon^{\frac{n}{2}} - \tfrac{n}{n-1}\varepsilon + \varepsilon = c(\tfrac{n}{n-1})^{\frac{n}{2}}\varepsilon^{\frac{n}{2}} - \tfrac{1}{n-1}\varepsilon < 0,$$

which holds if and only if $\varepsilon < (\frac{1}{c(n-1)})^{\frac{2}{n-2}}(\frac{n-1}{n})^{\frac{n}{n-2}}$. □

Lemma 3.6. *Let $\varepsilon > 0$ satisfy condition (8). Then $G(w)$ in (5) is sense-preserving at its zeros $\rho_1 e^{i\frac{(2k+1)\pi}{n}}$ and sense-reversing at its zeros $\rho_2 e^{i\frac{2k\pi}{n}}$, $1 \le k \le n$.*

Proof. We verify directly Definition 2.1 for both types of zeros. For ease of notation we denote the analytic part of $G(w)$ by $R_G(w) := cw^{n-1} + \frac{\varepsilon}{w}$. We have

$$R_G'(w) = (n-1)cw^{n-2} - \tfrac{\varepsilon}{w^2} = \tfrac{1}{w^2}((n-1)cw^n - \varepsilon).$$

Any zero w' of $G(w)$ is a solution of (6), thus satisfying $c(w')^n = |w'|^2 - \varepsilon$, so that

$$R_G'(w') = \tfrac{1}{(w')^2}((n-1)|w'|^2 - (n-1)\varepsilon - \varepsilon) = \tfrac{1}{(w')^2}((n-1)|w'|^2 - n\varepsilon)$$

and

$$|R_G'(w')| = |(n-1) - n\tfrac{\varepsilon}{|w'|^2}|.$$

Since ε satisfies (8), we have $\rho_1^2 < \varepsilon < \rho_2^2 < \frac{n}{n-1}\varepsilon$, see Lemma 3.5, which implies

$$(n-1) - n\tfrac{\varepsilon}{\rho_1^2} < (n-1) - n\tfrac{\varepsilon}{\rho_2^2} < (n-1) - n\tfrac{n-1}{n} = 0.$$

Then

$$|R_G'(\rho_1 e^{i\frac{(2k+1)\pi}{n}})| = n\tfrac{\varepsilon}{\rho_1^2} - (n-1) > n - (n-1) = 1,$$

which shows that $G(w)$ is sense-preserving at the zeros $\rho_1 e^{i\frac{(2k+1)\pi}{n}}$, and

$$|R_G'(\rho_2 e^{i\frac{2k\pi}{n}})| = n\tfrac{\varepsilon}{\rho_2^2} - (n-1) < n - (n-1) = 1,$$

which shows that $G(w)$ is sense-reversing at the zeros $\rho_2 e^{i\frac{2k\pi}{n}}$. □

The preceding lemma concludes the discussion of the zeros of $G(w)$. In the following main result of this section we prove *(i)* of Theorem 3.1. We will show that the zeros $\rho_1 e^{i\frac{(2k+1)\pi}{n}}$ and $\rho_2 e^{i\frac{2k\pi}{n}}$ of $G(w)$ give rise to zeros of $F(w)$.

Theorem 3.7. *Let $n \geq 3$ and $c > 0$ and set $\eta := (\frac{n}{n-1})^{\frac{1}{2}}$. Then, for all sufficiently small $\varepsilon > 0$, the function $F(w)$ in (4) has at least n zeros in $A(0, \eta^{-1}\sqrt{\varepsilon}, \sqrt{\varepsilon})$, at least n zeros in $A(0, \sqrt{\varepsilon}, \eta\sqrt{\varepsilon})$, and no zeros in $\overline{D}(0, \eta^{-1}\sqrt{\varepsilon})$. If $F(w)$ is regular, then at least n of its zeros in $A(0, \eta^{-1}\sqrt{\varepsilon}, \sqrt{\varepsilon})$ are sense-preserving and at least n of its zeros in $A(0, \sqrt{\varepsilon}, \eta\sqrt{\varepsilon})$ are sense-reversing.*

Proof. Let ε satisfy (8), so that in particular $G(w)$ in (5) has $3n$ zeros. We will show that the $2n$ zeros of $G(w)$ discussed in Lemma 3.6 give rise to $2n$ zeros of $F(w)$.

Consider a sense-preserving zero $w_+ = \rho_1 e^{i\frac{(2k+1)\pi}{n}}$ of $G(w)$. Then from Lemma 3.5 we have $\eta^{-1}\sqrt{\varepsilon} < |w_+| < \sqrt{\varepsilon}$. In particular, w_+ is the *only* exceptional point of $G(w)$ in the annular sector defined by the two radii $\eta^{-1}\sqrt{\varepsilon}$ and $\sqrt{\varepsilon}$, and the two half-lines $\arg(w) = \frac{2k\pi}{n}$ and $\arg(w) = \frac{(2k+2)\pi}{n}$;

see Figure 2(a). Let $\Gamma^+ = [\Gamma_1^+, \Gamma_2^+, \Gamma_3^+, \Gamma_4^+]$ be the boundary curve of this annular sector as indicated in Figure 2(a). Since $G(w)$ is sense-preserving at w_+ (see Lemma 3.6), we know that $V(G;\Gamma^+) = +1$ and we will show next that $V(F;\Gamma^+) = +1$.

In order to apply Rouché's theorem (Theorem 2.3), we will show that

$$|F(w) - G(w)| < |F(w)| + |G(w)|, \quad w \in \Gamma^+. \tag{9}$$

From (4) and (5), we see that inside a disk around $w = 0$ contained in the domain of convergence of the series of $R(w)$ we have $|F(w)-G(w)| \le M|w|^n$, for some $M > 0$ independent of ε. Hence, for sufficiently small $\varepsilon > 0$, Γ^+ is inside this disk. Thus, it suffices to show that $|G(w)| > M|w|^n$ on the arcs that compose Γ^+ (trivially, $|F(w)| + |G(w)| \ge |G(w)|$).

For $w \in \Gamma_1^+$ we have $|w| = \sqrt{\varepsilon}$, so that for sufficiently small $\varepsilon > 0$,

$$|G(w)| = |w|^{-1}|cw^n + \varepsilon - |w|^2| = c\sqrt{\varepsilon}^{n-1} > M\sqrt{\varepsilon}^n = M|w|^n. \tag{10}$$

For $w \in \Gamma_2^+$ or $w \in \Gamma_4^+$ we have $w^n = |w|^n$ and $\eta^{-1}\sqrt{\varepsilon} \le |w| \le \sqrt{\varepsilon}$. If $\varepsilon > 0$ is sufficiently small, then

$$\begin{aligned} |G(w)| &= |w|^{-1}|cw^n + \varepsilon - |w|^2| = |w|^{-1}(c|w|^n + \varepsilon - |w|^2) \ge c|w|^{n-1} \\ &\ge c\eta^{-(n-1)}\sqrt{\varepsilon}^{n-1} > M\sqrt{\varepsilon}^n \ge M|w|^n. \end{aligned}$$

For $w \in \Gamma_3^+$ we have $|w| = \eta^{-1}\sqrt{\varepsilon}$, so that for sufficiently small $\varepsilon > 0$,

$$\begin{aligned} |G(w)| &= |w|^{-1}|cw^n + \varepsilon - |w|^2| = |w|^{-1}|cw^n + (1-\eta^{-2})\varepsilon| \\ &\ge |w|^{-1}((1-\eta^{-2})\varepsilon - c|w|^n) \ge \tfrac{1-\eta^{-2}}{\eta^{-1}}\sqrt{\varepsilon} - c\eta^{-(n-1)}\sqrt{\varepsilon}^{n-1} \\ &> M\eta^{-n}\sqrt{\varepsilon}^n = M|w|^n. \end{aligned} \tag{11}$$

Hence for sufficiently small $\varepsilon > 0$ we find that (9) is satisfied on Γ^+ and thus $V(F;\Gamma^+) = 1$, so $F(w)$ has at least one zero inside this sector (by the argument principle). If $F(w)$ is regular, this zero is sense-preserving. Since $G(w)$ has n zeros of type w_+, $F(w)$ has at least n such zeros in the annulus $A(0, \eta^{-1}\sqrt{\varepsilon}, \sqrt{\varepsilon})$.

We can use exactly the same reasoning as above to show that the sense-reversing zeros $\rho_2 e^{i\frac{2k\pi}{n}}$ of $G(w)$ give zeros of $F(w)$. From Lemma 3.4 and Lemma 3.5 we see that $G(w)$ has n such zeros inside $A(0, \sqrt{\varepsilon}, \eta\sqrt{\varepsilon})$. Now, fix $w_- = \rho_2 e^{i\frac{2k\pi}{n}}$. Consider the boundary curve $\Gamma^- = [\Gamma_1^-, \Gamma_2^-, \Gamma_3^-, \Gamma_4^-]$ of the annular sector defined by the radii $\sqrt{\varepsilon}$ and $\eta\sqrt{\varepsilon}$ and the half-lines $\arg(w) = \frac{(2k-1)\pi}{n}$ and $\arg(w) = \frac{(2k+1)\pi}{n}$ (again, see Figure 2(a)). As before, we show that $|G(w)| > M|w|^n$ on Γ^-.

The arc Γ_3^- has been treated already in (10). For $w \in \Gamma_1^-$ we have $|w| = \eta\sqrt{\varepsilon}$, so that for sufficiently small $\varepsilon > 0$,

$$\begin{aligned} |G(w)| &= |w|^{-1}|cw^n + \varepsilon - |w|^2| = |w|^{-1}|cw^n + (1-\eta^2)\varepsilon| \\ &\ge |w|^{-1}((\eta^2-1)\varepsilon - c|w|^n) \ge \tfrac{\eta^2-1}{\eta}\sqrt{\varepsilon} - c\eta^{n-1}\sqrt{\varepsilon}^{n-1} \\ &> M\eta^n\sqrt{\varepsilon}^n = M|w|^n. \end{aligned} \tag{12}$$

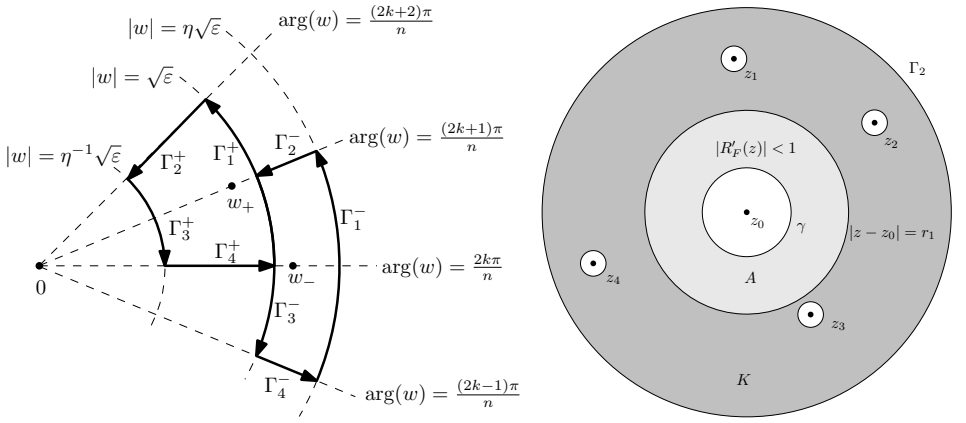

(a) (b) γ denotes the circle $|z - z_0| = \eta\sqrt{\varepsilon}$

Figure 2: Illustrations for the proofs of Theorems 3.7 (left) and 3.13 (right).

For $w \in \Gamma_2^-$ or $w \in \Gamma_4^-$ we have $w^n = -|w|^n$. Using that $\sqrt{\varepsilon} \le |w| \le \eta\sqrt{\varepsilon}$ we compute, for a sufficiently small $\varepsilon > 0$,

$$\begin{aligned}|G(w)| &= |w|^{-1}|cw^n + \varepsilon - |w|^2| = |w|^{-1}|-c|w|^n + \varepsilon - |w|^2| \\ &= |w|^{-1}(c|w|^n + |w|^2 - \varepsilon) \ge c|w|^{n-1} \ge c\sqrt{\varepsilon}^{n-1} > M\eta^n\sqrt{\varepsilon}^n \ge M|w|^n.\end{aligned}$$

As before we can now conclude that $V(F;\Gamma^-) = -1$, so $F(w)$ has at least one zero inside Γ^-, which is sense-reversing if $F(w)$ is regular. In total, n such zeros exist.

In order to complete the proof, let γ denote the circle $|w| = \eta^{-1}\sqrt{\varepsilon}$. From the computation (11) we see that Rouché's theorem applies to $F(w)$ and $G(w)$ on γ. Since $G(w)$ has a simple pole and no zeros inside γ, we obtain $V(F;\gamma) = V(G;\gamma) = -1$.

Let $R_F(w) := R(w) + \frac{\varepsilon}{w}$. For $0 \ne w \in \overline{D}(0, \eta^{-1}\sqrt{\varepsilon})$ we compute

$$|R_F'(w)| = |R'(w) - \tfrac{\varepsilon}{w^2}| \ge \tfrac{\varepsilon}{|w|^2} - |R'(w)| \ge \eta^2 - |R'(w)| > 1$$

for sufficiently small $\varepsilon > 0$, since $R'(0) = 0$. This shows that $F(w)$ is sense-preserving on the disk $\overline{D}(0, \eta^{-1}\sqrt{\varepsilon})$. Since 0 is a simple pole of $F(w)$ with Poincaré index $-1 = V(F;\gamma)$, there are no zeros of $F(w)$ in this disk. □

Remark 3.8. Theorem 3.7 gives a lower bound for $2n$ additional zeros close to 0. However, the proof does not show that there are *exactly* $2n$ such zeros, because the sector enclosed by Γ^+ may contain an open region where $|R_F'(w)| < 1$. In that case there may exist additional pairs of zeros inside this sector so that the total winding of $+1$ is maintained (similarly for Γ^-). We suspect that for sufficiently small $\varepsilon > 0$ exactly $2n$ additional zeros occur; but see also Section 4.2, where more than $2n$ additional zeros occur for somewhat larger ε.

We end this section with a result that follows easily from the proof of Theorem 3.7 and that will be helpful in the proof of Theorem 3.13 below.

Corollary 3.9. *Under the assumptions of Theorem 3.7, we have* $V(F;\gamma) = -1$*, where* γ *is the circle* $|w| = \eta\sqrt{\varepsilon}$*.*

Proof. From (12) we see that Rouché's theorem (Theorem 2.3) applies to $F(w)$ and $G(w)$ on the circle γ. But $G(w)$ has exactly one simple pole, n sense-preserving and n sense-reversing zeros inside γ, so $V(F;\gamma) = V(G;\gamma) = -1$. □

3.2 Behavior away from z_0 (Proof of *(ii)* and *(iii)* in Theorem 3.1)

In the previous section we substituted $w = z - z_0$ because it simplified the notation. This is no longer necessary, so we work in the z variable again. We will first prove *(ii)* of Theorem 3.1, but for a slightly more general setting, where we do not require $f(z_0) = 0$. This setting will be needed in the proof of Theorem 3.14.

Theorem 3.10. *Let* $f(z) = R(z) - \overline{z}$ *with* $\deg(R) \geq 2$*, and* $z_0 \in \mathbb{C}$*. Let* $z_1, \ldots, z_N \in \mathbb{C}$ *be the regular zeros of* $f(z)$*, except, possibly,* z_0*. Then there exist mutually disjoint disks* $\overline{D}(z_k, r)$ *not containing* z_0 *with the following property: For all sufficiently small* $\varepsilon > 0$ *the function*

$$F(z) = f(z) + \tfrac{\varepsilon}{z - z_0}$$

has exactly one zero in $D(z_k, r)$*, and the index of this zero is* $\operatorname{ind}(z_k; f)$*.*

Proof. Let $z_1, \ldots, z_M$, $M \geq N$, be all zeros of $f(z)$, except, possibly, z_0. Choose $r > 0$ with the following properties:

1. The disks $\overline{D}(z_k, r)$ do not intersect ($k = 1, \ldots, M$) and do neither contain z_0 nor the poles of $R(z)$.
2. If z_k is a regular zero, $f(z)$ is either sense-preserving or sense-reversing on $\overline{D}(z_k, r)$.

Fix a regular zero z_k, $1 \leq k \leq N$. Let Γ denote the circle around z_k with radius r. By construction, the continuous function $z \mapsto |f(z)(z - z_0)|$ admits a positive minimum on the compact set Γ. For any

$$0 < \varepsilon < \tfrac{1}{2} \min_{z \in \Gamma} |f(z)(z - z_0)|$$

we then have

$$|F(z)| = |f(z) + \tfrac{\varepsilon}{z - z_0}| \geq |f(z)| - |\tfrac{\varepsilon}{z - z_0}| > \tfrac{\varepsilon}{|z - z_0|}, \quad z \in \Gamma,$$

from which we find $|F(z) - f(z)| < |F(z)| + |f(z)|$ for $z \in \Gamma$. By Rouché's theorem (Theorem 2.3) we have $V(F;\Gamma) = V(-f;\Gamma) = \pm 1$, since $f(z)$ has

exactly one regular zero in the interior of Γ. Thus $F(z)$ also has (at least) one zero in the interior of Γ (by Theorem 2.6; see also the degree principle [20, Section 2.3.6] or [1, Theorem 2.3]).

Write $R_F(z) = R(z) + \frac{\varepsilon}{z-z_0}$, so that $F(z) = R_F(z) - \overline{z}$. Now suppose that $f(z)$ is sense-preserving at z_k, so that $|R'(z)| > 1$ on $\overline{D}(z_k, r)$. Note that $R'_F(z) = R'(z) - \frac{\varepsilon}{(z-z_0)^2}$, so that $|R'_F(z)| > 1$ on the disk if ε is chosen sufficiently small. Therefore $F(z)$ is also sense-preserving and its zeros have positive index ($+1$, see Proposition 2.7). Then $V(F;\Gamma) = V(f;\Gamma) = \operatorname{ind}(z_k; f) = +1$ shows that $F(z)$ has exactly one zero in this disk. A similar reasoning holds for sense-reversing zeros of $f(z)$. □

Remark 3.11. If all zeros of $f(z)$ have merely nonzero index, the first part of the proof still shows that $F(z)$ has *at least* one zero near every zero $z_k \neq z_0$ of $f(z)$.

Lemma 3.12. *Let $f(z) = R(z) - \overline{z}$ with $\deg(R) \geq 2$. Let $z_0, \zeta \in \mathbb{C}$ with $z_0 \neq \zeta$ and $f(\zeta) \neq 0$. Then there exists a neighborhood of ζ in which, for all sufficiently small $\varepsilon > 0$, the function*

$$F(z) = f(z) + \frac{\varepsilon}{z-z_0}$$

has no zeros.

Proof. Let us assume that ζ is not a pole of $R(z)$, else there is nothing to show. Then there exists $0 < r < |z_0 - \zeta|$ such that $f(z)$ is continuous and nonzero on $\overline{D}(\zeta, r)$. For

$$\varepsilon < \min_{z \in \overline{D}(\zeta,r)} |(z - z_0) f(z)|,$$

(the right hand side is positive by the choice of r), we see from

$$|F(z)| \geq |f(z)| - \frac{\varepsilon}{|z-z_0|}$$

that $F(z)$ has no zeros in $\overline{D}(\zeta, r)$. □

The following theorem completes the discussion of points "away" from the perturbation point z_0. Together with Theorem 3.7 and Theorem 3.10, it implies Theorem 3.1.

Theorem 3.13. *In the notation and under the assumptions of Theorem 3.1, let additionally $f(z)$ be regular. Then for sufficiently small $\varepsilon > 0$, the functions $F(z)$ and $f(z)$ have the same number of zeros outside $\overline{D}(z_0, \eta\sqrt{\varepsilon})$. More precisely:*

1. *If $z_1, \ldots, z_N$ are the zeros of $f(z)$ with $|z_k - z_0| > \eta\sqrt{\varepsilon}$, then there exist mutually disjoint disks $\overline{D}(z_k, r)$, $1 \leq k \leq N$, such that $F(z)$ has exactly one zero in each $D(z_k, r)$, and the index of this zero is $\operatorname{ind}(z_k; f)$.*

2. $F(z)$ has no further zeros outside $\overline{D}(z_0, \eta\sqrt{\varepsilon})$.

Proof. Since $\lim_{z\to\infty} f(z) = \infty$, there exists $r_2 > 0$ such that $|f(z)| \geq 1$ for $|z - z_0| \geq r_2$. Further we can choose r_2 so that $\Gamma_2 = \{z : |z - z_0| = r_2\}$ contains all poles of $f(z)$ in its interior. For $|z - z_0| \geq r_2$ we have

$$|F(z)| = |f(z) + \tfrac{\varepsilon}{z-z_0}| \geq |f(z)| - \tfrac{\varepsilon}{|z-z_0|} \geq 1 - \tfrac{\varepsilon}{r_2},$$

which is positive for sufficiently small $\varepsilon > 0$. Thus for each such ε the function $F(z)$ has no zeros on or exterior to Γ_2. We further have

$$|F(z) - f(z)| = \tfrac{\varepsilon}{|z-z_0|} = \tfrac{\varepsilon}{r_2} < 1 \leq |f(z)| \leq |F(z)| + |f(z)|, \quad z \in \Gamma_2.$$

Hence Rouché's theorem (Theorem 2.3) implies $V(F;\Gamma_2) = V(f;\Gamma_2)$. By Theorem 3.10 each zero of $f(z)$ inside Γ_2 has a corresponding zero of $F(z)$ with same index (except for z_0). We will now show that if $\varepsilon > 0$ is sufficiently small, then $F(z)$ has no further zeros inside Γ_2 than implied by Theorem 3.7 and Theorem 3.10. In order to achieve this, we will use Lemma 3.12 combined with a compactness argument.

By assumption $R'(z_0) = 0$. Thus we can choose $r_1 > 0$ such that $|R'(z)| < \frac{1}{n}$ for $|z - z_0| \leq r_1$, and such that z_0 is the only zero of $f(z)$ in $|z - z_0| \leq r_1$. We define the compact set K as follows. Consider the closed annulus $r_1 \leq |z - z_0| \leq r_2$ and denote by $z_1, \ldots, z_N$ the zeros of $f(z)$ in that annulus. By Theorem 3.10, there are mutually disjoint $\overline{D}(z_k, r)$, $0 \leq k \leq N$, such that $F(z)$ has exactly one zero $z'_k \in D(z_k, r)$ of the same index, $1 \leq k \leq N$. Cutting out these neighborhoods in the annulus, we obtain the compact set K (Figure 2(b)).

For each $\zeta \in K$ we have $f(\zeta) \neq 0$, so there exists a neighborhood of ζ as in Lemma 3.12. These neighborhoods constitute an open covering of K, of which a finite subset is sufficient to cover K. On each neighborhood $F(z)$ is nonzero for all sufficiently small ε; see Lemma 3.12. Hence, only a finite number of smallness constraints on ε are sufficient to guarantee that $F(z)$ has no zeros inside K.

Recall that inside each of the cut out disks $D(z_k, r)$, $1 \leq k \leq N$, the function $F(z)$ has exactly one zero of same index as $f(z)$. Thus, it remains to show that $F(z)$ has no additional zeros inside the annulus $A := A(z_0, \eta\sqrt{\varepsilon}, r_1)$. As before set $R_F(z) = R(z) + \frac{\varepsilon}{z-z_0}$. Then, for $z \in A$,

$$|R'_F(z)| \leq |R'(z)| + \tfrac{\varepsilon}{|z-z_0|^2} < \tfrac{1}{n} + \tfrac{n-1}{n} = 1,$$

and thus $F(z)$ is sense-reversing on A. Denote by γ the circle $\{z : |z - z_0| = \eta\sqrt{\varepsilon}\}$, and by n_- the number of (sense-reversing) zeros of $F(z)$ in A. By the argument principle we find

$$-1 + \sum_{k=1}^{N} \operatorname{ind}(z_k; f) = V(f;\Gamma_2) = V(F;\Gamma_2) = V(F;\gamma) + \sum_{k=1}^{N} \operatorname{ind}(z'_k; F) - n_-,$$

which shows $n_- = 0$, since $\operatorname{ind}(z_k; f) = \operatorname{ind}(z'_k; F)$ for $k = 1, \ldots, N$, and $V(F;\gamma) = -1$; see Corollary 3.9. □

3.3 Perturbation at arbitrary points

We now consider perturbations at points where the assumptions of Theorem 3.1 are not satisfied. The situation is simpler than in the setting of Theorem 3.1 and for the proof the same techniques as in Section 3.1 can be applied. We therefore only give a sketch of the proof. Furthermore, we assume for simplicity that both $f(z)$ and $F(z)$ are regular, although this requirement could be weakened somewhat.

Theorem 3.14. *Let $f(z) = R(z) - \overline{z}$ with $\deg(R) \geq 2$ be regular and satisfy $\lim_{z\to\infty} f(z) = \infty$, and let $z_0 \in \mathbb{C}$. For sufficiently small $\varepsilon > 0$, if*

$$F(z) = f(z) + \tfrac{\varepsilon}{z - z_0}$$

is regular, then the following holds:

1. *If z_0 is a pole of $f(z)$, then $F(z)$ and $f(z)$ have the same number of zeros.*
2. *If $0 < |f(z_0)| < \infty$, then there exists $r > 0$ such that $0 < |f(z)| < \infty$ on $D(z_0, r)$, and $F(z)$ has at least one sense-preserving zero in $D(z_0, r)$.*
3. *If $f(z_0) = 0$, and $|R'(z_0)| > 1$, there exists $r > 0$ such that $F(z)$ has at least two sense-preserving zeros in $D(z_0, r)$.*
4. *If $f(z_0) = 0$, and $0 < |R'(z_0)| < 1$, there exists $r > 0$ such that $F(z)$ has at least two sense-preserving zeros and two sense-reversing zeros in $D(z_0, r)$.*

Further, in 2., 3. and 4., $F(z)$ and $f(z)$ have the same number of zeros outside $D(z_0, r)$.

Proof. (Sketch)

In *1.* we have $R(z) = (z - z_0)^{-m}\widetilde{R}(z)$ with $\widetilde{R}(z_0) \notin \{0, \infty\}$, $m \geq 1$. In some disk $\overline{D}(z_0, \delta)$ we have $|z| \leq M$ and $|\widetilde{R}(z)| \geq M' > 0$. If need be, reduce δ such that $\delta^m < \frac{M'}{2M}$ holds. Noting that

$$R_F(z) = R(z) + \tfrac{\varepsilon}{z - z_0} = \tfrac{1}{(z-z_0)^m}(\widetilde{R}(z) + \varepsilon(z - z_0)^{m-1}),$$

one can compute that $|F(z)| > 0$ on $\overline{D}(z_0, \delta)$ for all sufficiently small ε. Consider the annulus $A(z_0, \delta, r_2)$ which contains all zeros of $f(z)$ (r_2 is chosen as in the proof of Theorem 3.13). After cutting out appropriate disks about the zeros of $f(z)$, a compact set K remains. As in the proof of Theorem 3.13, for sufficiently small $\varepsilon > 0$, each disk around a zero of $f(z)$ contains exactly one zero of $F(z)$, and the set K does not contain any zeros of $F(z)$.

In *2.* there exists $r > 0$ such that $0 < |f(z)| < \infty$ on $\overline{D}(z_0, r)$. By the argument principle the winding of $f(z)$ along the boundary curve is 0. Apply Rouché's theorem (Theorem 2.3) to $f(z)$ and $F(z)$ on the boundary to see that $F(z)$ has at least one sense-preserving zero inside this disk, provided $\varepsilon > 0$ is sufficiently small.

Let r_2 and Γ_2 be defined as in the proof of Theorem 3.13, and construct the compact set K by removing from the annulus $\overline{A}(z_0, r, r_2)$ suitable disks centered at the zeros of $f(z)$. Proceeding exactly as in the proof of Theorem 3.13 we see that $F(z)$ and $f(z)$ have the same number of zeros outside $D(z_0, r)$.

In both *3.* and *4.* we substitute $w := z - z_0$ for simplicity of notation, as in Section 3.1. Set $c := R'(0)$, which can be assumed to be real positive. Truncation of the Laurent series of the analytic part of $F(w) = f(w) + \frac{\varepsilon}{w}$ yields the function $G(w) = cw + \frac{\varepsilon}{w} - \overline{w}$.

In *3.* we have $c > 1$ and one computes that $G(w)$ has exactly two sense-preserving zeros $\pm i(\frac{\varepsilon}{1+c})^{\frac{1}{2}}$. Applying Rouché's theorem to $F(w)$ and $G(w)$ on the circle $|w| = \sqrt{\varepsilon}$ gives the result. An example is shown in Section 4.3.

Since $c > 1$, there exists $r_1 > 0$ such that $|R'(w)| > \frac{1+c}{2}$ on $\overline{D}(0, r_1)$. We then have for $w \in A := A(0, \sqrt{\varepsilon}, r_1)$

$$|R'_F(w)| = |R'(w) - \tfrac{\varepsilon}{w^2}| \geq |R'(w)| - \tfrac{\varepsilon}{|w|^2} \geq 1 + \tfrac{c-1}{2} - \tfrac{\varepsilon}{r_1^2},$$

which is larger than 1 if ε is chosen sufficiently small. Thus $F(w)$ is sense-preserving on A. Now, the same reasoning as in the proof of Theorem 3.13 (with the modified A) shows that $F(w)$ and $f(w)$ have the same number of zeros outside $D(z_0, r)$, where $r = \sqrt{\varepsilon}$.

In *4.* we have $0 < c < 1$ and one computes that $G(w)$ has exactly the two sense-preserving zeros $\pm i(\frac{\varepsilon}{1+c})^{\frac{1}{2}}$, and the two sense-reversing zeros $\pm(\frac{\varepsilon}{1-c})^{\frac{1}{2}}$. Applying Rouché's theorem to $F(w)$ and $G(w)$ on $\gamma_1 = \{w \in \mathbb{C} : |w| = \sqrt{\varepsilon}\}$ shows that $F(w)$ has two sense-preserving zeros inside γ_1, and applying it on the circle $\gamma_2 = \{w \in \mathbb{C} : |w| = \frac{2}{\sqrt{1-c}}\sqrt{\varepsilon}\}$ shows that $F(w)$ has two sense-reversing zeros between γ_1 and γ_2. An example for this case can be seen in Section 4.4, more specifically in Figure 5(b).

Since $0 < c < 1$ there exists $r_1 > 0$ such that $|R'(w)| < \frac{1+c}{2}$ on $\overline{D}(0, r_1)$. Then, we have for $w \in A := A(0, \frac{2}{\sqrt{1-c}}\sqrt{\varepsilon}, r_1)$

$$|R'_F(w)| = |R'(w) - \tfrac{\varepsilon}{w^2}| \leq |R'(w)| + \tfrac{\varepsilon}{|w|^2} \leq \tfrac{1+c}{2} + \varepsilon\tfrac{1-c}{4\varepsilon} < 1,$$

so that $F(w)$ is sense-reversing in A. The same reasoning as in the proof of Theorem 3.13 now shows that $F(w)$ and $f(w)$ have the same number of zeros outside $D(z_0, r)$, where $r = \frac{2}{\sqrt{1-c}}\sqrt{\varepsilon}$. □

4 Examples

We briefly discuss the Poincaré index and its connection with phase portraits. (Recall the example given in the Introduction; see Figure 1.) Let z_0 be an isolated exceptional point of the continuous function $f(z)$, and let γ be a circle around z_0 suitable for the computation of $\mathrm{ind}(z_0; f)$. Clearly, the Poincaré index measures the overall change of the argument of $f(z)$ while

z travels once around γ (in the positive sense). This corresponds exactly to the *chromatic number* of γ, as discussed in [23, p. 772]. Thus, less formally, the Poincaré index corresponds to the number of times each color appears in the phase portrait while travelling once around z_0, and the sign of the Poincaré index is revealed by the ordering in which the colors appear. This observation allows to determine the Poincaré index of an isolated exceptional point of $f(z)$ by looking at the phase portrait of $f(z)$.

For the color scheme we use in the phase portraits, the color ordering while travelling around some point is exemplified for the indices $+1$, -1 and -2 as follows (left to right):

This is the same "color wheel" as used, for example, in [23]. For the computation of the phase portraits in this paper we used a slightly modified version of the MATLAB package "Phase Plots of Complex Functions" by Elias Wegert[1].

Thus the index of an exceptional point of $f(z) = R(z) - \overline{z}$ can be determined from the phase portrait. Poles and zeros of $f(z)$, which are the only exceptional points, are marked with white squares (poles) or black disks (zeros). Additionally, all phase portraits are visually divided in slightly brightened regions, where $f(z)$ is sense-preserving (i.e., the analytic part dominates), and slightly darkened regions, where $f(z)$ is sense-reversing (i.e., the co-analytic part dominates). Notice that the indices of zeros in the latter case are always -1, while the indices of sense-preserving zeros are $+1$.

4.1 Circular point lenses

Recall Rhie's construction described in the Introduction, which is based on the function $R_0(z) = \frac{z^{d-1}}{z^d - r^d}$, for some $d \geq 2$ and $r > 0$. It is easy to see that $R_0^{(k)}(0) = 0$ for $1 \leq k \leq d-2$, while $R_0^{(d-1)}(0) \neq 0$. An application of *(i)* in Theorem 3.1 with $n = d$ shows that $F(z) = R_0(z) + \frac{\varepsilon}{z} - \overline{z}$ has $2d$ zeros located in two annuli around the perturbation point $z_0 = 0$. Moreover, if $r > 0$ and $\varepsilon > 0$ are sufficiently small, then there exist further $3d$ zeros corresponding to the $3d$ zeros of $R_0(z) - \overline{z}$ away from $z_0 = 0$. The results in [16] show that the same perturbation behavior can be observed for Rhie's original function $(1-\varepsilon)R_0(z) + \frac{\varepsilon}{z} - \overline{z}$. A numerical example for this function with $d = 7$ is shown in Figure 1.

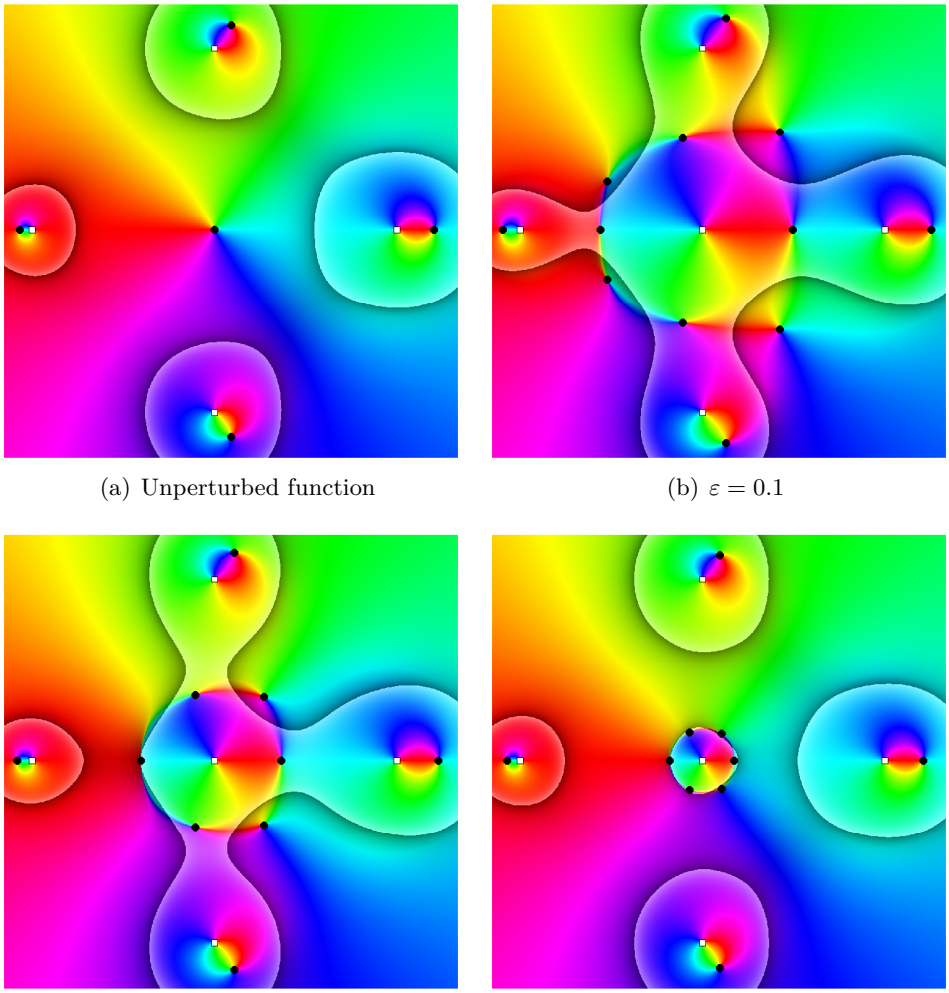

(a) Unperturbed function

(b) $\varepsilon = 0.1$

(c) $\varepsilon = 0.05$

(d) $\varepsilon = 0.01$

Figure 3: More than $2n$ additional zeros may occur; see Section 4.2.

4.2 Generation of more than $2n$ zeros

Theorem 3.7 *(i)* gives the lower bound $2n$ on the number of additional zeros due to the perturbation. While we suspect that actually exactly $2n$ zeros appear for sufficiently small ε (see also Remark 3.8), we will now see that *more* than $2n$ zeros may appear if ε is not small enough.

Consider the function

$$R(z) = \frac{\frac{1}{6}z^3 + \frac{1}{20}z^2}{z^4 - \frac{1}{10}},$$

for which $R(0) = R'(0) = 0$, $|R''(0)| = 1$ and $|R'''(0)| = 10$. A phase portrait

[1] `http://www.visual.wegert.com/`

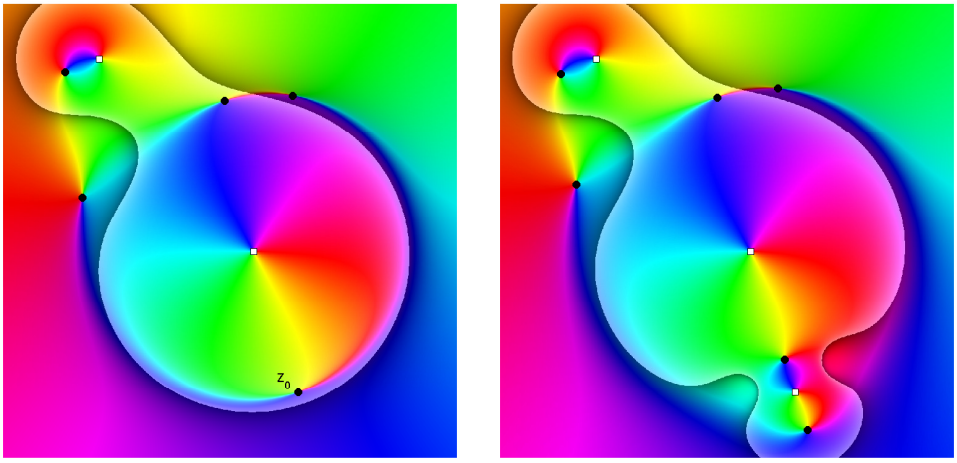

Figure 4: Perturbation at a sense-preserving zero; see Section 4.3.

of $R(z) - \overline{z}$ is shown in Figure 3(a).

Figure 3(b) shows a phase portrait of $R(z) + \frac{\varepsilon}{z} - \overline{z}$ with $\varepsilon = 0.1$. The perturbation results in 8 additional zeros in the vicinity of 0, although $n = 3$. In this example the first non-vanishing derivative is dominated by a higher derivative and hence our analysis from Section 3 does not apply, since ε is not small enough.

However, the second derivative becomes dominant as soon as ε is sufficiently small. Figure 3(c) shows the result of perturbing with $\varepsilon = 0.05$. Now only $2n = 6$ additional zeros occur, as suggested by Theorem 3.1. If ε is reduced further, as can be seen in Figure 3(d) for $\varepsilon = 0.01$, the additional zeros approach those of the function $G(w)$ in Section 3, but the number of additional zeros (six) remains the same.

4.3 Perturbing a sense-preserving zero

Figure 4 shows the result of perturbing a sense-preserving zero by a pole. The left plot shows a randomly generated[2] rational harmonic function $f(z) = R(z) - \overline{z}$, where $R(z)$ is of degree two (both the numerator and denominator polynomials of $R(z)$ have degree two) and extremal. The point z_0 is a sense-preserving zero of $f(z)$ with $|R'(z_0)| \approx 1.176 > 1$. We add a pole at z_0 with $\varepsilon = 0.025$; the resulting function is shown in Figure 4 (right). As suggested by Theorem 3.14, two sense-preserving zeros appear.

[2]More precisely, we chose 5 points in the complex plane, with real and imaginary parts drawn uniformly at random from $[-1, 1]$. We then constructed $R(z)$ such that these random points are the zeros of $R(z) - \overline{z}$.

4.4 Iterative perturbation

Starting from the randomly chosen extremal rational function $R(z)$ of degree two introduced in the previous section, our goal is now to successively add two poles at sense-reversing zeros such that extremality is maintained by each perturbation. We will thus obtain extremal rational functions of degrees three and four. This procedure is displayed in Figure 5, which we will discuss in detail now.

The initial situation with $R_1(z) = R(z)$ is depicted in Figure 5(a), where we plot the phase portrait of $R_1(z) - \overline{z}$. Black triangles show zeros of $R_1'(z)$ and white squares show the poles of $R_1(z)$. The picture shows that $R_1(z) - \overline{z}$ has three sense-preserving zeros (black disks in the bright region), and two sense-reversing zeros (black disks in the dark region).

Clearly, neither of the two sense-reversing zeros satisfies the conditions of Theorem 3.1. Denote by z_1 the leftmost sense-reversing zero of $R_1(z) - \overline{z}$; we have $|R_1'(z_1)| \approx 0.5572$. Numerical experiments show that perturbing $R_1(z) - \overline{z}$ with the pole $\frac{\varepsilon_1}{z - z_1}$ results for all $\varepsilon_1 > 0$ small enough in a function that has four additional zeros nearby z_1. The result of such a perturbation is shown in Figure 5(b). The four additional zeros are explained by Theorem 3.14, and reducing ε_1 further does not result in further zeros in our numerical experiments.

Figure 5(c) shows the phase portrait of the function $R_2(z) - \overline{z}$, where $R_2(z) = R_1(z) + c$ with a deliberately chosen constant $c \in \mathbb{C}$ such that $R_2(z) - \overline{z}$ has a sense-reversing zero z_2 that coincides (numerically) with a zero of $R_2'(z) = R_1'(z)$ (leftmost zero of $R_2'(z)$).

The effect of adding a pole at z_2 to $R_2(z)$, i.e., forming $R_3(z) = R_2(z) + \frac{\varepsilon_2}{z - z_2}$, is shown in the phase portrait of $R_3(z) - \overline{z}$ in Figure 5(d). An enlarged view on the perturbed region is given in Figure 5(e). We see that $R_3(z) - \overline{z}$ has 5 more zeros than $R_2(z) - \overline{z}$. Here $\varepsilon_2 = 4.5 \cdot 10^{-3}$, and we have chosen this value because a newly created zero of $R_3(z) - \overline{z}$ lies in the immediate vicinity of a zero of $R_3'(z)$ (rightmost zero in Figure 5(e)).

In order to obtain conditions that allow another application of Theorem 3.1, we could have tried to add another constant to $R_3(z)$ such that the conditions of the theorem are met. However, the rightmost zero of $R_3(z) - \overline{z}$, say, z_3, is already very close to a zero of $R_3'(z)$. Figure 5(f) shows the effect of adding a pole at this position, i.e. setting $R_4(z) = R_3(z) + \frac{\varepsilon_3}{z - z_3}$ and considering the function $R_4(z) - \overline{z}$. Although the conditions of the theorem are not exactly met (we have $|R_3'(z_3)| \approx 0.7936$), the same effect as in Figures 5(c)–5(d) can be observed. In particular, $R_4(z)$ is again extremal.

Notice also that it has been possible to choose the value ε_3 such that two newly created zeros of $R_4(z) - \overline{z}$ are very close to newly created zeros of $R_4'(z)$, suggesting that it may be possible to repeat this perturbation procedure at least one more time.

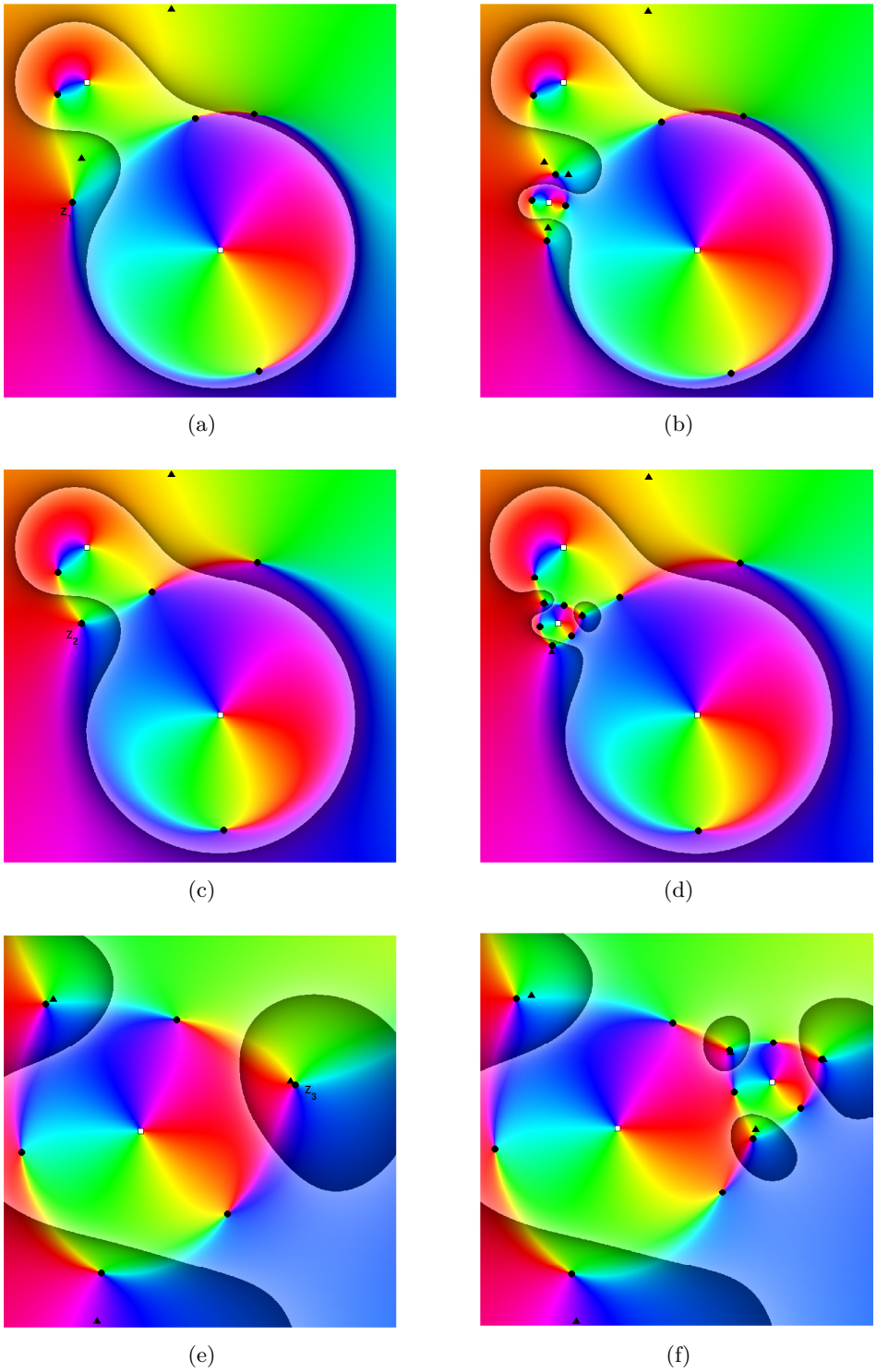

(a) (b) (c) (d) (e) (f)

Figure 5: Iterative perturbation of a random rational function; see Section 4.4. Black triangles indicate the zeros of $R'(z)$.

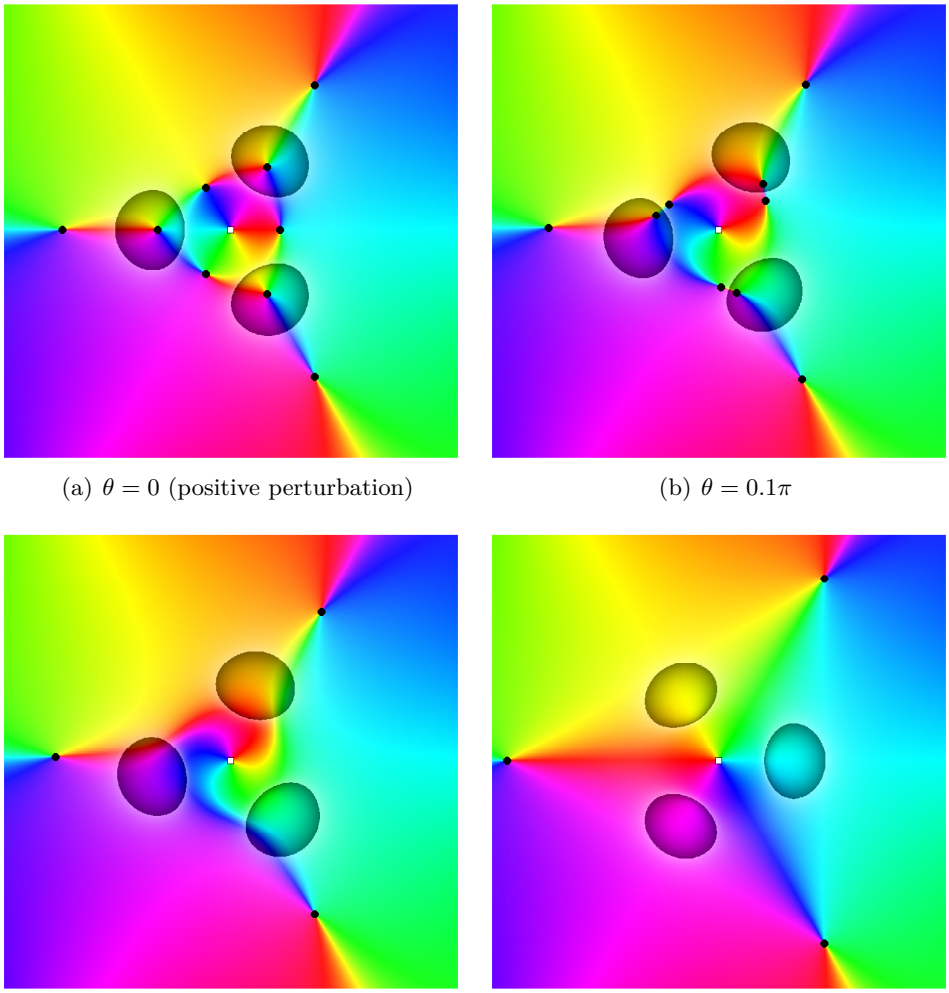

(a) $\theta = 0$ (positive perturbation)

(b) $\theta = 0.1\pi$

(c) $\theta = 0.2\pi$

(d) $\theta = \pi$ (negative perturbation)

Figure 6: Phase portraits of Rhie's function $R_\varepsilon(z)$ from (1) with $\varepsilon > 0$ replaced by $\varepsilon e^{i\theta}$; see Section 4.5.

4.5 Extension to complex residues

Our motivation for studying the effect of adding poles to $R(z) - \overline{z}$ comes from an astrophysical application in gravitational microlensing. This astrophysical application requires adding simple poles with *positive* residues. From a mathematical point of view, one may wonder about the effect of adding poles with *complex* residues on the number of (newly created) zeros. We will now give a brief and informal discussion of this case.

Consider Rhie's function from (1), where we now replace ε by $\varepsilon e^{i\theta}$, with $\varepsilon > 0$ and $\theta \in \mathbb{R}$. Figure 6 shows phase portraits of $R_{\varepsilon e^{i\theta}}(z)$ centered at the origin for $n = 3$ and several values of θ. For positive perturbation ($\theta = 0$)

the function $R_\varepsilon(z) - \overline{z}$ has $2n = 6$ zeros close to the origin (Figure 6(a)). We observe that with increasing argument, the zeros close to the origin approach each other (Figure 6(b)) and finally vanish (Figures 6(c) and 6(d)).

Heuristically this effect can be explained as follows. Let z_0 be a zero of $f(z) = R(z) - \overline{z}$, where $R(z)$ is rational with $\deg(R) \geq 2$. Consider the perturbed function $F(z) = f(z) + \frac{\varepsilon}{z - z_0}$. This function can be approximated (after translation $w := z - z_0$) by the function $G(w)$ in (5). The zeros of $G(w)$ close to z_0 give rise to zeros of $F(z)$; see Sections 3.1 and 3.3. The zeros of $G(w)$ are the solutions of the equation

$$cw^n + \varepsilon - |w|^2 = 0.$$

For small values of w, this equation is *approximated* by $\varepsilon - |w|^2 = 0$, which has solutions only for $\varepsilon \geq 0$. This suggests that $F(z)$ has no zeros near z_0 for sufficiently small ε chosen "away from the positive real axis".

4.6 Extension to poles of higher order

So far we considered perturbations by simple poles. One may wonder about the effects of adding poles of higher order. We give a brief and informal discussion of this case.

For simplicity, let $f(z)$ be as in Theorem 3.14. Suppose $z_0 \in \mathbb{C}$ is not a pole of $f(z)$ and consider the function $F(z) = f(z) + \frac{\varepsilon}{(z - z_0)^k}$, where now $k \geq 1$, and assume that $F(z)$ is regular as well. As before, we can show that on a sufficiently large circle Γ we have $V(f; \Gamma) = V(F; \Gamma)$. Further, there exists a circle γ centered at z_0, not containing any zero or pole of $f(z)$ (except possibly z_0), such that for sufficiently small ε the functions $f(z)$ and $F(z)$ have the same number of zeros with same indices outside γ, and that $V(f; \gamma) = V(F; \gamma)$ holds. Let us denote by n_+^{new} and n_-^{new} the number of sense-preserving and sense-reversing zeros of $F(z)$ inside γ, respectively. By the argument principle (Theorem 2.6) we then have

$$\operatorname{ind}(z_0; f) = V(f; \gamma) = V(F; \gamma) = -k + n_+^{\text{new}} - n_-^{\text{new}},$$

or, equivalently, $n_+^{\text{new}} - n_-^{\text{new}} = k + \operatorname{ind}(z_0; f)$. Thus the total number of zeros of the regular function $F(z)$ inside γ is

$$n_+^{\text{new}} + n_-^{\text{new}} = k + \operatorname{ind}(z_0; f) + 2n_-^{\text{new}} \geq k + \operatorname{ind}(z_0; f). \tag{13}$$

We illustrate this result in Figure 7. In Figure 7(a), the same function as used in Section 4.3 is shown; the indicated points correspond to a sense-preserving zero ($\operatorname{ind}(z_1; f) = 1$), a sense-reversing zero ($\operatorname{ind}(z_2; f) = -1$) and a non-exceptional point ($\operatorname{ind}(z_3; f) = 0$).

Adding a pole of order $k = 4$ with residue $\varepsilon = 10^{-5}$ at the designated positions z_1, z_2 and z_3 results in 5, 3, and 4 new solutions nearby the position

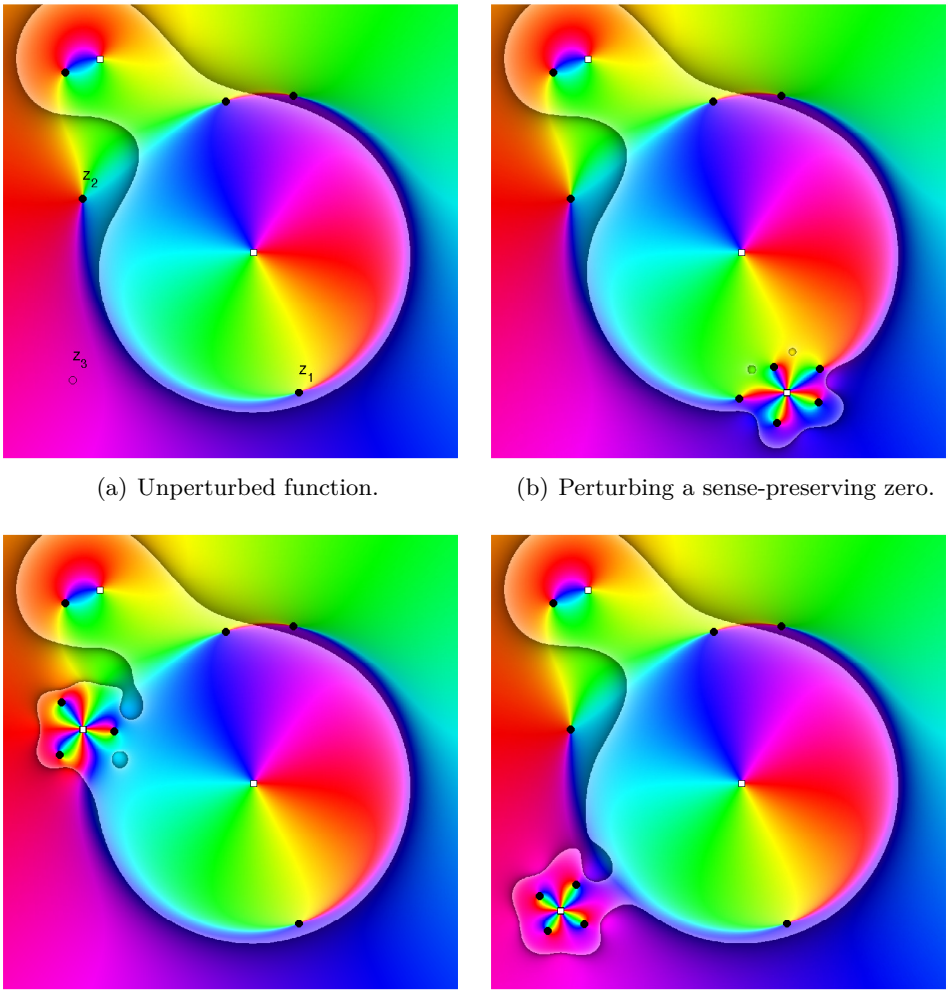

(a) Unperturbed function.

(b) Perturbing a sense-preserving zero.

(c) Perturbing a sense-reversing zero.

(d) Perturbing a non-zero.

Figure 7: Perturbations with poles of higher order; see Section 4.6.

of the pole, which is shown in Figures 7(b)–7(d). In each case, the minimum number of zeros are created (see the bound (13)), and $n_-^{\text{new}} = 0$.

We performed extensive numerical experiments for various combinations of k, index of z_0 and the number of vanishing derivatives at z_0. In each case, if ε was chosen sufficiently small, the minimum number of zeros was created and $n_-^{\text{new}} = 0$. This observed behaviour is different from the case of adding a simple pole, which can create $n_-^{\text{new}} = n_+^{\text{new}} = n$ new zeros when perturbing a zero at which $n-1$ derivatives of $R(z)$ vanish. Thus, perturbing with a simple pole seems to be a more effective means to create extremal rational functions. Further, the effect of complex residues ε we observed was significantly different from the situation in Section 4.5; the created zeros are

merely rotated according to the value of $\arg(\varepsilon)$.

5 Conclusions and Outlook

We have generalized Rhie's technique [19] for constructing extremal point lenses to arbitrary rational harmonic functions of the form $f(z) = R(z) - \overline{z}$. We have shown that if $f(z_0) = 0$ and the first $n-2$ derivatives of $R(z)$ vanish at z_0, while $R^{(n-1)}(z_0) \neq 0$, then the function $f(z) + \frac{\varepsilon}{z-z_0}$ has at least $2n$ zeros near the circle $|z - z_0| = \sqrt{\varepsilon}$, provided $\varepsilon > 0$ is sufficiently small. In particular, our general results cover Rhie's original construction; see Corollary 3.3. We also gave lower bounds on the number of additional zeros if $f(z)$ is perturbed by a pole at any other point $z_0 \in \mathbb{C}$.

We have briefly studied extensions of our results to complex residues (Section 4.5) and poles of higher order (Section 4.6) by means of examples, but we did not pursue these directions with full rigor.

Theorems 3.1 and 3.14 give *sufficient conditions* for *lower bounds* on the number of newly created zeros in the vicinity of the point where the pole is added, which raises two open questions. Firstly, the examples in Section 4.2 demonstrate that the stated conditions are not *necessary* for the creation of the stated number of zeros. They show that more images can be created if the perturbation residue ε is chosen somewhat "too large". It would be interesting to quantify this effect. Secondly, we believe that for sufficiently small perturbations, no more than the stated number of zeros are created; see also Remark 3.8. We have performed extensive numerical experiments that support this claim. However, a rigorous analysis is yet to be done.

Acknowledgements We would like to thank Elias Wegert for comments on the manuscript and creating the color scheme used in the illustrations. We are grateful to the anonymous referee for carefully reading the manuscript and for giving us many useful suggestions.

The work of R. Luce was supported by Deutsche Forschungsgemeinschaft, Cluster of Excellence "UniCat".

References

[1] Mark Benevich Balk. *Polyanalytic Functions.* Mathematical Research. 63. Berlin: Akademie-Verlag. 197 p. , 1991.

[2] Johann Bayer and Charles C. Dyer. Maximal lensing: mass constraints on point lens configurations. *Gen. Relativity Gravitation*, 39(9):1413–1418, 2007.

[3] Johann Bayer and Charles C. Dyer. Erratum: Maximal lensing: mass constraints on point lens configurations. *Gen. Relativity Gravitation*, 41(3):669, 2009.

[4] Pavel M. Bleher, Youkow Homma, Lyndon L. Ji, and Roland K. W. Roeder. Counting zeros of harmonic rational functions and its application to gravitational lensing. *Int. Math. Res. Not. IMRN*, (8):2245–2264, 2014.

[5] John B. Conway. *Functions of one complex variable*, volume 11 of *Graduate Texts in Mathematics*. Springer-Verlag, New York, second edition, 1978.

[6] Peter Duren. *Harmonic mappings in the plane*, volume 156 of *Cambridge Tracts in Mathematics*. Cambridge University Press, Cambridge, 2004.

[7] Peter Duren, Walter Hengartner, and Richard S. Laugesen. The argument principle for harmonic functions. *Amer. Math. Monthly*, 103(5):411–415, 1996.

[8] Lukas Geyer. Sharp bounds for the valence of certain harmonic polynomials. *Proc. Amer. Math. Soc.*, 136(2):549–555, 2008.

[9] I. Glicksberg. A remark on Rouché's theorem. *Amer. Math. Monthly*, 83(3):186–187, 1976.

[10] Peter Henrici. *Applied and computational complex analysis*. Wiley-Interscience [John Wiley & Sons], New York, 1974.

[11] Dmitry Khavinson and Genevra Neumann. On the number of zeros of certain rational harmonic functions. *Proc. Amer. Math. Soc.*, 134(4):1077–1085, 2006.

[12] Dmitry Khavinson and Genevra Neumann. From the fundamental theorem of algebra to astrophysics: a "harmonious" path. *Notices Amer. Math. Soc.*, 55(6):666–675, 2008.

[13] Dmitry Khavinson and Grzegorz Świątek. On the number of zeros of certain harmonic polynomials. *Proc. Amer. Math. Soc.*, 131(2):409–414, 2003.

[14] S.-Y. Lee, A. Lerario, and E. Lundberg. Remarks on Wilmshurst's theorem. *ArXiv e-prints*, August 2013.

[15] Jörg Liesen. When is the adjoint of a matrix a low degree rational function in the matrix? *SIAM J. Matrix Anal. Appl.*, 29(4):1171–1180, 2007.

[16] Robert Luce, Olivier Sète, and Jörg Liesen. Sharp parameter bounds for certain maximal point lenses. *Gen. Relativity Gravitation*, 46(5):46:1736, 2014.

[17] S. Mao, A. O. Petters, and H. J. Witt. Properties of Point Mass Lenses on a Regular Polygon and the Problem of Maximum Number of Images. In T. Piran and R. Ruffini, editors, *Recent Developments in Theoretical and Experimental General Relativity, Gravitation, and Relativistic Field Theories*, pages 1494–1496, 1999.

[18] A. O. Petters and M. C. Werner. Mathematics of gravitational lensing: multiple imaging and magnification. *Gen. Relativity Gravitation*, 42(9):2011–2046, 2010.

[19] S. H. Rhie. n-point Gravitational Lenses with 5(n-1) Images. *ArXiv Astrophysics e-prints*, May 2003.

[20] T. Sheil-Small. *Complex polynomials*, volume 75 of *Cambridge Studies in Advanced Mathematics*. Cambridge University Press, Cambridge, 2002.

[21] T. J. Suffridge and J. W. Thompson. Local behavior of harmonic mappings. *Complex Variables Theory Appl.*, 41(1):63–80, 2000.

[22] Elias Wegert. *Visual complex functions*. Birkhäuser/Springer Basel AG, Basel, 2012.

[23] Elias Wegert and Gunter Semmler. Phase plots of complex functions: a journey in illustration. *Notices Am. Math. Soc.*, 58(6):768–780, 2011.

[24] A. S. Wilmshurst. The valence of harmonic polynomials. *Proc. Amer. Math. Soc.*, 126(7):2077–2081, 1998.

Creating images by adding masses to gravitational point lenses*

Olivier Sète† Robert Luce† Jörg Liesen†

Abstract

A well-studied maximal gravitational point lens construction of S. H. Rhie produces $5n$ images of a light source using $n+1$ deflector masses. The construction arises from a circular, symmetric deflector configuration on n masses (producing only $3n+1$ images) by adding a tiny mass in the center of the other mass positions (and reducing all the other masses a little bit).

In a recent paper we studied this "image creating effect" from a purely mathematical point of view (Sète, Luce & Liesen, Comput. Methods Funct. Theory 15(1):9-35, 2015). Here we discuss a few consequences of our findings for gravitational microlensing models. We present a complete characterization of the effect of adding small masses to these point lens models, with respect to the number of images. In particular, we give several examples of maximal lensing models that are different from Rhie's construction and that do not share its highly symmetric appearance. We give generally applicable conditions that allow the construction of maximal point lenses on $n+1$ masses from maximal lenses on n masses.

1 Introduction

We consider the phenomenon of multiple lensed images in the framework of gravitational microlensing. Specifically, given $n \geq 2$ point masses $m_j > 0$ at positions $z_j \in \mathbb{C}$ in the complexified lens plane, we consider the lensing map $\eta : L \to S$ from the lens plane $L = \mathbb{C}\backslash\{z_1, \ldots, z_n\}$ to the light source plane $S = \mathbb{C}$,

$$\eta(z) = z - \gamma\overline{z} - \sum_{j=1}^{n} \frac{m_j}{\overline{z} - \overline{z}_j}, \tag{1}$$

*A final version of this preprint manuscript appeared as follows: O. Sète, R. Luce and J. Liesen. Creating images by adding masses to gravitational point lenses. *Gen. Relativity Gravitation* (2015) 47, Art. 42, pp. 1–8.

†TU Berlin, Institute of Mathematics, MA 4-5, Straße des 17. Juni 136, 10623 Berlin, Germany (`{sete,luce,liesen}@math.tu-berlin.de`)

where $\gamma \in \mathbb{C}$ is the (constant) external shear. This lens model can be seen as a generalization of the Chang-Refsdal lens to n point massses; see [1]. Given a light source position (projected on the lens plane) $\zeta \in \mathbb{C}$, the (projected) images of the light source are exactly the solutions of the equation $\eta(z) = \zeta$. See [15] for a general introduction to gravitational lensing and [14] for gravitational lensing in terms of complex variables; see also [11, 6].

The important question of the maximal number of images that can be produced by a gravitational lens on n point masses modeled by (1) was answered in 2006 by Khavinson & Neumann [5]. Their result is as follows.

Theorem 1.1. *The maximal number of images that can be produced by the lensing map η in* (1) *is $5n-5$ if $\gamma = 0$ and $5n$ if $\gamma \neq 0$.*

In the case of *nonzero* shear, the bound of $5n$ images can be improved slightly. As shown by An & Evans [1], the maximal number of images in that case is $5n-1$. The "missing image" accounts for a solution to the lens equation at the point infinity in the extended complex plane; see also [7].

A particular class of point lenses that realizes the maximal number of images has been devised by Rhie [12]. Her construction (and the variant discussed in [2, 3]) has been recently studied in great detail [8]. We will very briefly recall the construction with a small *additive* mass (in contrast to her original construction in [12]).

Consider the lens on n equal point masses $m_j = 1/n$ located at the vertices of a regular polygon of a certain radius r, i.e., $z_j = re^{i\frac{2j\pi}{n}}$, and without external shear ($\gamma = 0$). This yields the lensing map

$$\eta(z) = z - \frac{\overline{z}^{n-1}}{\overline{z}^n - r^n}. \tag{2}$$

For a light source located at the origin of the lens plane, i.e., $\zeta = 0$, it is known that this lens produces $3n+1$ images [9]. In order to arrive at a maximal lens, a tiny mass ε is added at the image position $z = 0$, i.e., we define

$$\eta_\varepsilon(z) = \eta(z) - \frac{\varepsilon}{\overline{z}}. \tag{3}$$

If $\varepsilon > 0$ is sufficiently small, this "perturbation" of the lens induces $2n$ "new" images on two circles around the origin [8] (and the previous image at $z = 0$ vanishes). So the lens on $n+1$ point masses modeld by η_ε produces $5n$ images, and thus is a maximal lens.

We recently showed (in a purely mathematical context) that this "image creating effect" of adding masses is *not specific* to the particular (symmetric) lens described by (2) [13]. Our goal here is to present some implications of the mathematical results in [13] for gravitational point lens models.

In Section 2 we present a general classification of the image creating effect that is induced by adding tiny masses to an existing lens. The results are applicable to point lens models with or without external shear. The extremal

case of *maximal lensing* is studied in Section 3. To our knowledge, the only known maximal point lens models are based on the lens (2) from above. We will present conditions that allow the construction of maximal point lenses different from these lenses. We give several examples for maximal lenses.

2 Adding tiny masses to a lens

Recall that the solutions to the lens equation $\eta(z) = \zeta$ can be classified using the sign of the determinant of the Jacobian of η (e.g. [10]). In terms of Wirtinger derivatives, we find for the functional determinant of the lensing map

$$\det D\eta(z) = |\partial_z \eta(z)|^2 - |\partial_{\bar{z}} \eta(z)|^2 = 1 - |R'(z)|^2,$$

where we have abbreviated $R(z) = \overline{\gamma} z + \sum_{j=1}^{n} \frac{m_j}{z - z_j}$, so that $\eta(z) = z - \overline{R(z)}$.

We will call an image $z^* \in \mathbb{C}$, i.e, a solution to the equation $\eta(z) = \zeta$, a *sense-preserving* image if $|R'(z^*)| < 1$, and a *sense-reserving* image if $|R'(z^*)| > 1$. The sense-reversing images correspond to saddle images (i.e., the Jacobian of η is indefinite), whereas sense-preserving images correspond to minimum or maximum images (where the Jacobian is definite). Recall that an image is called a minimal, saddle or maximal image if it is a (local) minimum, saddle point or (local) maximum of the time delay function (induced from the lens potential corresponding to η); see e.g. [10, 11]. The characterization via $|R'|$ then follows from the equality of the Jacobian determinant of the lensing map and the determinant of the Hessian of the time delay function.

Note that the functional determinant vanishes at an image z^* only if ζ lies on a caustic (i.e., infinite magnification), and we will assume in the following that this is not the case. Further we will assume in the following that $|\gamma| \neq 1$.

We will now rephrase Theorems 3.1 and 3.14 of [13] into the setting of gravitational microlensing. In short, the following theorem can be summarized as follows: If a sufficiently small mass is inserted at position z_{n+1} of the lens plane, there will always appear some "new" images nearby z_{n+1}, and all the previously existing images will only alter their positions slightly (except for possibly z_{n+1}, if it is an image position itself). The number of new images depends on certain properties of the lensing map at z_{n+1}, which we can fully classify.

Theorem 2.1. *Let $\eta_n(z) = z - \gamma\overline{z} - \sum_{j=1}^{n} \frac{m_j}{\overline{z} - \overline{z}_j} = z - \overline{R(z)}$ be the lensing map corresponding to $n \geq 2$ point masses $m_j > 0$ at positions $z_j \in \mathbb{C}$ with external shear $|\gamma| \neq 1$. Denote by $m_{n+1} > 0$ a tiny mass and $z_{n+1} \in \mathbb{C}$, $z_{n+1} \neq z_j$ for $1 \leq j \leq n$, a point on the lens plane at which the mass is added, i.e., consider the lensing map*

$$\eta_{n+1}(z) = \eta_n(z) - \frac{m_{n+1}}{\overline{z} - \overline{z}_{n+1}}.$$

If m_{n+1} is sufficiently small, and if the source ζ does not lie on a caustic of η_n or η_{n+1}, then there exists an open disk D around z_{n+1} such that $D\backslash\{z_{n+1}\}$ contains no mass point of η_n and no image of ζ under η_n. Further η_n and η_{n+1} have the same number of images outside D, and the following holds:

1. *If z_{n+1} is not an image of ζ under η_n, then η_{n+1} has at least one image of ζ in D.*
2. *If z_{n+1} is a sense-reversing image of ζ under η_n, then η_{n+1} has at least two images of ζ in D.*
3. *If z_{n+1} is a sense-preserving image of ζ under η_n, and $|R'(z_{n+1})| \neq 0$, then η_{n+1} has at least four images of ζ in D.*
4. *If z_{n+1} is a sense-preserving image of ζ under η_n, $R'(z_{n+1}) = \cdots = R^{(d-2)}(z_{n+1}) = 0$, and $R^{(d-1)}(z_{n+1}) \neq 0$, then η_{n+1} has at least $2d$ images of ζ in D.*

Remark 2.2.

1. The lens (3) in the introduction is covered by case 4 in the preceding theorem with $m_{n+1} = \varepsilon$ and $d = n$. For this lens, appropriate values of m_{n+1} are completely characterized in [8].
2. In cases 2–4, the point z_{n+1} is –of course– no longer a solution of the lens equation $\eta_{n+1}(z) = \zeta$.
3. The lenses modeld by η_n and η_{n+1} have the same number of images outside D, and these images are located at approximately the same positions and retain their type (sense-reversing or sense-preserving).
4. If one and two images are created in cases 1 and 2, respectively, these images are sense-reversing. In cases 3 and 4 an equal number of sense-reversing and sense-preserving images are created; see [13, thms. 3.1,3.14].
5. In all cases of the above theorem, it is guaranteed that "at least" a certain number of images are created (provided that m_{n+1} is sufficiently small). We believe that in fact no more than the stated number of images are created, and extensive numerical experiments support this claim. A mathematical proof of this claim is, however, a topic of future research.
6. The effect of adding a mass larger than the "sufficiently small" mass in the previous theorem is twofold: Either the mass is so large that the lens is globally affected and images of η_n "far away" from z_{n+1} may disappear. Otherwise, even if the effect is still local to z_{n+1} with respect to η_n, *more* than the claimed number of images may be created; see [13, sect. 4.2] or [8, fig. 5]. This effect is also shown in the example in section 3. A quantification of this effect is subject of further research; see also [13].
7. The proofs in [13] show that in each of the cases the created images are located nearby (possibly rotated) roots of unity with radius *approximately* $\sqrt{m_{n+1}}$. The smaller the added mass m_{n+1} is, the closer

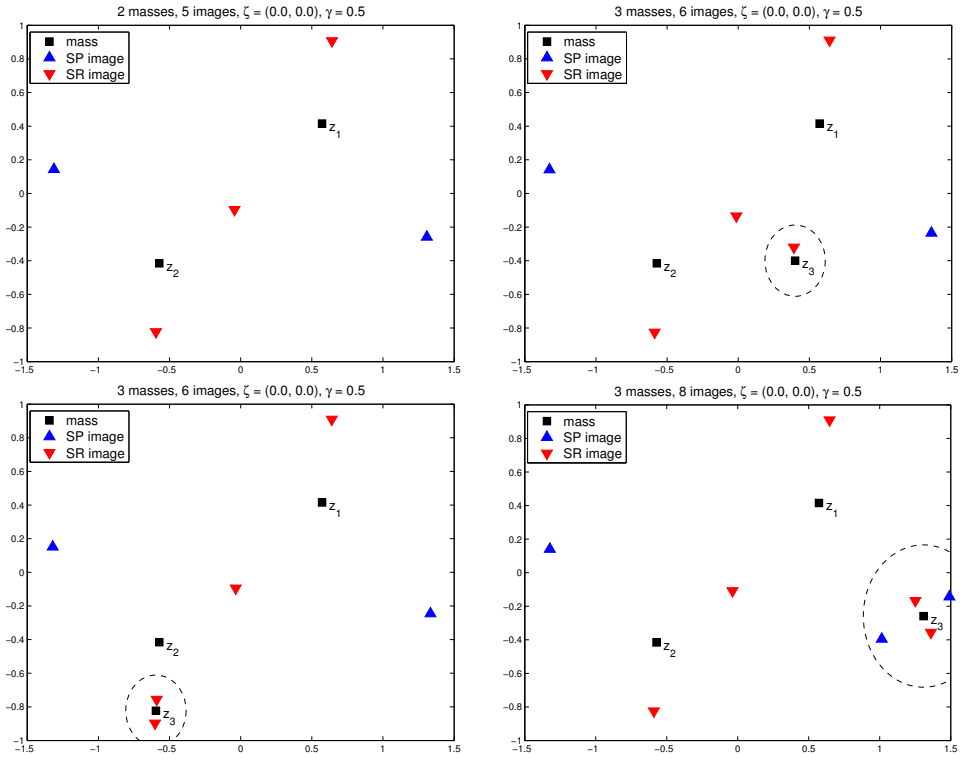

Figure 1: Illustration for Theorem 2.1. The black squares indicate mass points, and triangles show the location of the induced images of the light source. The images are classified by "SP" (sense-preserving, blue, upward pointing) and "SR" (sense-reversing, red, downward pointing). The initial binary lens is shown in the top left picture. The other pictures show the lens after adding a mass at the indicated point z_3, which is no image (top right), a sense-reversing image (bottom left) and a sense-preserving image (bottom right) of the initial lens.

the images assume these positions. The radii of the new images can be quantified; see [13, thm. 3.1].

Numerical examples for the cases 1–3 are shown in Fig. 1. The initial lens (top left image) is a binary lens with masses $m_1 = 0.6$ and $m_2 = 0.4$, external shear $\gamma = 0.5$, and a light source at $\zeta = 0$. The other three pictures (top right, bottom left, bottom right) display the effect of adding a small mass of $m_3 = 0.02$ at a position z_3 for each of the cases 1–3. As implied by Theorem 2.1, one, two and four images are created nearby the mass position z_3, while the other images only alter their positions slightly. Examples for the case 4 with exactly one vanishing derivative of R are given in Section 3.

3 Construction of maximal point lenses

In the introduction we noted that the only known examples for maximal point lens models seem to arise from modifications of the point lens of Mao, Petters and Witt [9]. In this section we show how to construct from a given maximal point lens on n masses another maximal point lens on $n+1$ masses by adding a tiny mass to the given lens. The conditions we give are in fact a special case of Theorem 2.1, but applying this theorem to this *maximal lensing* case simplifies the conditions imposed on the lensing map η_n considerably and deserves a statement on its own. In the statement of this theorem we set the external shear γ to zero, but an analogous statement holds for gravitational lenses with external shear.

Theorem 3.1. *Let $\eta_n(z) = z - \sum_{j=1}^{n} \frac{m_j}{\overline{z}-\overline{z}_j} = z - \overline{R(z)}$ model a point lens on n masses $m_j > 0$ at positions $z_j \in \mathbb{C}$, that produces the maximal number of $5n-5$ images. Let $z_{n+1} \in \mathbb{C}$ be an image with $R'(z_{n+1}) = 0$. Then for all sufficiently small masses $m_{n+1} > 0$, the lens modeled by the lensing map $\eta_{n+1}(z) = \eta_n(z) - \frac{m_{n+1}}{\overline{z}-\overline{z}_{n+1}}$, which is of degree $n+1$, produces the maximal number of $5n$ images, provided that the source ζ does not lie on a caustic of η_n or η_{n+1}.*

Note that $R''(z_{n+1}) \neq 0$, because η_n is a maximal lens. Also, the image z_{n+1} is necessarily an unmagnified image, since the magnification of z_{n+1} is

$$\mathrm{Mag}(z_{n+1}, \zeta) = |\det D\eta(z_{n+1})|^{-1} = |1 - |R'(z_{n+1})|^2|^{-1} = 1.$$

The theorem is illustrated in Figure 2. The initial lens is depicted in the top left image. This binary lens with masses $m_1 = 0.6$ and $m_2 = 0.4$ at positions z_1 and z_2 and zero external shear produces five images of the source, thus it is a maximal lens. The projected position of the light source ζ on the lens plane is the origin. At the image z_3 indicated in the plot, we have $|R'(z_3)| \approx 5 \cdot 10^{-16}$, so the image z_3 satisfies (numerically) the condition of Theorem 3.1.

The result of adding a third mass of $m_3 = 0.05$ at z_3 is shown in the top right picture. As implied by the theorem, six "new" images around the newly created mass appear. As the "old" images only alter their positions slightly, but no image disappears (except for z_3), the constructed lens is maximal again.

After adding the mass m_3 at the position z_3 to the lens plane, the derivative of R does not vanish at any of the ten images. However, for the image z_4 indicated in the plot, we have $|R'(z_4)| \approx 0.0954$, which is already quite small. By shifting the projected source position ζ slightly within the caustic from $(0,0)$ to approximately $(0.00537, 0.00989)$, the image z_4 moves to a nearby point in the lens plane, at which R' vanishes. Adding a mass of size $m_4 = 0.005$ at this displaced image again produces 6 new images in the

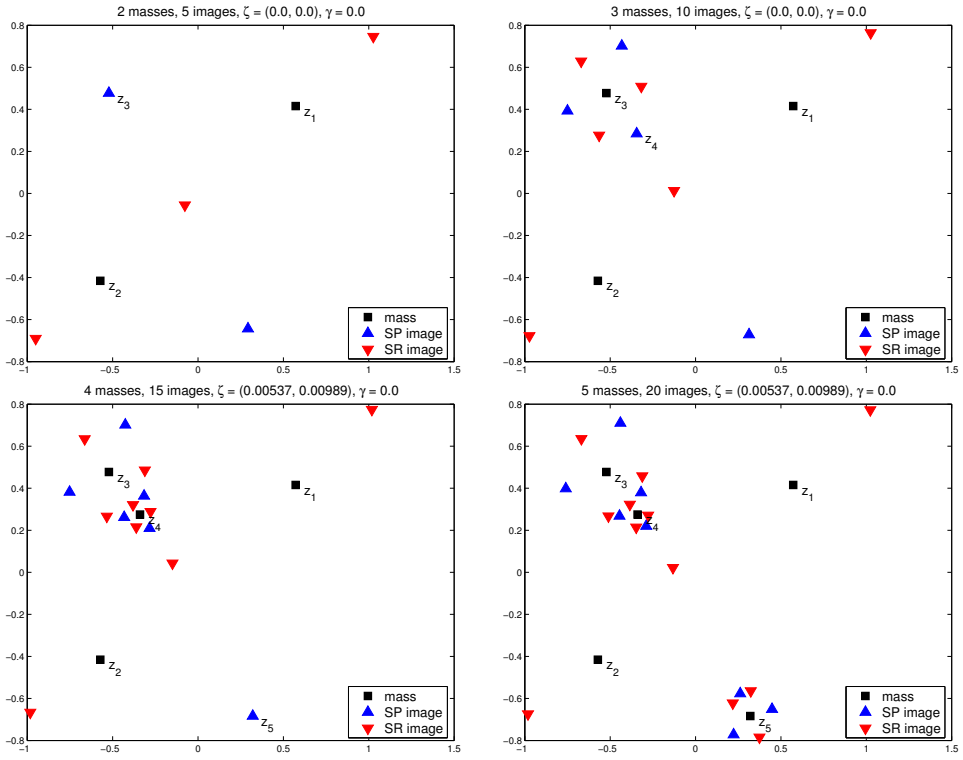

Figure 2: Numerical example for the image-creating effect of adding small masses at certain images of a maximal lens. See Section 3 for a detailed discussion. The symbols used are the same as in Fig. 1.

vicinity of the newly added mass, and thus we have constructed a maximal point lens on four masses. The resulting lens configuration is shown in the bottom left plot.

Finally we wish to emphasize that the condition specified in Theorem 3.1, viz., that the derivative must vanish at the point where the mass is to be added, is only *sufficient* for obtaining again a maximal lens, but not necessary. It may well be that the maximum number of images, six, is already produced if the derivative is sufficiently small. This aspect is exemplified by the image z_5 in the bottom left plot. Here we have $|R'(z_5)| \approx 0.09$, but yet adding a small mass of $m_5 = 0.015$ produces six new images. Fewer images (four) are created, however, if m_5 is somewhat smaller, as implied by case 3 of Theorem 2.1. The resulting maximal lens is shown in the bottom right picture.

4 Conclusions and outlook

In this note we have presented a complete characterization of the image creating effect when a mass is inserted into a given microlensing model. The assumptions in the mathematical assertions cover microlensing models with and without shear and are applicable to any number of point masses. Our findings generalize a particular construction for maximal point lenses by Rhie and we have given a general methodology for the construction of maximal point lens models.

The two most important open questions in the context of Theorem 2.1 are, firstly, to prove that the lower bounds on the number of created images are in fact equalities and, secondly, to quantify the allowable mass such that the claimed number of images are created.

Finally we mention that the question of maximal lensing in models with objects of radial mass density is much less understood than in point lens models [4].

Ackowledgements Robert Luce's work is supported by Deutsche Forschungsgemeinschaft, Cluster of Excellence "UniCat".

References

[1] Jin H. An and N. Wyn Evans. The Chang-Refsdal lens revisited. *Monthly Notices of the Royal Astronomical Society*, 369(1):317–334, 2006.

[2] Johann Bayer and Charles C. Dyer. Maximal lensing: mass constraints on point lens configurations. *Gen. Relativity Gravitation*, 39(9):1413–1418, 2007.

[3] Johann Bayer and Charles C. Dyer. Erratum: Maximal lensing: mass constraints on point lens configurations. *Gen. Relativity Gravitation*, 41(3):669, 2009.

[4] Dmitry Khavinson and Erik Lundberg. Gravitational lensing by a collection of objects with radial densities. *Anal. Math. Phys.*, 1(2-3):139–145, 2011.

[5] Dmitry Khavinson and Genevra Neumann. On the number of zeros of certain rational harmonic functions. *Proc. Amer. Math. Soc.*, 134(4):1077–1085, 2006.

[6] Dmitry Khavinson and Genevra Neumann. From the fundamental theorem of algebra to astrophysics: a "harmonious" path. *Notices Amer. Math. Soc.*, 55(6):666–675, 2008.

[7] Robert Luce, Olivier Sète, and Jörg Liesen. A Note on the Maximum Number of Zeros of $r(z) - \bar{z}$. *ArXiv e-prints*, October 2014. To appear in Comput. Methods Funct. Theory.

[8] Robert Luce, Olivier Sète, and Jörg Liesen. Sharp parameter bounds for certain maximal point lenses. *Gen. Relativity Gravitation*, 46(5):1–16, 2014.

[9] S. Mao, A. O. Petters, and H. J. Witt. Properties of point mass lenses on a regular polygon and the problem of maximum number of images. In *The Eighth Marcel Grossmann Meeting, Part A, B (Jerusalem, 1997)*, pages 1494–1496. World Sci. Publ., River Edge, NJ, 1999.

[10] A. O. Petters and M. C. Werner. Mathematics of gravitational lensing: multiple imaging and magnification. *Gen. Relativity Gravitation*, 42(9):2011–2046, 2010.

[11] Arlie O. Petters, Harold Levine, and Joachim Wambsganss. *Singularity theory and gravitational lensing*, volume 21 of *Progress in Mathematical Physics*. Birkhäuser Boston, Inc., Boston, MA, 2001.

[12] S. H. Rhie. n-point Gravitational Lenses with 5(n-1) Images. *ArXiv Astrophysics e-prints*, May 2003.

[13] Olivier Sète, Robert Luce, and Jörg Liesen. Perturbing rational harmonic functions by poles. *Comput. Methods Funct. Theory*, 15(1):9–35, 2015.

[14] Norbert Straumann. Complex formulation of lensing theory and applications. *Helv. Phys. Acta*, 70(6):894–908, 1997.

[15] Joachim Wambsganss. Gravitational lensing in astronomy. *Living Reviews in Relativity*, 1(12 (cited on May 12, 2014)), 1998.

On conformal maps from multiply connected domains onto lemniscatic domains*

Olivier Sète† Jörg Liesen†

Abstract

We study conformal maps from multiply connected domains in the extended complex plane onto lemniscatic domains. Walsh proved the existence of such maps in 1956 and thus obtained a direct generalization of the Riemann mapping theorem to multiply connected domains. For certain polynomial pre-images of simply connected sets we derive a construction principle for Walsh's conformal map in terms of the Riemann map for the simply connected set. Moreover, we explicitly construct examples of Walsh's conformal map for certain radial slit domains and circular domains.

Keywords conformal mapping; multiply connected domains; lemniscatic domains.

Mathematics Subject Classification (2010) 30C35; 30C20

1 Introduction

Let $\mathcal{K}$ be any simply connected domain (open and connected set) in the extended complex plane $\widehat{\mathbb{C}}$ with $\infty \in \mathcal{K}$ and with at least two boundary points. Then the Riemann mapping theorem guarantees the existence of a conformal map Φ from $\mathcal{K}$ onto the exterior of the unit disk, which is uniquely determined by the normalization conditions $\Phi(\infty) = \infty$ and $\Phi'(\infty) > 0$. The exterior of the unit disk therefore is considered *the canonical domain* every such domain $\mathcal{K}$ can be conformally identified with (in the Riemann sense). For domains $\mathcal{K}$ that are not simply connected the conformal identification

*A final version of this preprint manuscript appeared as follows: O. Sète and J. Liesen. On conformal maps from multiply connected domains onto lemniscatic domains *Electron. Trans. Numer. Anal.* (2016) 45, pp. 1–15.

†TU Berlin, Institute of Mathematics, MA 4-5, Straße des 17. Juni 136, 10623 Berlin, Germany. {sete,liesen}@math.tu-berlin.de

with a suitable canonical domain is significantly more challenging. This fact has been well described already by Nehari in his classical monograph on conformal mappings from 1952 [31, Chapter 7], which identified five of the "more important" canonical slit domains (originally due to Koebe [23, p. 311]).

In recent years there has been a surge of interest in the theory and computation of conformal maps for multiply connected sets, which has been driven by the wealth of applications of conformal mapping techniques throughout the mathematical sciences. Many recent publications have dealt with canonical slit domains as those described by Nehari; see, e.g., [1, 5, 9, 12, 28, 29]. A related line of recent research in this context has focussed on the theory and computation of Schwarz-Christoffel mapping formulas from (the exterior of) finitely many non-intersecting disks (circular domains, see, e.g., [19]) onto (the exterior of) the same number of non-intersecting polygons; see, e.g., [3, 4, 7, 8, 10]. A review and comparison of both approaches is given in [11].

In this work we explore yet another idea which goes back to a paper of Walsh from 1956 [37]. Walsh's canonical domain is a *lemniscatic domain* of the form

$$\mathcal{L} := \{w \in \widehat{\mathbb{C}} : |U(w)| > \mu\}, \quad \text{where} \quad U(w) := \prod_{j=1}^{n} (w - a_j)^{m_j}, \tag{1}$$

$a_1, \ldots, a_n \in \mathbb{C}$ are pairwise distinct, $m_1, \ldots, m_n > 0$ satisfy $\sum_{j=1}^{n} m_j = 1$, and $\mu > 0$. Note that the function U in the definition of $\mathcal{L}$ is an analytic but in general multiple-valued function. Its absolute value is, however, single-valued. Walsh proved that if $\mathcal{K}$ is the exterior of $n \geq 1$ non-intersecting simply connected components, then $\mathcal{K}$ can be conformally identified with *some* lemniscatic domain $\mathcal{L}$ of the form (1); see Theorem 2.1 below for the complete statement. Walsh's theorem is a direct generalization of the Riemann mapping theorem, and for $n = 1$ the two results are in fact equivalent. Alternative proofs of Walsh's theorem were given by Grunsky [15, 16] (see also [17, Theorem 3.8.3]), Jenkins [21] and Landau [24]. For some further remarks on Walsh's theorem we refer to Gaier's commentary in Walsh's Selected Papers [39, pp. 374-377].

To our knowledge, apart from the different *existence proofs*, conformal maps related to Walsh's lemniscatic domains, which we call *lemniscatic maps*, have rarely been studied. In particular, we are not aware of any example for lemniscatic maps in the previously published literature. In this work we derive a general construction principle for lemniscatic maps for

polynomial pre-images of simply connected sets and we construct some explicit examples. We believe that our results are of interest not only from a theoretical but also from a practical point of view. Walsh's lemniscatic map easily reveals the logarithmic capacity of $E = \widehat{\mathbb{C}}\backslash\mathcal{K}$ as well as the Green's function with pole at infinity for $\mathcal{K}$, whose contour lines or level curves are important in polynomial approximation. Moreover, analogously to the construction of the classical Faber polynomials on compact and simply connected sets (cf. [6, 35]), lemniscatic maps allow to define generalized Faber polynomials on compact sets with several components; see [38]. While the classical Faber polynomials have found a wide range of applications in particular in numerical linear algebra (see, e.g., [2, 20, 26, 27, 34]) and more general numerical polynomial approximation (see, e.g., [13, 14]), the *Faber–Walsh polynomials* have not been used for similar purposes yet, as no explicit examples for lemniscatic maps have been known. In our follow-up paper [33] we present more details on the theory of Faber–Walsh polynomials as well as explicitly computed examples.

In Section 2 we state Walsh's theorem, and discuss general properties of the conformal map onto lemniscatic domains. We then consider the explicit construction of lemniscatic maps: In Section 3 we derive a construction principle for the lemniscatic map for certain polynomial pre-images of simply connected compact sets. In Section 4 we construct the lemniscatic map for the exterior of two equal disks. Some brief concluding remarks in Section 5 close the paper.

2 General properties of the conformal map onto lemniscatic domains

Let us first consider a lemniscatic domain $\mathcal{L}$ as in (1). It is easy to see that its Green's function with pole at infinity is given by

$$g_{\mathcal{L}}(w) = \log|U(w)| - \log(\mu).$$

Moreover,

$$c(\widehat{\mathbb{C}}\backslash\mathcal{L}) := \lim_{w\to\infty} \exp(\log|w| - g_{\mathcal{L}}(w)) = \mu$$

is the logarithmic capacity of $\widehat{\mathbb{C}}\backslash\mathcal{L}$. The following theorem on the conformal equivalence of lemniscatic domains and certain multiply connected domains is due to Walsh [37, Theorems 3 and 4].

Theorem 2.1. *Let $E := \cup_{j=1}^{n} E_j$, where $E_1, \ldots, E_n \subseteq \mathbb{C}$ are mutually exterior simply connected compact sets (none a single point) and let $\mathcal{K} := \widehat{\mathbb{C}} \backslash E$. Then there exist a unique lemniscatic domain $\mathcal{L}$ of the form* (1) *and a unique bijective conformal map*

$$\Phi : \mathcal{K} \to \mathcal{L} \quad \text{with} \quad \Phi(z) = z + \mathcal{O}\left(\frac{1}{z}\right) \quad \text{for } z \text{ near infinity.} \tag{2}$$

In particular,

$$g_{\mathcal{K}}(z) = g_{\mathcal{L}}(\Phi(z)) = \log|U(\Phi(z))| - \log(\mu) \tag{3}$$

is the Green's function with pole at infinity of $\mathcal{K}$, and the logarithmic capacity of E is $c(E) = c(\widehat{\mathbb{C}} \backslash \mathcal{L}) = \mu$. The function Φ is called the lemniscatic map *of $\mathcal{K}$ (or of E).*

Note that for $n = 1$ the lemniscatic domain $\mathcal{L}$ is the exterior of a disk with radius $\mu > 0$, and Theorem 2.1 is equivalent to the classical Riemann mapping theorem.

If, for the given set $\mathcal{K}$, the function $\widetilde{\Phi} : \mathcal{K} \to \widetilde{\mathcal{L}}$ is any conformal map onto a lemniscatic domain that is normalized by $\widetilde{\Phi}(\infty) = \infty$ and $\widetilde{\Phi}'(\infty) = 1$, then $\widetilde{\Phi}(z) = \Phi(z) + b$ with Φ from Theorem 2.1 and some $b \in \mathbb{C}$. This uniqueness up to translation of lemniscatic domains follows from a more general theorem of Walsh [37, Theorem 4] by taking into account the normalization of $\widetilde{\Phi}$. This fact has already been noted by Motzkin in his MathSciNet review of [38].

Let $\sigma > 1$, and let

$$\Gamma_\sigma = \{z \in \mathcal{K} : g_{\mathcal{K}}(z) = \log(\sigma)\} \quad \text{and} \quad \Lambda_\sigma = \{w \in \mathcal{L} : g_{\mathcal{L}}(w) = \log(\sigma)\}$$

be the level curves of $g_{\mathcal{K}}$ and $g_{\mathcal{L}}$, respectively. Then (3) implies $\Phi(\Gamma_\sigma) = \Lambda_\sigma$, and thus

$$\Phi : \operatorname{ext}(\Gamma_\sigma) \to \operatorname{ext}(\Lambda_\sigma) = \{w \in \widehat{\mathbb{C}} : |U(w)| > \sigma\mu\}$$

is the lemniscatic map of the exterior of Γ_σ, provided that Γ_σ still has n components. (This holds exactly when the zeros of $g'_{\mathcal{K}}$ lie exterior to Γ_σ.) Thus, we may "thicken" the given set $E = \widehat{\mathbb{C}} \backslash \mathcal{K}$, and Φ still is the corresponding lemniscatic map. An illustration is given in Figure 1 for a compact set composed of three radial slits from Corollary 3.3 below (with parameters $n = 3$, $C = 1$ and $D = 2$) and for Γ_σ with $\sigma = 1.15$.

The next result shows that certain symmetry properties of the domain $\mathcal{K}$ imply corresponding properties of its lemniscatic map Φ and the lemniscatic domain $\mathcal{L}$. Here we consider rotational symmetry as well as symmetry with respect to the real and the imaginary axis.

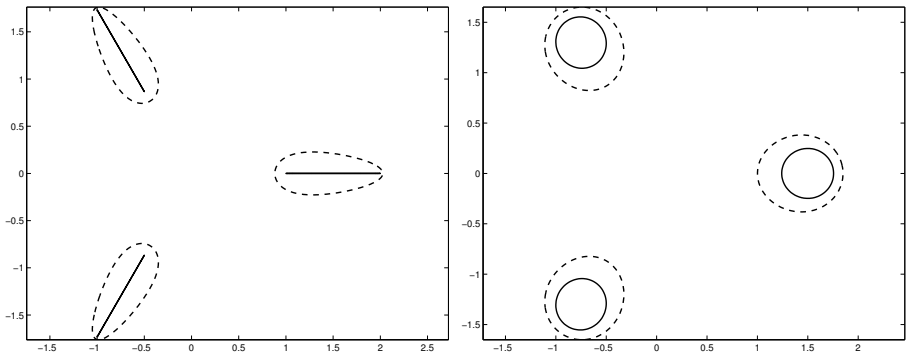

Figure 1: Left: The set E consisting of three radial slits (solid) and the "thickened" set bounded by Γ_σ for $\sigma = 1.15$ (dashed). Right: The corresponding lemniscatic domains.

Lemma 2.2. *In the notation of Theorem 2.1 we have:*

1. *If* $\mathcal{K} = e^{i\theta}\mathcal{K} := \{e^{i\theta}z : z \in \mathcal{K}\}$, *then* $\Phi(z) = e^{-i\theta}\Phi(e^{i\theta}z)$ *and* $\mathcal{L} = e^{i\theta}\mathcal{L}$.
2. *If* $\mathcal{K} = \mathcal{K}^* := \{\overline{z} : z \in \mathcal{K}\}$, *then* $\Phi(z) = \overline{\Phi(\overline{z})}$ *and* $\mathcal{L} = \mathcal{L}^*$.
3. *If* $\mathcal{K} = -\mathcal{K}^*$, *then* $\Phi(z) = -\overline{\Phi(-\overline{z})}$ *and* $\mathcal{L} = -\mathcal{L}^*$.

In each case Φ^{-1} *has the same symmetry property as* Φ.

Proof. We only prove the first assertion; the proofs of the others are similar. Define the function $\widetilde{\Phi}$ on $\mathcal{K}$ by $\widetilde{\Phi}(z) := e^{-i\theta}\Phi(e^{i\theta}z)$. Then

$$\widetilde{\Phi}(\mathcal{K}) = e^{-i\theta}\Phi(e^{i\theta}\mathcal{K}) = e^{-i\theta}\Phi(\mathcal{K}) = e^{-i\theta}\mathcal{L},$$

and $\widetilde{\Phi} : \mathcal{K} \to e^{-i\theta}\mathcal{L}$ is a bijective conformal map onto a lemniscatic domain with a normalization as in (2). Since the lemniscatic map of $\mathcal{K}$ is unique, we have $\Phi(z) = \widetilde{\Phi}(z) = e^{-i\theta}\Phi(e^{i\theta}z)$ and $\mathcal{L} = e^{-i\theta}\mathcal{L}$, or equivalently $\mathcal{L} = e^{i\theta}\mathcal{L}$.

Suppose that $\Phi(z) = e^{-i\theta}\Phi(e^{i\theta}z)$ for all $z \in \mathcal{K}$. Writing $w = \Phi(z)$ we get

$$\Phi^{-1}(e^{i\theta}w) = \Phi^{-1}(e^{i\theta}\Phi(z)) = \Phi^{-1}(\Phi(e^{i\theta}z)) = e^{i\theta}z = e^{i\theta}\Phi^{-1}(w),$$

which completes the proof. □

Finally, we show how a linear transformation of the set affects the lemniscatic map.

Lemma 2.3. *In the notation of Theorem 2.1, consider a linear transformation $\tau(w) = aw + b$ with $a \neq 0$, then*

$$\tau(\mathcal{L}) = \Big\{ \widetilde{w} \in \widehat{\mathbb{C}} : \prod_{j=1}^{n} |\widetilde{w} - \tau(a_j)|^{m_j} > |a|\mu \Big\}$$

is a lemniscatic domain and $\widetilde{\Phi} := \tau \circ \Phi \circ \tau^{-1}$ is the lemniscatic map of $\tau(\mathcal{K})$.

Proof. With $\widetilde{w} = \tau(w) = aw + b$ we have

$$\prod_{j=1}^{n} |\widetilde{w} - \tau(a_j)|^{m_j} = \prod_{j=1}^{n} |aw - aa_j|^{m_j} = |a| \prod_{j=1}^{n} |w - a_j|^{m_j},$$

and hence $\tau(\mathcal{L})$ is a lemniscatic domain. Clearly, $\widetilde{\Phi} : \tau(\mathcal{K}) \to \tau(\mathcal{L})$ is a bijective and conformal map with Laurent series at infinity

$$\widetilde{\Phi}(z) = a\Phi\Big(\frac{z-b}{a}\Big) + b = z + \mathcal{O}\left(\frac{1}{z}\right).$$

Thus, $\widetilde{\Phi}$ is the lemniscatic map of $\tau(\mathcal{K})$. □

Lemma 2.3 can be applied to the lemniscatic maps we will derive in Sections 3 and 4 in order to obtain lemniscatic maps for further sets.

3 Lemniscatic maps and polynomial pre-images

In this section we discuss the construction of lemniscatic maps if the set E is a polynomial pre-image of a simply connected compact set Ω. We first exhibit the intricate relation between the lemniscatic map for E and the exterior Riemann map for Ω in the general case. Under some additional assumptions we obtain an explicit formula for the lemniscatic map in terms of the Riemann map; see Theorem 3.1 below.

Let $\Omega \subseteq \mathbb{C}$ be a compact and simply connected set (not a single point) and let

$$\widetilde{\Phi} : \widehat{\mathbb{C}} \backslash \Omega \to \{ w \in \widehat{\mathbb{C}} : |w| > 1 \} \quad \text{with} \quad \widetilde{\Phi}(\infty) = \infty, \quad \widetilde{\Phi}'(\infty) > 0, \tag{4}$$

be the exterior Riemann map of Ω. Suppose that

$$E := P^{-1}(\Omega)$$

consists of $n \geq 2$ simply connected compact components (none a single point), where $P(z) = \alpha_d z^d + \alpha_{d-1} z^{d-1} + \ldots + \alpha_0$ is a polynomial with $\alpha_d \neq 0$. As above, let $\mathcal{K} := \widehat{\mathbb{C}} \backslash E$ and let

$$\Phi : \mathcal{K} \to \mathcal{L} = \{w \in \widehat{\mathbb{C}} : |U(w)| > \mu\}$$

be the lemniscatic map of $\mathcal{K}$. Then the Green's function with pole at infinity for $\mathcal{K}$ is given by (3), and can also be expressed as

$$g_{\mathcal{K}}(z) = \log|U(\Phi(z))| - \log(\mu) = \frac{1}{d} g_{\widehat{\mathbb{C}} \backslash \Omega}(P(z)) = \frac{1}{d} \log|\widetilde{\Phi}(P(z))|;$$

see the proof of Theorem 5.2.5 in [32]. This shows that Φ and $\widetilde{\Phi}$ are related by

$$|U(\Phi(z))| = \mu |\widetilde{\Phi}(P(z))|^{1/d}, \tag{5}$$

where

$$\mu = c(E) = \left(\frac{c(\Omega)}{|\alpha_d|}\right)^{1/d} = \left(\frac{1}{|\alpha_d| \widetilde{\Phi}'(\infty)}\right)^{1/d};$$

see [32, Theorem 5.2.5]. If $\widetilde{\Phi}$ and P are known, the equality (5) yields a formula for (the modulus of) $U \circ \Phi$. However, this does not lead to *separate* expressions for U and Φ. In other words, we can in general neither obtain the lemniscatic domain nor the lemniscatic map directly via (5) from the knowledge of $\widetilde{\Phi}$ and P.

For certain sets Ω and polynomials P, we obtain by a direct construction explicit formulas for U and Φ in terms of the Riemann map $\widetilde{\Phi}$.

Theorem 3.1. *Let $\Omega = \Omega^* \subseteq \mathbb{C}$ be compact and simply connected (not a single point) with exterior Riemann map $\widetilde{\Phi}$ as in (4). Let $P(z) = \alpha z^n + \alpha_0$ with $n \geq 2$, $\alpha_0 \in \mathbb{R}$ to the left of Ω, and $\alpha > 0$.*

Then $E := P^{-1}(\Omega)$ is the disjoint union of n simply connected compact sets, and

$$\Phi : \widehat{\mathbb{C}} \backslash E \to \mathcal{L} = \{w \in \widehat{\mathbb{C}} : |U(w)| > \mu\}, \tag{6}$$

$$\Phi(z) = z\Big(\frac{\mu^n}{z^n}[(\widetilde{\Phi} \circ P)(z) - (\widetilde{\Phi} \circ P)(0)]\Big)^{\frac{1}{n}}, \tag{7}$$

is the lemniscatic map of E, where we take the principal branch of the nth root, and where

$$\mu := \Big(\frac{1}{\alpha \widetilde{\Phi}'(\infty)}\Big)^{\frac{1}{n}} > 0, \quad \textit{and} \quad U(w) := (w^n + \mu^n (\widetilde{\Phi} \circ P)(0))^{\frac{1}{n}}. \tag{8}$$

Proof. We construct the lemniscatic map Φ first in the sector

$$S = \Big\{ z \in \mathbb{C}\backslash\{0\} : -\frac{\pi}{n} < \arg(z) < \frac{\pi}{n} \Big\},$$

and then extend it by the Schwarz reflection principle.

Since $z \in E$ if and only if $z^n \in \frac{1}{\alpha}(\Omega - \alpha_0)$, the set E has a single component E_1 in the sector S, obtained by taking the principal branch of the nth root. Note that $E_1 = E_1^* \subseteq S$ is again a simply connected compact set. Then $E = \cup_{j=1}^n e^{i2\pi j/n} E_1$ is the disjoint union of n simply connected compact sets.

Starting in $S\backslash E_1$, we construct the lemniscatic map as a composition of bijective conformal maps, see Figure 2:

1. The function $z_1 = P(z)$ maps $S\backslash E_1$ onto the complement of $]-\infty, \alpha_0] \cup \Omega$.

2. Then $z_2 = \widetilde{\Phi}(z_1)$ maps this domain onto the complement of $]-\infty, \widetilde{\Phi}(\alpha_0)] \cup \{z_2 : |z_2| \le 1\}$. Note that $\Omega = \Omega^*$ implies that $\widetilde{\Phi}(z) = \overline{\widetilde{\Phi}(\overline{z})}$, so that $]-\infty, \alpha_0]$ is mapped to the real line. In particular, $\widetilde{\Phi}(\alpha_0) < -1$.

3. The function $z_3 = \mu^n(z_2 - \widetilde{\Phi}(\alpha_0))$ maps the previous domain onto the complement of $]-\infty, 0] \cup \{z_3 \in \mathbb{C} : |z_3 + \mu^n \widetilde{\Phi}(\alpha_0)| \le \mu^n\}$. Here $\mu > 0$ is defined by (8).

4. Finally, $w = z_3^{1/n}$, where we take the principal branch of the square root, maps this domain onto $S \cap \{w : |w^n + \mu^n \widetilde{\Phi}(\alpha_0)| > \mu^n\}$.

Since each map is bijective and conformal, their composition Φ is a bijective conformal map from $S\backslash E_1$ to $S \cap \{w \in \widehat{\mathbb{C}} : |U(w)| > \mu\}$. A short computation shows that

$$\Phi(z) = (\mu^n[(\widetilde{\Phi} \circ P)(z) - (\widetilde{\Phi} \circ P)(0)])^{\frac{1}{n}} = z\Big(\frac{\mu^n}{z^n}[(\widetilde{\Phi} \circ P)(z) - (\widetilde{\Phi} \circ P)(0)]\Big)^{\frac{1}{n}}$$

for $z \in S\backslash E_1$. Since Φ maps the half-lines $\arg(z) = \pm\frac{\pi}{n}$ onto themselves, Φ can be extended by Schwarz' reflection principle to a bijective and conformal map from $(\widehat{\mathbb{C}}\backslash E)\backslash\{0, \infty\}$ to $\mathcal{L}\backslash\{0, \infty\}$. Note that Φ is given by (7) for every $z \in (\widehat{\mathbb{C}}\backslash E)\backslash\{0, \infty\}$, since the right hand side of (7) is analytic there. This follows since the expression under the nth root lies in $\mathbb{C}\backslash]-\infty, 0]$ for every $z \in (\widehat{\mathbb{C}}\backslash E)\backslash\{0, \infty\}$.

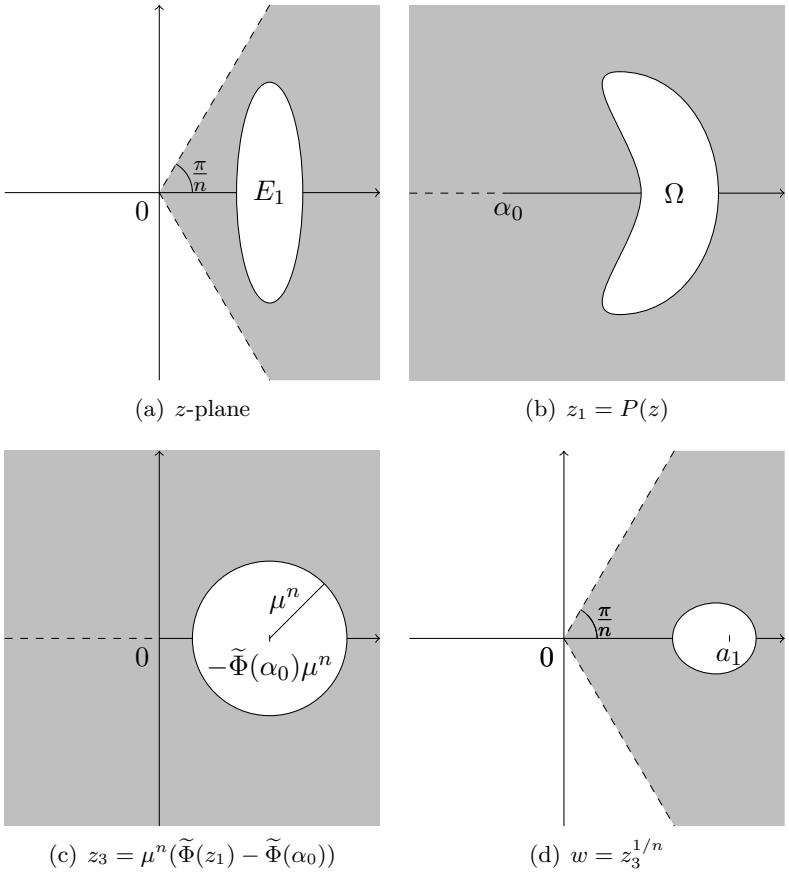

(a) z-plane (b) $z_1 = P(z)$

(c) $z_3 = \mu^n(\widetilde{\Phi}(z_1) - \widetilde{\Phi}(\alpha_0))$ (d) $w = z_3^{1/n}$

Figure 2: Construction of the lemniscatic map in the proof of Theorem 3.1.

It remains to show that Φ is defined and conformal in 0 and ∞, and that it satisfies the normalization in (2). We begin with the point $z = 0$. Near α_0 the Riemann mapping $\widetilde{\Phi}$ has the form

$$\widetilde{\Phi}(z) = \widetilde{\Phi}(\alpha_0) + \widetilde{\Phi}'(\alpha_0)(z - \alpha_0) + \mathcal{O}((z - \alpha_0)^2).$$

Then near 0 we have

$$\Phi(z) = z\Big(\frac{\mu^n}{z^n}[\widetilde{\Phi}'(\alpha_0)\alpha z^n + \mathcal{O}(z^{2n})]\Big)^{\frac{1}{n}} = z\Big(\mu^n\widetilde{\Phi}'(\alpha_0)\alpha + \mathcal{O}(z^n)\Big)^{\frac{1}{n}},$$

so that $\Phi(0) = 0$, and $\Phi'(0) = (\mu^n\widetilde{\Phi}'(\alpha_0)\alpha)^{\frac{1}{n}} \neq 0$, showing that Φ is defined and conformal at 0.

Near $z = \infty$, we have $\widetilde{\Phi}(z) = \widetilde{\Phi}'(\infty)z + \mathcal{O}(1)$, so that, together with (8),

$$\Phi(z) = z\Big(\frac{\mu^n}{z^n}[\widetilde{\Phi}'(\infty)\alpha z^n + \mathcal{O}(1)]\Big)^{\frac{1}{n}} = z\Big(1 + \mathcal{O}\Big(\frac{1}{z^n}\Big)\Big)^{\frac{1}{n}} = z + \mathcal{O}\Big(\frac{1}{z^{n-1}}\Big).$$

Thus Φ satisfies (2) and is a bijective conformal map from $\widehat{\mathbb{C}}\backslash E$ to $\mathcal{L}$, as claimed. □

The assumption $\alpha > 0$ in Theorem 3.1 has been made for simplicity only. In the notation of the theorem, if $P_\theta(z) = \alpha e^{i\theta}z^n + \alpha_0$ with $\theta \in \mathbb{R}$, then $P_\theta(z) = P(e^{i\theta/n}z)$. Hence $P_\theta^{-1}(\Omega) = e^{-i\theta/n}E = \tau(E)$, with $\tau(z) = e^{-i\theta/n}z$. Then the lemniscatic map of $\widehat{\mathbb{C}}\backslash P_\theta^{-1}(\Omega)$ is $\tau \circ \Phi \circ \tau^{-1}$; see Lemma 2.3.

Also note that if Ω is symmetric with respect to the line through the origin and some point $e^{i\theta}$, then, taking α_0 on that line to the left of Ω, the assertion of Theorem 3.1 remains unchanged.

Example 3.2. As an example we consider the compact set Ω in Figure 3(b), which is of the form introduced in [22, Theorem 3.1]. It is defined with the parameters $\lambda = -1$, $\phi = \frac{\pi}{2}$ and $R = 1.1$ through the inverse of its Riemann map

$$\widetilde{\Phi}^{-1}(w) = \frac{(w - \lambda N)(w - \lambda M)}{(N - M)w + \lambda(MN - 1)},$$

where

$$Q = \tan(\phi/4) + \frac{1}{\cos(\phi/4)}, \quad N = \frac{1}{2}\left(\frac{Q}{R} + \frac{R}{Q}\right), \quad M = \frac{R^2 - 1}{2R\tan(\phi/4)}.$$

Then Ω is the compact set bounded by $\widetilde{\Phi}^{-1}(\{w \in \mathbb{C} : |w| = 1\})$, and thus has, in particular, an analytic boundary. Since $\Omega = \Omega^*$ and $\alpha_0 = 0$ lies to the left of Ω, we can apply Theorem 3.1 with $P(z) = z^3$. Figure 3(a) shows the set $E = P^{-1}(\Omega)$, and Figure 3(c) shows the corresponding lemniscatic domain.

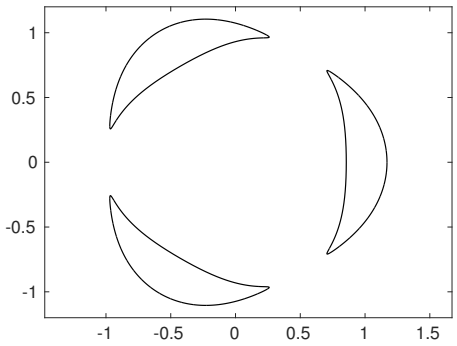

(a) $E = P^{-1}(\Omega)$ with $P(z) = z^3$

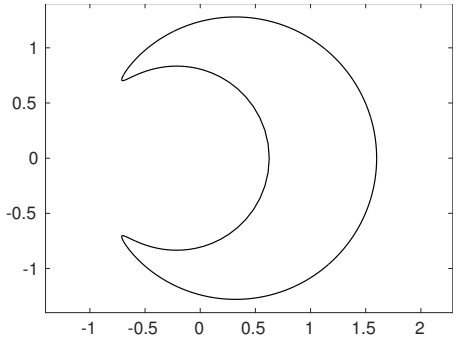

(b) Compact set $\Omega = \Omega^*$.

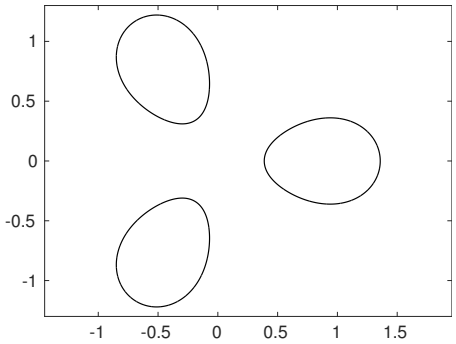

(c) Lemniscatic domain $\mathcal{L}$

Figure 3: Illustration of Theorem 3.1 with a set from [22, Theorem 3.1].

Using Theorem 3.1 we now derive the lemniscatic conformal map for a radial slit domain.

Corollary 3.3. *Let $E = \cup_{j=1}^{n} e^{i2\pi j/n}[C, D]$ with $0 < C < D$. Then*

$$\Phi(z) = z\Big(\frac{1}{2} + \frac{\sqrt{D}^n\sqrt{C}^n}{2}\frac{1}{z^n} \pm \frac{1}{2z^n}\sqrt{(z^n - C^n)(z^n - D^n)}\Big)^{\frac{1}{n}} \tag{9}$$

is the lemniscatic map of E with corresponding lemniscatic domain

$$\mathcal{L} = \left\{ w \in \widehat{\mathbb{C}} : |U(w)| = \left| w^n - \frac{(\sqrt{D}^n + \sqrt{C}^n)^2}{4} \right|^{\frac{1}{n}} > \mu = \Big(\frac{D^n - C^n}{4}\Big)^{\frac{1}{n}} \right\}. \tag{10}$$

The inverse of Φ is given by

$$\Phi^{-1}(w) = w\left(1 + \frac{(\sqrt{D}^n - \sqrt{C}^n)^2}{4}\frac{1}{w^n - \frac{(\sqrt{D}^n + \sqrt{C}^n)^2}{4}}\right)^{\frac{1}{n}}, \tag{11}$$

where we take the principal branch of the nth root.

Proof. With $P(z) = z^n$ and $\Omega = [C^n, D^n]$ we have $E = P^{-1}(\Omega)$, and Theorem 3.1 applies. We need the conformal map

$$\widetilde{\Phi} : \widehat{\mathbb{C}}\backslash[C^n, D^n] \to \{w \in \widehat{\mathbb{C}} : |w| > 1\}, \quad \widetilde{\Phi}(\infty) = \infty, \quad \widetilde{\Phi}'(\infty) > 0.$$

Clearly, its inverse is given by

$$\widetilde{\Phi}^{-1}(w) = \frac{D^n - C^n}{4}\Big(w + \frac{1}{w}\Big) + \frac{D^n + C^n}{2},$$

so that

$$\widetilde{\Phi}(z) = \frac{2}{D^n - C^n}\Big(z - \frac{D^n + C^n}{2} \pm \sqrt{(z - C^n)(z - D^n)}\Big),$$

where the branch of the square root is chosen such that $|\widetilde{\Phi}(z)| > 1$. In particular, $\widetilde{\Phi}'(\infty) = \frac{4}{D^n - C^n}$. Using this in Theorem 3.1 yields (9) and (10). By reversing the construction in the proof of Theorem 3.1, we see that

$$\Phi^{-1}(w) = \Big(\widetilde{\Phi}^{-1}\Big(\frac{w^n}{\mu^n} + \widetilde{\Phi}(0)\Big)\Big)^{\frac{1}{n}},$$

which, after a short computation, yields (11). □

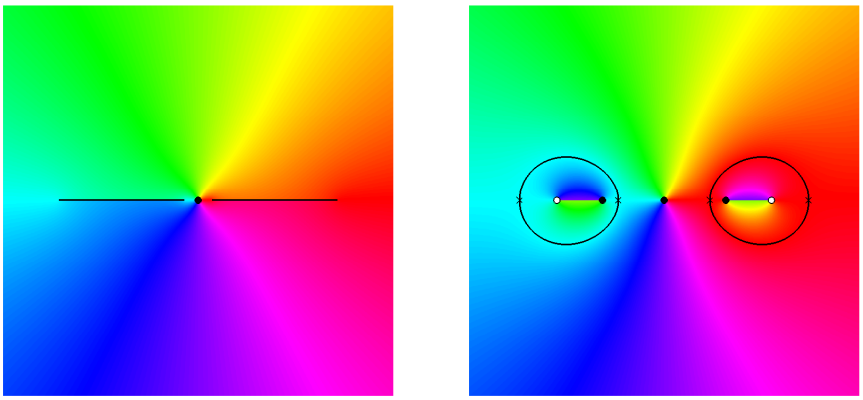

(a) Phase portrait of Φ. (b) Phase portrait of Φ^{-1}.

Figure 4: Phase portraits of Φ and Φ^{-1} from Corollary 3.3 for $n = 2$ and $C = 0.1$ and $D = 1$.

Corollary 3.3 shows, in particular, that $\left(\frac{D^n - C^n}{4}\right)^{1/n}$ is the logarithmic capacity of $E = \cup_{j=1}^{n} e^{i2\pi j/n}[C, D]$; see [18].

Let us have a closer look at Corollary 3.3 in the case $n = 2$, i.e.,

$$E = [-D, -C] \cup [C, D].$$

First note that in this case Corollary 3.3 gives a new proof for the well-known fact that the logarithmic capacity of E is $c(E) = \frac{\sqrt{D^2 - C^2}}{2}$; see, e.g., [32, Corollary 5.2.6] and [18]. Figure 4 shows phase portraits of Φ and $\psi := \Phi^{-1}$ for the values $C = 0.1$ and $D = 1$; see [40, 41] for details on phase portraits. The black lines in the left figure are the two intervals forming E, and the black curves in the right figure are the boundary of $\mathcal{L}$. At the black and white dots the functions have the values 0 and ∞, respectively. The zeros of ψ are 0 and $\pm\sqrt{DC}$. The function $\psi : \mathcal{L} \to \mathcal{K}$ can be continued analytically (but not conformally) to a full neighbourhood of the lemniscate $\{w : |w^2 - \frac{(D+C)^2}{4}| = \frac{D^2 - C^2}{4}\}$. The zeros of ψ' are denoted by black crosses. Note the discontinuity of the phase of ψ between the zeros and singularities interior to the lemniscate. This suggests that ψ will be analytic and single-valued in $\{w \in \widehat{\mathbb{C}} : |U(w)| > \frac{D-C}{2}\}$.

4 Lemniscatic map for two equal disks

In this section we analytically construct the lemniscatic map of a set E that is the union of two disjoint equal disks. Let us denote by $D_r(z_0) = \{z \in \mathbb{C} : |z - z_0| \le r\}$ the closed disk with radius $r > 0$ and center $z_0 \in \mathbb{C}$. By Lemma 2.3 we can assume without loss of generality that $E = D_r(z_0) \cup D_r(-z_0)$ with real z_0 and $0 < r < z_0$. Let $P(z) = \alpha z^2 + \alpha_0$ with $\alpha > 0$, then

$$\Omega = \{\alpha(z_0 + \rho e^{it})^2 + \alpha_0 : 0 \le \rho \le r, 0 \le t \le 2\pi\}$$

is a simply connected compact set with $E = P^{-1}(\Omega)$, so that in principle we could apply Theorem 3.1. However, the Riemann map for the set Ω seems not to be readily available. Therefore, we directly construct the lemniscatic map as a composition of certain conformal maps. The main ingredients are the map from the exterior of two disks onto the exterior of two intervals and from there onto a lemniscatic domain (according to Corollary 3.3).

We need the following conformal map from [31, pp. 293–295].

Lemma 4.1. *Let $0 < \rho < 1$ and define*

$$L = L(\rho) := 2\rho \prod_{n=1}^{\infty} \Big(\frac{1+\rho^{8n}}{1+\rho^{8n-4}}\Big)^2, \tag{12}$$

and the complete elliptic integral of the first kind

$$K = K(k) := \int_0^1 \frac{dt}{\sqrt{(1-t^2)(1-k^2t^2)}} \quad \text{with } k := L^2. \tag{13}$$

Then the function

$$w = f(z) = L\,\mathrm{sn}\Big(\frac{2K}{\pi} i \log\Big(\frac{z}{\rho}\Big) + K; k\Big) \tag{14}$$

is a bijective and conformal map from the annulus $\rho < |z| < \rho^{-1}$ onto the w-plane with the slits $-\infty < w \le -\frac{1}{L}$, $-L \le w \le L$ and $\frac{1}{L} \le w < \infty$. Further, we have $f(-1) = -1$ and $f'(-1) = (1-L^2)\frac{2K}{\pi} > 0$, and $f(z^{-1}) = (f(z))^{-1}$.

Proof. See [31, pp. 293–295] for the existence and mapping properties of f. Note that f is independent of the choice of the branch of the logarithm. By construction f is also symmetric with respect to the real axis and to the unit circle, i.e., $f(z) = \overline{f(\overline{z})}$, and $f(z) = 1/\overline{f(1/\overline{z})}$. This implies $f(1/z) = 1/\overline{f(\overline{z})} = 1/f(z)$.

It remains to compute $f(-1)$ and $f'(-1)$. Recall the identity

$$\operatorname{sn}'(z;k) = \operatorname{cn}(z;k)\operatorname{dn}(z;k),$$

where $\operatorname{cn}(z;k) = \sqrt{1-\operatorname{sn}(z;k)^2}$, $\operatorname{cn}(0) = 1$, and $\operatorname{dn}(z) = \sqrt{1-k^2\operatorname{sn}(z;k)^2}$, $\operatorname{dn}(0) = 1$. We compute

$$f'(z) = L\operatorname{cn}(\zeta(z);k)\operatorname{dn}(\zeta(z);k)\frac{2K}{\pi}i\frac{1}{z}, \quad \text{where} \quad \zeta(z) = \frac{2K}{\pi}i\log\Big(-i\frac{z}{\rho}\Big).$$

For $z=-1$ we have $\zeta(-1) = -K - i\frac{2K}{\pi}\log(\rho) =: -K + i\frac{K'}{2}$; see [31, p. 294]. With the special values

$$\operatorname{sn}(K+i\tfrac{K'}{2};k) = \frac{1}{\sqrt{k}}, \quad \operatorname{cn}(K+i\tfrac{K'}{2};k) = -i\sqrt{\frac{1}{k}-1},$$
$$\operatorname{dn}(K+i\tfrac{K'}{2};k) = \sqrt{1-k},$$

see [25, p. 381] or [36, p. 145], and the identities

$$\operatorname{sn}(z+2K;k) = -\operatorname{sn}(z;k), \quad \operatorname{cn}(z+2K;k) = -\operatorname{cn}(z;k),$$
$$\operatorname{dn}(z+2K;k) = \operatorname{dn}(z;k),$$

see [42, p. 500], we obtain

$$f(-1) = L\operatorname{sn}\Big(-K+i\frac{K'}{2};k\Big) = -L\frac{1}{\sqrt{k}} = -1,$$
$$f'(-1) = Li\sqrt{\frac{1-k}{k}}\sqrt{1-k}\frac{2K}{\pi}i(-1) = L\frac{1-k}{\sqrt{k}}\frac{2K}{\pi} = (1-L^2)\frac{2K}{\pi} > 0.$$

In the last equalities we used $k = L^2$. □

We now construct the lemniscatic map of the exterior of two disjoint equal disks.

Theorem 4.2. *Let $r, z_0 \in \mathbb{R}$ with $0 < r < z_0$, and $E = D_r(z_0) \cup D_r(-z_0)$. Let T be the Möbius transformation*

$$T(z) = \frac{\alpha+z}{\alpha-z}, \quad \alpha = \sqrt{z_0^2 - r^2} > 0,$$

f, K, L be given as in Lemma 4.1 with

$$0 < \rho = \frac{\sqrt{z_0+r}-\sqrt{z_0-r}}{\sqrt{z_0+r}+\sqrt{z_0-r}} < 1,$$

and let Φ_1 be the lemniscatic map from (9) for $n = 2$, with

$$C = \frac{2K\alpha}{\pi}(1-L)^2, \quad D = \frac{2K\alpha}{\pi}(1+L)^2. \tag{15}$$

Then

$$\Phi(z) = \Phi_1(f'(-1)\cdot(T^{-1}\circ f\circ T)(z)) \tag{16}$$

is the lemniscatic map of E with corresponding lemniscatic domain

$$\mathcal{L} = \left\{ w\in\widehat{\mathbb{C}} : \left| w^2 - \left(\frac{2K\alpha}{\pi}(1+L^2)\right)^2 \right|^{\frac{1}{2}} > \sqrt{2L(1+L^2)}\frac{2K\alpha}{\pi} \right\}, \tag{17}$$

and hence, in particular, $c(E) = \sqrt{2L(1+L^2)}\frac{2K\alpha}{\pi}$.

Proof. Our proof is constructive. First, Φ is obtained as composition of conformal maps which map $\widehat{\mathbb{C}}\backslash E$ to a lemniscatic domain. In a second step, we show that Φ is normalized as in (2), and thus is a lemniscatic map. The first steps in the construction, namely $T^{-1}\circ f\circ T$, modify and generalize a conformal map in [31, p. 297], and are illustrated in Figure 5.

Since T maps the points $-\alpha, 0, \alpha$ to $0, 1, \infty$, respectively, T maps $\mathbb{R}$ to $\mathbb{R}$ (with same orientation). We compute the images of the two disks under $z_1 = T(z)$. Let

$$\rho := T(-z_0+r) = \frac{\sqrt{z_0+r}-\sqrt{z_0-r}}{\sqrt{z_0+r}+\sqrt{z_0-r}} \in]0,1[.$$

A short computation shows that $T(-z_0-r) = -\rho$. Since the circle $|z+z_0| = r$ cuts the real line in a right angle, this holds true for its image under T, and T maps the circle $|z+z_0| = r$ onto the circle $|z_1| = \rho$. Further, $T(-z) = 1/T(z)$ implies that T maps $|z-z_0| = r$ to $|z_1| = \frac{1}{\rho}$. Hence we see that T maps $\widehat{\mathbb{C}}\backslash E$ onto the annulus $\frac{1}{\rho} < |z_1| < \rho$.

This annulus is mapped by $z_2 = f(z_1)$ onto the complex plane with the slits $-\infty \le z_2 \le -\frac{1}{L}$, $-L \le z_2 \le L$ and $\frac{1}{L} \le z_2 \le \infty$, where $L = L(\rho)$ is given by (12); see Lemma 4.1.

For $T^{-1}(z_2) = \alpha\frac{z_2-1}{z_2+1}$ we have $T^{-1}(1/z_2) = -T^{-1}(z_2)$. Then, setting for brevity $b = \frac{1-L}{1+L}$, we compute

$$T^{-1}(L^{-1}) = \alpha b,\ T^{-1}(-L^{-1}) = \alpha b^{-1},\ T^{-1}(-L) = -\alpha b^{-1},\ T^{-1}(L) = -\alpha b.$$

This shows that T^{-1} maps the z_2-plane with the slits $-\infty \le z_2 \le -L^{-1}$, $-L \le z_2 \le L$ and $L^{-1} \le z_2 \le \infty$ onto the z_3-plane with the two slits

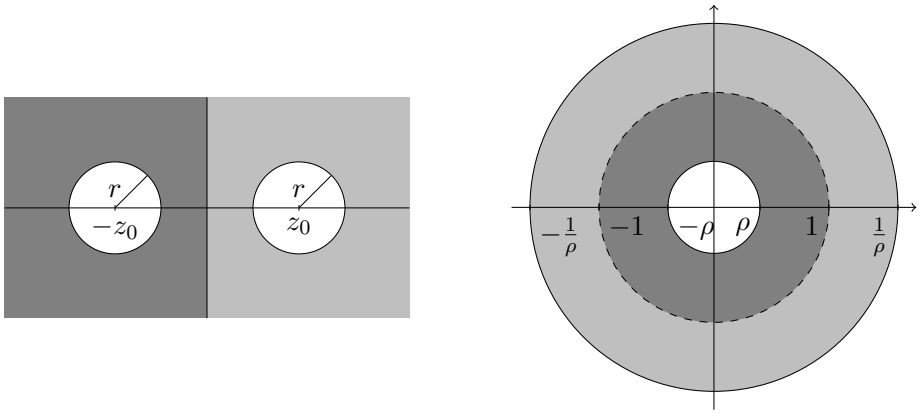

(a) exterior of two disks in the z-plane

(b) $z_1 = T(z) = \frac{\alpha+z}{\alpha-z}$

(c) $z_2 = f(z_1)$

(d) $z_3 = T^{-1}(z_2) = \alpha\frac{z_2-1}{z_2+1}$

Figure 5: Conformal map from the exterior of two disks to the exterior of two intervals; see the proof of Theorem 4.2.

$[-\alpha b^{-1}, -\alpha b]$ and $[\alpha b, \alpha b^{-1}]$. Multiplying with $f'(-1)$ we obtain the exterior of $[-D, -C] \cup [C, D]$, with C and D as in (15). The lemniscatic map for this set is Φ_1 from (9) with lemniscatic domain $\mathcal{L}$ given by (10). A short calculation shows that $\mathcal{L}$ has the form (17).

This shows that $\Phi : \widehat{\mathbb{C}} \backslash E \to \mathcal{L}$ is a bijective and conformal map onto a lemniscatic domain, and it remains to verify (2).

We have $\Phi(\infty) = \infty$, since $T(\infty) = -1$ and $f(-1) = -1$, see Lemma 4.1, and since Φ_1 satisfies the normalization in (2). Next we show that $\Phi'(\infty) = 1$. Let us begin with the derivative of $g = T^{-1} \circ f \circ T$ at $z \neq \infty$, which is

$$g'(z) = (T^{-1})'(f(T(z))) \cdot f'(T(z)) \cdot T'(z).$$

We compute $T'(z) = \frac{2\alpha}{(\alpha - z)^2}$ and $(T^{-1})'(z) = \frac{2\alpha}{(z+1)^2}$, so that

$$\begin{aligned}(T^{-1})'(f(T(z))) \cdot T'(z) &= (f(T(z)) - f(-1))^{-2} \frac{4\alpha^2}{(\alpha - z)^2} \\ &= \Big(\frac{f(T(z)) - f(-1)}{T(z) - (-1)}\Big)^{-2} \frac{4\alpha^2}{(T(z)+1)^2(\alpha - z)^2} \\ &= \Big(\frac{f(T(z)) - f(-1)}{T(z) - (-1)}\Big)^{-2}.\end{aligned}$$

We therefore find

$$g'(\infty) = \lim_{z \to \infty} g'(z) = \lim_{z \to \infty} f'(T(z)) \Big(\frac{f(T(z)) - f(-1)}{T(z) - (-1)}\Big)^{-2} = \frac{1}{f'(-1)}.$$

This implies $\Phi'(\infty) = \Phi_1'(\infty) f'(-1) g'(\infty) = 1$, so that $\Phi(z) = z + \mathcal{O}(1)$ near infinity. We further show that Φ is odd, so that the constant term in the Laurent series at infinity vanishes, showing (2). The function f satisfies $f(1/z) = 1/f(z)$; see Lemma 4.1. Together with $T(-z) = 1/T(z)$ and $T^{-1}(1/w) = -T^{-1}(w)$ this gives

$$g(-z) = T^{-1}(f(T(-z))) = T^{-1}(f(1/T(z))) = T^{-1}(1/f(T(z))) = -g(z).$$

Since also Φ_1 is odd, which can be seen either from Lemma 2.2 or directly from (9), Φ is an odd function and is normalized as in (2). □

Note that the construction in the proof of Theorem 4.2 can be generalized to doubly connected domains $\mathcal{K} = \widehat{\mathbb{C}} \backslash E$ as follows. Let $h : \mathcal{K} \to \{w \in \mathbb{C} : 1/\rho < |w| < \rho\}$ be a bijective conformal map that satisfies $|h(\infty)| = 1$. In this case we can assume (after rotation) that $h(\infty) = -1$. We then have

$$h(z) = -1 + a_1/z + \mathcal{O}(1/z^2) \quad \text{for } z \text{ near infinity,}$$

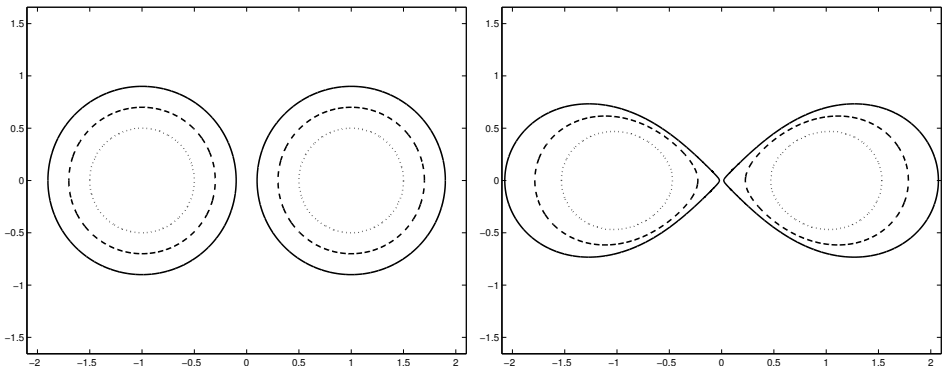

Figure 6: Illustration of Theorem 4.2.

with $a_1 \neq 0$ since h is conformal. Let $S(z) = \frac{z-1}{z+1}$. Then the lemniscatic map of E is given by

$$\Phi(z) = \Phi_1 \left(-\frac{a_1 f'(-1)}{2} (S \circ f \circ h)(z) \right) + \beta$$

with f as in Lemma 4.1, Φ_1 the lemniscatic map of two (possibly rotated) intervals of same length, and $\beta \in \mathbb{C}$ is chosen so that the normalization (2) holds.

In Figure 6 we plot the sets $E = E(z_0, r)$ for $z_0 = 1$ and $r = 0.5$, 0.7 and 0.9 (left) and the corresponding lemniscatic domains (right). We evaluated the complete elliptic integral of the first kind (13) using the MATLAB function `ellipk`. The product in the formula (12) for L converges very quickly, so that it suffices to compute the first few terms in order to obtain the correct value up to machine precision.

5 Concluding remarks

In this article we investigated properties of lemniscatic maps, i.e., conformal maps from multiply connected domains in the extended complex plane onto lemniscatic domains. We derived a general construction principle of lemniscatic maps in terms of the Riemann map for certain polynomial pre-images of simply connected sets, and we constructed the first (to our knowledge) analytic examples: One for the exterior of n radial slits, and one for the exterior of two disks.

Lemniscatic maps allow the construction of the Faber–Walsh polynomials, which are a direct generalization of the classical Faber polynomials to

compact sets consisting of several components. A study of these polynomials is given in our paper [33]. Moreover, we have addressed the numerical computation of lemniscatic maps in [30].

Acknowledgements. We thank Bernd Beckermann for many helpful remarks, and in particular for suggesting to generalize the construction of the conformal map for the radial slit domain in Corollary 3.3 to Theorem 3.1. We also thank the anonymous referees for helpful comments.

References

[1] V. V. Andreev and T. H. McNicholl, *Computing conformal maps of finitely connected domains onto canonical slit domains*, Theory Comput. Syst., 50 (2012), pp. 354–369.

[2] B. Beckermann and L. Reichel, *Error estimates and evaluation of matrix functions via the Faber transform*, SIAM J. Numer. Anal., 47 (2009), pp. 3849–3883.

[3] D. Crowdy, *The Schwarz-Christoffel mapping to bounded multiply connected polygonal domains*, Proc. R. Soc. Lond. Ser. A Math. Phys. Eng. Sci., 461 (2005), pp. 2653–2678.

[4] ——, *Schwarz-Christoffel mappings to unbounded multiply connected polygonal regions*, Math. Proc. Cambridge Philos. Soc., 142 (2007), pp. 319–339.

[5] D. Crowdy and J. Marshall, *Conformal mappings between canonical multiply connected domains*, Comput. Methods Funct. Theory, 6 (2006), pp. 59–76.

[6] J. H. Curtiss, *Faber polynomials and the Faber series*, Amer. Math. Monthly, 78 (1971), pp. 577–596.

[7] T. K. DeLillo, *Schwarz-Christoffel mapping of bounded, multiply connected domains*, Comput. Methods Funct. Theory, 6 (2006), pp. 275–300.

[8] T. K. DeLillo, T. A. Driscoll, A. R. Elcrat, and J. A. Pfaltzgraff, *Computation of multiply connected Schwarz-Christoffel maps for exterior domains*, Comput. Methods Funct. Theory, 6 (2006), pp. 301–315.

[9] ——, *Radial and circular slit maps of unbounded multiply connected circle domains*, Proc. R. Soc. Lond. Ser. A Math. Phys. Eng. Sci., 464 (2008), pp. 1719–1737.

[10] T. K. DeLillo, A. R. Elcrat, and J. A. Pfaltzgraff, *Schwarz-Christoffel mapping of multiply connected domains*, J. Anal. Math., 94 (2004), pp. 17–47.

[11] T. K. Delillo and E. H. Kropf, *Slit maps and Schwarz-Christoffel maps for multiply connected domains*, Electron. Trans. Numer. Anal., 36 (2009/10), pp. 195–223.

[12] ——, *Numerical computation of the Schwarz-Christoffel transformation for multiply connected domains*, SIAM J. Sci. Comput., 33 (2011), pp. 1369–1394.

[13] S. W. Ellacott, *Computation of Faber series with application to numeri-*

cal polynomial approximation in the complex plane, Math. Comp., 40 (1983), pp. 575–587.

[14] ——, *A survey of Faber methods in numerical approximation*, Comput. Math. Appl. Part B, 12 (1986), pp. 1103–1107.

[15] H. Grunsky, *Über konforme Abbildungen, die gewisse Gebietsfunktionen in elementare Funktionen transformieren. I*, Math. Z., 67 (1957), pp. 129–132.

[16] ——, *Über konforme Abbildungen, die gewisse Gebietsfunktionen in elementare Funktionen transformieren. II*, Math. Z., 67 (1957), pp. 223–228.

[17] ——, *Lectures on theory of functions in multiply connected domains*, Vandenhoeck & Ruprecht, Göttingen, 1978.

[18] M. Hasson, *The capacity of some sets in the complex plane*, Bull. Belg. Math. Soc. Simon Stevin, 10 (2003), pp. 421–436.

[19] P. Henrici, *Applied and computational complex analysis. Vol. 3*, Pure and Applied Mathematics (New York), John Wiley & Sons, Inc., New York, 1986.

[20] V. Heuveline and M. Sadkane, *Arnoldi-Faber method for large non-Hermitian eigenvalue problems*, Electron. Trans. Numer. Anal., 5 (1997), pp. 62–76 (electronic).

[21] J. A. Jenkins, *On a canonical conformal mapping of J. L. Walsh*, Trans. Amer. Math. Soc., 88 (1958), pp. 207–213.

[22] T. Koch and J. Liesen, *The conformal "bratwurst" maps and associated Faber polynomials*, Numer. Math., 86 (2000), pp. 173–191.

[23] P. Koebe, *Abhandlungen zur Theorie der konformen Abbildung, IV. Abbildung mehrfach zusammenhängender schlichter Bereiche auf Schlitzbereiche*, Acta Math., 41 (1916), pp. 305–344.

[24] H. J. Landau, *On canonical conformal maps of multiply connected domains*, Trans. Amer. Math. Soc., 99 (1961), pp. 1–20.

[25] W. Magnus, F. Oberhettinger, and R. P. Soni, *Formulas and theorems for the special functions of mathematical physics*, Third enlarged edition. Die Grundlehren der mathematischen Wissenschaften, Band 52, Springer-Verlag New York, Inc., New York, 1966.

[26] I. Moret and P. Novati, *The computation of functions of matrices by truncated Faber series*, Numer. Funct. Anal. Optim., 22 (2001), pp. 697–719.

[27] ——, *An interpolatory approximation of the matrix exponential based on Faber polynomials*, J. Comput. Appl. Math., 131 (2001), pp. 361–380.

[28] M. M. S. Nasser, *Numerical conformal mapping of multiply connected regions onto the second, third and fourth categories of Koebe's canonical slit domains*, J. Math. Anal. Appl., 382 (2011), pp. 47–56.

[29] ——, *Numerical conformal mapping of multiply connected regions onto the fifth category of Koebe's canonical slit regions*, J. Math. Anal. Appl., 398 (2013), pp. 729–743.

[30] M. N. S. Nasser, J. Liesen, and O. Sète, *Numerical computation of the conformal map onto lemniscatic domains*, arXiv:1505.04916, (2015).

[31] Z. Nehari, *Conformal mapping*, McGraw-Hill Book Co., Inc., New York,

Toronto, London, 1952.

[32] T. Ransford, *Potential theory in the complex plane*, vol. 28 of London Mathematical Society Student Texts, Cambridge University Press, Cambridge, 1995.

[33] O. Sète and J. Liesen, *Properties and examples of Faber–Walsh polynomials*, arXiv:1502.07633, (2015).

[34] G. Starke and R. S. Varga, *A hybrid Arnoldi-Faber iterative method for nonsymmetric systems of linear equations*, Numer. Math., 64 (1993), pp. 213–240.

[35] P. K. Suetin, *Series of Faber polynomials*, vol. 1 of Analytical Methods and Special Functions, Gordon and Breach Science Publishers, Amsterdam, 1998.

[36] F. Tricomi, *Elliptische Funktionen*, Mathematik und ihre Anwendungen in Physik und Technik, Reihe A, Band 20, Akademische Verlagsgesellschaft Geest & Portig K.-G., Leipzig, 1948.

[37] J. L. Walsh, *On the conformal mapping of multiply connected regions*, Trans. Amer. Math. Soc., 82 (1956), pp. 128–146.

[38] ——, *A generalization of Faber's polynomials*, Math. Ann., 136 (1958), pp. 23–33.

[39] J. L. Walsh, *Selected papers*, Springer-Verlag, New York, 2000. Edited by Theodore J. Rivlin and Edward B. Saff.

[40] E. Wegert, *Visual Complex Functions*, Birkhäuser/Springer Basel AG, Basel, 2012.

[41] E. Wegert and G. Semmler, *Phase plots of complex functions: a journey in illustration*, Notices Am. Math. Soc., 58 (2011), pp. 768–780.

[42] E. T. Whittaker and G. N. Watson, *A course of modern analysis. An introduction to the general theory of infinite processes and of analytic functions: with an account of the principal transcendental functions*, Fourth edition. Reprinted, Cambridge University Press, New York, 1962.

Properties and examples of Faber–Walsh polynomials

Olivier Sète[†] Jörg Liesen[†]

Abstract

The Faber–Walsh polynomials are a direct generalization of the (classical) Faber polynomials from simply connected sets to sets with several simply connected components. In this paper we derive new properties of the Faber–Walsh polynomials, where we focus on results of interest in numerical linear algebra, and on the relation between the Faber–Walsh polynomials and the classical Faber and Chebyshev polynomials. Moreover, we present examples of Faber–Walsh polynomials for two real intervals as well as some non-real sets consisting of several simply connected components.

Keywords Faber–Walsh polynomials, generalized Faber polynomials, multiply connected domains, lemniscatic domains, lemniscatic maps, conformal maps, asymptotic convergence factor

Mathematics Subject Classification (2010) 30C10; 30E10; 30C20

1 Introduction

The (classical) Faber polynomials associated with a simply connected compact set $\Omega \subset \mathbb{C}$ have found numerous applications in numerical approximation [10, 11] and in particular in numerical linear algebra [4, 6, 20, 29, 30, 41]. The main idea behind their construction, originally due to Faber [12], is to have a sequence of polynomials $F_0, F_1, F_2, \ldots$, so that each analytic function on Ω can be expanded in a convergent series of the form $\sum_{j=0}^{\infty} \gamma_j F_j(z)$, where the polynomials depend only on the set Ω. The definition and practical computation of the Faber polynomials is based on the Riemann map from the exterior of Ω (in the extended complex plane) onto the exterior of the unit disk. The Faber polynomials therefore exist for simply connected sets only. For surveys of the theory of Faber polynomials we refer to [5, 42].

In 1956, Walsh found a direct generalization of the Riemann mapping theorem to sets consisting of several simply connected components (none a single point). He showed that the exterior of each such set can be mapped conformally onto a *lemniscatic domain* [43]; see Theorem 2.1 below for a complete

[†]TU Berlin, Institute of Mathematics, MA 4-5, Straße des 17. Juni 136, 10623 Berlin, Germany. {sete,liesen}@math.tu-berlin.de

statement. Further existence proofs of Walsh's *lemniscatic map* were given by Grunsky [15, 16] and [17, Theorem 3.8.3], Jenkins [21] and Landau [24]. We recently studied lemniscatic maps in [39] and derived several explicit examples, which are among the first in the literature (see also the technical report [38]).

In a subsequent paper of 1958, Walsh used his lemniscatic map for obtaining a generalization of the Faber polynomials from simply connected sets to sets consisting of several simply connected components [44]; see Theorem 2.3 below for a complete statement. While the literature on Faber polynomials is quite extensive, the *Faber–Walsh polynomials* have rarely been studied in the literature. One notable exception is Suetin's book [42], which contains a proper subsection on the Faber–Walsh polynomials as well as a few further references (see also the technical report [38]).

Clearly, the mathematical theory and practical applicability of the Faber–Walsh polyomials have not been fully explored yet. Our goal in this paper is to contribute to a better understanding. To this end we derive some new theoretical results on Faber–Walsh polynomials and give several analytic as well as numerically computed examples. In our theoretical study we focus on results that are of interest in constructive approximation and numerical linear algebra applications, and on the relation between Faber–Walsh polynomials and the classical Faber as well as Chebyshev polynomials. In our examples we consider sets consisting of two distinct real intervals, as well as non-real sets consisting of several components. In particular, our numerical results demonstrate that the Faber–Walsh polynomials are computable for a wide range of sets via a numerical conformal mapping technique for multiply connected domains introduced in [31].

The paper is organized as follows. In Section 2 we give a summary of Walsh's results, and recall the definition of Faber–Walsh polynomials. We then derive general properties of Faber–Walsh polynomials in Section 3. In Section 4 we consider Faber–Walsh polynomials for two real intervals and particularly study their relation to the classical Chebyshev polynomials. In Section 5 we show numerical examples of Faber–Walsh polynomials for two different nonreal sets.

2 The Faber–Walsh polynomials

We first discuss Walsh's generalization of the Riemann mapping theorem. For a given integer $N \geq 1$, let $a_1, \ldots, a_N \in \mathbb{C}$ be pairwise distinct and let the positive real numbers $m_1, \ldots, m_N$ satisfy $\sum_{j=1}^{N} m_j = 1$. Then for any $\mu > 0$ the set

$$\mathcal{L} := \{w \in \widehat{\mathbb{C}} : |U(w)| > \mu\}, \quad \text{where} \quad U(w) := \prod_{j=1}^{N} (w - a_j)^{m_j}, \tag{2.1}$$

is called a *lemniscatic domain* in the extended complex plane $\widehat{\mathbb{C}} = \mathbb{C} \cup \{\infty\}$. The following theorem of Walsh shows that lemniscatic domains are canonical domains for certain N-times connected domains (open and connected sets).

Theorem 2.1 ([43, Theorems 3 and 4]). *Let $E := \cup_{j=1}^{N} E_j$, where $E_1, \ldots, E_N \subseteq \mathbb{C}$ are mutually exterior simply connected compact sets (none a single point), and let $\mathcal{K} := \widehat{\mathbb{C}} \backslash E$. Then there exists a unique lemniscatic domain $\mathcal{L}$ of the form (2.1) with $\mu > 0$ equal to the logarithmic capacity of E, and a unique bijective conformal map*

$$\Phi : \mathcal{K} \to \mathcal{L} \quad \text{with} \quad \Phi(z) = z + \mathcal{O}\left(\frac{1}{z}\right) \quad \text{for } z \text{ near infinity.}$$

We call the function Φ the lemniscatic map *of $\mathcal{K}$ (or of E), and denote $\psi = \Phi^{-1}$.*

For $N = 1$ the set E is simply connected and a lemniscatic domain is the exterior of a disk. Hence in this case Theorem 2.1 is equivalent with the Riemann mapping theorem. In [39] we studied the properties of lemniscatic maps and derived several analytic examples. In the subsequent paper [31], written jointly with Nasser, we presented a numerical method for computing lemniscatic maps. Both the analytic results from [39] and the numerical method from [31] will be used in Sections 4 and 5 below.

In [44] Walsh used Theorem 2.1 for proving the existence of a direct generalization of the (classical) Faber polynomials to sets E with several components. The second major ingredient is the following. For the unit disk, the monomials w^k are fundamental for Taylor and Laurent series of analytic functions, and the zeros of w^k are at the center of the unit disk. For a lemniscatic domain $\mathcal{L}$, we need a generalization of w^k to a polynomial with zeros at the centers $a_1, \ldots, a_N$ of $\mathcal{L}$, and the multiplicity of each zero a_j must fit its "importance" for $\mathcal{L}$, given by the exponent m_j.

Lemma 2.2 ([44, Lemma 2]). *Let $\mathcal{L}$ be a lemniscatic domain as in (2.1).*

1. *There exists a sequence $(\alpha_j)_{j=1}^{\infty}$, chosen from the centers $a_1, \ldots, a_N$, such that*

$$|N_{k,j} - k m_j| \le A \quad \text{for } j = 1, 2, \ldots, N, \quad k = 1, 2, \ldots, \tag{2.2}$$

   where $N_{k,j}$ denotes the number of times a_j appears in the sequence $\alpha_1, \ldots, \alpha_k$, and where A is a positive constant.

2. *Any such sequence has the following property: For any closed set $S \subseteq \widehat{\mathbb{C}}$ not containing any of the points $a_1, \ldots, a_N$ there exist constants $A_1, A_2 > 0$, such that*

$$A_1 < \frac{|u_k(w)|}{|U(w)|^k} < A_2 \quad \text{for } k = 0, 1, 2, \ldots \text{ and any } w \in S, \tag{2.3}$$

   where $u_k(w) := \prod_{j=1}^{k}(w - \alpha_j) = \prod_{j=1}^{N}(w - a_j)^{N_{k,j}}$.

For $N = 1$ a lemniscatic domain is the exterior of a disk, and we have $\alpha_j = a_1$ for all $j \ge 1$ and $u_k(w) = (w - a_1)^k$. For $N \ge 2$, the sequence $(\alpha_j)_{j=1}^{\infty}$ is *not unique*, but it can be chosen constructively from $a_1, \ldots, a_N$; see [44]. Note that

a smaller constant A in (2.2) implies better bounds in (2.3). For $N = 2$ one possible choice is $\alpha_j = a_1$ if $\lfloor jm_1 \rfloor > \lfloor (j-1)m_1 \rfloor$, and $\alpha_j = a_2$ otherwise, where $\lfloor \cdot \rfloor$ denotes the integer part. We use this choice in our examples in Sections 4 and 5.1 below.

In the notation of Theorem 2.1, the Green's functions with pole at infinity for $\mathcal{L}$ and $\mathcal{K} = \widehat{\mathbb{C}} \backslash E$ are

$$g_{\mathcal{L}}(w) = \log|U(w)| - \log(\mu) \quad \text{and} \quad g_{\mathcal{K}}(z) = g_{\mathcal{L}}(\Phi(z)), \tag{2.4}$$

respectively; see [39, 44]. For $\sigma > 1$ we denote their level curves by

$$\Gamma_\sigma = \{z \in \mathcal{K} : g_{\mathcal{K}}(z) = \log(\sigma)\},$$
$$\Lambda_\sigma = \{w \in \mathcal{L} : g_{\mathcal{L}}(w) = \log(\sigma)\} = \{w \in \mathcal{L} : |U(w)| = \sigma\mu\}.$$

Note that $\Phi(\Gamma_\sigma) = \Lambda_\sigma$. Further, we denote by int and ext the interior and exterior of a closed curve (or union of closed curves), respectively. In particular, we have

$$\operatorname{int}(\Lambda_\sigma) = \{w \in \widehat{\mathbb{C}} : |U(w)| < \sigma\mu\}, \quad \operatorname{ext}(\Lambda_\sigma) = \{w \in \widehat{\mathbb{C}} : |U(w)| > \sigma\mu\}.$$

We can now state Walsh's main result from [44].

Theorem 2.3 ([44, Theorem 3])**.** *Let E, $\mathcal{L}$ and $\psi = \Phi^{-1}$ be as in Theorem 2.1. Let $(\alpha_j)_{j=1}^\infty$ and the corresponding polynomials $u_k(w)$, $k = 0, 1, \ldots$, be as in Lemma 2.2. Then the following hold:*

1. *For $z \in \Gamma_\sigma$ and $w \in \operatorname{ext}(\Lambda_\sigma)$ we have*

$$\frac{\psi'(w)}{\psi(w) - z} = \sum_{k=0}^{\infty} \frac{b_k(z)}{u_{k+1}(w)}, \tag{2.5}$$

where

$$b_k(z) = \frac{1}{2\pi i} \int_{\Lambda_\lambda} u_k(\tau) \frac{\psi'(\tau)}{\psi(\tau) - z}\, d\tau = \frac{1}{2\pi i} \int_{\Gamma_\lambda} \frac{u_k(\Phi(\zeta))}{\zeta - z}\, d\zeta \tag{2.6}$$

for any $\lambda > \sigma$. The function b_k is a monic polynomial of degree k, which is called the kth Faber–Walsh polynomial *for E and $(\alpha_j)_{j=1}^\infty$.*

2. *Let f be analytic on E, and let $\rho > 1$ be the largest number such that f is analytic and single-valued in* $\operatorname{int}(\Gamma_\rho)$*. Then f has a unique representation as a* Faber–Walsh series

$$f(z) = \sum_{k=0}^{\infty} a_k b_k(z), \quad a_k = \frac{1}{2\pi i} \int_{\Lambda_\lambda} \frac{f(\psi(\tau))}{u_{k+1}(\tau)}\, d\tau, \quad 1 < \lambda < \rho,$$

which converges absolutely in $\operatorname{int}(\Gamma_\rho)$ *and maximally on E, i.e.,*

$$\limsup_{n\to\infty} \|f - \sum_{k=0}^{n} a_k b_k\|_E^{\frac{1}{n}} = \frac{1}{\rho},$$

where $\|\cdot\|_E$ denotes the maximum norm on E.

Note that the assertions about the Faber–Walsh polynomials hold for any admissible sequence $(\alpha_j)_{j=1}^{\infty}$ as in Lemma 2.2. In this article, if we do not explicitly mention the sequence, the corresponding results hold for any such sequence.

For $N = 1$ the Faber–Walsh polynomials reduce to the *monic* Faber polynomials for the (simply connected) set E as considered in [10, 28, 40].

For an entire function f we have $\rho = \infty$ and hence $\operatorname{int}(\Gamma_\rho) = \mathbb{C}$ in part *2.* of the theorem.

In our proof of Proposition 3.7 below we will use that for each given $\sigma > 1$ there exists positive constants C_1, C_2 independent of k such that

$$0 < C_1|u_k(\Phi(z))| \le |b_k(z)| \le C_2|u_k(\Phi(z))| \quad \text{for } z \in \Gamma_\sigma. \tag{2.7}$$

Here the upper bound on $|b_k(z)|$ holds for all k and the lower bound holds only for sufficiently large k; see [42, p. 253].

In (2.5)–(2.6) the Faber–Walsh polynomials are defined as the (polynomial) coefficients in the expansion of the function $\psi'(w)/(\psi(w) - z)$. Similar to the (classical) Faber polynomials, the Faber–Walsh polynomials can also be defined using the coefficients of the Laurent series of the conformal map ψ in a neighborhood of infinity. Using this approach one can derive a recursive formula for computing the Faber–Walsh polynomials. In the following result we state the recursion that we have used in our numerical computations that are described in Section 4.1. A variant of this recursion was first published in the technical report [38].

Proposition 2.4. *In the notation of Theorem 2.3, the Laurent series at infinity of the conformal map $\psi = \Phi^{-1}$ has the form*

$$\psi(w) = w + \sum_{k=1}^{\infty} \frac{c_k}{w^k}.$$

Then the Faber–Walsh polynomials are recursively given by

$$\begin{aligned} b_0(z) &= 1 \\ b_k(z) &= (z - \alpha_k)b_{k-1}(z) + \beta_{k-1,1}(z), \quad k \ge 1, \end{aligned}$$

where the "correction terms" $\beta_{k,\ell}(z)$ are polynomials given by $\beta_{0,1}(z) = 0$ and

$$\begin{aligned} \beta_{1,\ell}(z) &= \alpha_1(\ell - 1)c_{\ell-1} - (\ell + 1)c_\ell, \quad \ell \ge 1, \\ \beta_{k,\ell}(z) &= -c_\ell b_{k-1}(z) - \alpha_k\beta_{k-1,\ell}(z) + \beta_{k-1,\ell+1}(z), \quad k \ge 2, \quad \ell \ge 1, \end{aligned}$$

with $c_0 = 0$.

3 On the theory of Faber–Walsh polynomials

In this section we derive several new results about Faber–Walsh polynomials. We begin with an alternative representation, and then relate Faber polynomials

for a simply connected set Ω to the Faber–Walsh polynomials for a polynomial pre-image of Ω. Finally, we will show that the normalized Faber–Walsh polynomials are asymptotically optimal.

Our first result is an easy consequence of Theorem 2.3.

Corollary 3.1. *In the notation of Theorem 2.3, the kth Faber–Walsh polynomial $b_k(z)$ is the polynomial part of the Laurent series at infinity of $u_k(\Phi(z))$.*

Proof. By Theorem 2.1, the Laurent series at infinity of the lemniscatic map Φ has the form $\Phi(\zeta) = \zeta + \sum_{j=1}^{\infty} \frac{d_j}{\zeta^j}$, and the series converges locally uniformly in a neighbourhood of infinity. Then the Laurent series at infinity of

$$u_k(\Phi(\zeta)) = \prod_{j=1}^{k} (\Phi(\zeta) - \alpha_j) = p_k(\zeta) + \sum_{j=1}^{\infty} \frac{\widetilde{d}_j}{\zeta^j} \tag{3.1}$$

converges locally uniformly in a neighbourhood of infinity. Here p_k is a monic polynomial of degree k. Let $z \in \mathbb{C}$. Let $\lambda > 1$ be such that $z \in \operatorname{int}(\Gamma_\lambda)$ and such that Γ_λ is in the region of convergence of (3.1). Using (2.6) we obtain

$$\begin{aligned} b_k(z) &= \frac{1}{2\pi i} \int_{\Gamma_\lambda} \frac{u_k(\Phi(\zeta))}{\zeta - z}\, d\zeta = \frac{1}{2\pi i} \int_{\Gamma_\lambda} \frac{p_k(\zeta)}{\zeta - z}\, d\zeta + \frac{1}{2\pi i} \int_{\Gamma_\lambda} \sum_{j=1}^{\infty} \frac{\widetilde{d}_j}{\zeta^j} \frac{1}{\zeta - z}\, d\zeta \\ &= p_k(z). \end{aligned}$$

The second integral vanishes by virtue of Cauchy's integral formula for domains with infinity as interior point; see, e.g., [27, Problem 14.14]. □

Note that in the case $N = 1$ this result reduces to the classical fact that the kth Faber polynomial $F_k(z)$ is the polynomial part of the Laurent series at infinity of $(\Phi(z))^k$.

We will now consider sets E that are polynomial pre-images of simply connected sets Ω. We first recall the following result from [39] about the corresponding lemniscatic maps.

Theorem 3.2 ([39, Theorem 3.1])**.** *Let $\Omega = \Omega^* \subseteq \mathbb{C}$ be a simply connected compact set (not a single point) with exterior Riemann mapping*

$$\widetilde{\Phi} : \widehat{\mathbb{C}} \backslash \Omega \to \{w \in \widehat{\mathbb{C}} : |w| > 1\}, \quad \widetilde{\Phi}(\infty) = \infty, \quad \widetilde{\Phi}'(\infty) > 0.$$

Let $P(z) = \alpha z^n + \alpha_0$ with $\alpha_0 \in \mathbb{R}$ to the left of Ω, $\alpha > 0$, and $n \geq 2$. Then $E := P^{-1}(\Omega)$ is the disjoint union of n simply connected compact sets, and

$$\Phi : \widehat{\mathbb{C}} \backslash E \to \mathcal{L} = \{w \in \widehat{\mathbb{C}} : |U(w)| > \mu\}, \quad \Phi(z) = z\Big(\frac{\mu^n}{z^n}[\widetilde{\Phi}(P(z)) - \widetilde{\Phi}(P(0))]\Big)^{\frac{1}{n}},$$

is the lemniscatic map of E, where we take the principal branch of the nth root, and where

$$\mu := \Big(\frac{1}{\alpha \widetilde{\Phi}'(\infty)}\Big)^{\frac{1}{n}} > 0, \quad \textit{and} \quad U(w) := (w^n + \mu^n \widetilde{\Phi}(P(0)))^{\frac{1}{n}}.$$

Note that we consider the Riemann map onto the exterior of the unit disk, so that $\widetilde{\Phi}'(\infty)$ is positive, but is not necessarily 1. Therefore, the Faber polynomials F_k associated with this map have the leading coefficients $(\widetilde{\Phi}'(\infty))^k$, and will in general not be monic.

We then obtain the following "transplantation" result for Faber–Walsh polynomials, which is an analogue of a similar result for Chebyshev polynomials shown in [14, 22]. For related results on polynomial pre-images see also [32, 34].

Theorem 3.3. *In the notation of Theorem 3.2, denote the $n \geq 2$ distinct roots of the polynomial $(U(w))^n$ by $a_1, \ldots, a_n$. Then, the (kn)th Faber–Walsh polynomial for E and $(\alpha_j)_{j=1}^{\infty} = (a_1, a_2, \ldots, a_n, a_1, a_2, \ldots, a_n, \ldots)$ satisfies*

$$b_{kn}(z) = \frac{1}{(\alpha\widetilde{\Phi}'(\infty))^k} F_k(P(z)), \tag{3.2}$$

for all $k \geq 0$, where F_k is the kth Faber polynomial for Ω.

Proof. Theorem 3.2 implies that

$$\prod_{j=1}^{n}(\Phi(z) - a_j) = (U(\Phi(z)))^n = \mu^n \widetilde{\Phi}(P(z)) = \frac{1}{\alpha\widetilde{\Phi}'(\infty)}\widetilde{\Phi}(P(z)).$$

Then, for $k \geq 0$, we find

$$u_{kn}(\Phi(z)) = \prod_{j=1}^{n}(\Phi(z) - a_j)^k = \frac{1}{(\alpha\widetilde{\Phi}'(\infty))^k}(\widetilde{\Phi}(P(z)))^k.$$

Considering on both sides the polynomial part of the Laurent series at infinity, we find (3.2); see Corollary 3.1 for the Faber–Walsh polynomials, and, for instance, [42, p. 33] for the Faber polynomials. □

In Theorem 3.3 other choices of the sequence $(\alpha_j)_{j=1}^{\infty}$ are possible: If $(\alpha_j)_{j=1}^{\infty}$ satisfies $u_{kn}(w) = \prod_{j=1}^{n}(w - a_j)^k$ for some k, then (3.2) holds.

For a polynomial of degree 1 the sitation is different from the one in Theorem 3.3, since the polynomial then is a linear transformation and thus preserves the number of components of a set. In this case we obtain the following stronger result.

Proposition 3.4. *Let the notation be as in Theorem 2.3, and let $P(z) = az + b$ with $a \neq 0$. Then the Faber–Walsh polynomials $\widetilde{b}_k$ for $P(E)$ and $(P(\alpha_j))_{j=1}^{\infty}$ satisfy $b_k(z) = \frac{1}{a^k}\widetilde{b}_k(P(z))$ for all $k \geq 0$.*

Proof. Let $\Phi : \widehat{\mathbb{C}}\backslash E \to \mathcal{L}$ be the lemniscatic map of E. Then $P(\mathcal{L})$ is a lemniscatic domain and $\widetilde{\Phi} := P \circ \Phi \circ P^{-1}$ is the lemniscatic map of $P(E)$; see [39, Lemma 2.3]. In particular, the polynomials $u_k(w) = \prod_{j=1}^{k}(w - \alpha_j)$ for $\mathcal{L}$ and $\widetilde{u}_k(\widetilde{w}) = \prod_{j=1}^{k}(\widetilde{w} - P(\alpha_j))$ for $P(\mathcal{L})$ satisfy

$$\widetilde{u}_k(\widetilde{\Phi}(P(z))) = \widetilde{u}_k(P(\Phi(z))) = \prod_{j=1}^{k}(P(\Phi(z)) - P(\alpha_j)) = a^k u_k(\Phi(z)).$$

Corollary 3.1 implies that $\widetilde{b}_k(P(z)) = a^k b_k(z)$. □

We now show that Faber–Walsh polynomials are *asymptotically optimal* in the sense of the following definition introduced by Eiermann, Niethammer and Varga [8, 9] in the context of semi-iterative methods for solving linear algebraic systems.

Definition 3.5. For a compact set $E \subseteq \mathbb{C}$ and $z_0 \in \mathbb{C}$ the number

$$R_{z_0}(E) := \limsup_{k\to\infty} \Big(\min_{p\in\mathcal{P}_k(z_0)} \|p\|_E \Big)^{1/k}$$

is called the *asymptotic convergence factor* for polynomials from $\mathcal{P}_k(z_0) := \{1 + \sum_{j=1}^{k} a_j(z-z_0)^j : a_1, \ldots, a_k \in \mathbb{C}\}$ on E. A sequence of polynomials $p_k \in \mathcal{P}_k(z_0)$, $k = 0, 1, \ldots$, is called *asymptotically optimal* on E and with respect to z_0, if

$$\lim_{k\to\infty} \|p_k\|_E^{1/k} = R_{z_0}(E).$$

For any compact set E and $z_0 \in \mathbb{C}$ we have $R_{z_0}(E) \le 1$, and $R_{z_0}(E) = 1$ if $z_0 \in E$. (More precisely, one can show that $R_{z_0}(E) < 1$ if and only if z_0 is in the unbounded component of $\widehat{\mathbb{C}}\backslash E$.) For sets as in Theorem 2.1, the asymptotic convergence factor can be characterized with the Green's function.

Proposition 3.6. *In the notation of Theorem 2.1, let $g_{\mathcal{K}}$ be the Green's function with pole at infinity for $\mathcal{K}$; see* (2.4)*. Then*

$$R_{z_0}(E) = \exp(-g_{\mathcal{K}}(z_0)) = \frac{\mu}{|U(\Phi(z_0))|} \quad \textit{for each } z_0 \in \mathbb{C}\backslash E.$$

Moreover, any polynomial $p_k \in \mathcal{P}_k(z_0)$ satisfies

$$\|p_k\|_E \ge R_{z_0}(E)^k.$$

This result was shown for $z_0 = 1 \notin E$ in [7], and the proof given there can be easily extended to all $z_0 \in \mathbb{C}\backslash E$. For E consisting of a finite number of real intervals and $z_0 = 0$, a sharp lower bound for $\|p_k\|_E$, $p_k \in \mathcal{P}_k(0)$, has been derived in [37].

We stress that Proposition 3.6 gives a characterization of the asymptotic convergence factor for complex sets E as in Theorem 2.1 and *any* $z_0 \in \mathbb{C}\backslash E$. Numerical examples using the method from [31] for computing lemniscatic maps are given in Sections 4 and 5 below.

Proposition 3.7. *In the notation of Theorem 2.3, let $z_0 \in \mathbb{C}\backslash E$ and let $\sigma_0 > 1$ be such that $z_0 \in \Gamma_{\sigma_0}$. Then*

$$R_{z_0}(E) = \frac{1}{\sigma_0} \quad \textit{and} \quad R_{z_0}(\overline{\mathrm{int}(\Gamma_\sigma)}) = \frac{\sigma}{\sigma_0} \quad \textit{for } 1 < \sigma \le \sigma_0,$$

and the Faber–Walsh polynomials for E satisfy

$$\lim_{k\to\infty}\Big(\frac{\|b_k\|_E}{|b_k(z_0)|}\Big)^{1/k}=\frac{1}{\sigma_0}=R_{z_0}(E), \tag{3.3}$$

$$\lim_{k\to\infty}\Big(\frac{\|b_k\|_{\Gamma_\sigma}}{|b_k(z_0)|}\Big)^{1/k}=\frac{\sigma}{\sigma_0}\quad \textit{for any } \sigma>1. \tag{3.4}$$

Hence the normalized Faber–Walsh polynomials $b_k(z)/b_k(z_0)\in\mathcal{P}_k(z_0)$ are asymptotically optimal on E, and on $\overline{\operatorname{int}(\Gamma_\sigma)}$ whenever $1<\sigma\le\sigma_0$.

Proof. The Green's function with pole at infinity for $\mathcal{K}=\widehat{\mathbb{C}}\backslash E$ is $g_{\mathcal{K}}$ as in (2.4). By the definition of σ_0, we have $g_{\mathcal{K}}(z_0)=\log(\sigma_0)$, so that $R_{z_0}(E)=\frac{1}{\sigma_0}$ by Proposition 3.6. The Green's function with pole at infinity for $\operatorname{ext}(\Gamma_\sigma)$ is $g_{\mathcal{K}}(z)-\log(\sigma)$. Hence, for $1<\sigma\le\sigma_0$, $R_{z_0}(\overline{\operatorname{int}(\Gamma_\sigma)})=\frac{\sigma}{\sigma_0}$ by Proposition 3.6.

Let $\sigma>1$. By (2.7) there exists constants $C_1,C_2>0$ such that for sufficiently large k we have

$$C_1|u_k(\Phi(z))|<|b_k(z)|<C_2|u_k(\Phi(z))|,\quad z\in\Gamma_\sigma.$$

Apply Lemma 2.2 to bound $|u_k(\Phi(z))|$: There exist $A_1,A_2>0$ such that (2.3) holds for $w\in\Phi(\Gamma_\sigma)=\Lambda_\sigma=\{w:|U(w)|=\sigma\mu\}$. We thus have

$$C_1A_1(\sigma\mu)^k<|b_k(z)|<C_2A_2(\sigma\mu)^k,\quad z\in\Gamma_\sigma. \tag{3.5}$$

We then have $b_k(z)\neq 0$ for $z\in\Gamma_\sigma$ and, in particular, $b_k(z_0)\neq 0$ for sufficiently large k. Now (3.5) implies $\lim_{k\to\infty}|b_k(z)|^{1/k}=\sigma\mu$ for any $z\in\Gamma_\sigma$, and, in particular,

$$\lim_{k\to\infty}|b_k(z_0)|^{1/k}=\sigma_0\mu. \tag{3.6}$$

Moreover $\lim_{k\to\infty}\|b_k\|_{\Gamma_\sigma}^{1/k}=\sigma\mu$, since (3.5) holds uniformly for $z\in\Gamma_\sigma$. This establishes (3.4).

In order to show (3.3), let $\mu_k:=\min\{\|p\|_E:p \text{ monic of degree } k\}$. From [40, Sect. 1.3.4] it is known that the sequence $\big(\mu_k^{1/k}\big)_k$ converges to the capacity μ of E. Since the Faber–Walsh polynomials b_k are monic of degree k, we have the estimate

$$\mu_k\le\|b_k\|_E\le\|b_k\|_{\Gamma_\sigma}\le C_2A_2(\sigma\mu)^k,$$

where $\sigma>1$ is arbitrary; see (3.5). This shows that

$$\mu\le\liminf_{k\to\infty}\|b_k\|_E^{1/k}\le\limsup_{k\to\infty}\|b_k\|_E^{1/k}\le\sigma\mu,$$

and $\lim_{k\to\infty}\|b_k\|_E^{1/k}=\mu$, since $\sigma>1$ was arbitrary. Together with (3.6) we obtain (3.3). □

4 Faber–Walsh polynomials on two intervals

In this section we consider Faber–Walsh polynomials on sets consisting of two real intervals.

Polynomial approximation problems on such sets have been studied in numerous publications, dating back (at least) to the classical works of Achieser [2, 3], who derived analytic formulae for the Chebyshev polynomials and the Green's function in terms of Jacobi's elliptic and theta functions. For a modern treatment of this area with many references up to 1996 we refer to Fischer's book [13]. It also contains an analytic formula for the asymptotic convergence factor for two intervals and real z_0 in terms of Jacobi's elliptic and theta functions (through its characterization with the Green's function), as well as a MATLAB code for its numerical computation [13, p. 130]. More recently, Peherstorfer and Schiefermayr studied Chebyshev polynomials on several real intervals in [33], and Schiefermayr derived bounds on the asymptotic convergence factor for two intervals in terms of elementary functions [36]. Related approximation problems have been studied in [19, 35, 37].

In this section we show how the Faber–Walsh polynomials fit into this widely studied area. We first consider the case of two intervals of the same length. Here the lemniscatic map is known explicitly, so that the Faber–Walsh polynomials can be explicitly computed and related to the classical Faber and Chebyshev polynomials. We then consider the general case of two arbitrary intervals, where we compute the lemniscatic map and the Faber–Walsh polynomials numerically.

4.1 Two intervals of same length

We consider the sets consisting of two real intervals of same length which are symmetric with respect to the origin, i.e.,

$$E = [-D, -C] \cup [C, D] \quad \text{with } 0 < C < D. \tag{4.1}$$

The lemniscatic map of such a set is known analytically from [39].

Proposition 4.1. *Let E be as in* (4.1)*. Then*

$$w = \Phi(z) = z\left(\frac{1}{2} + \frac{DC}{2}\frac{1}{z^2} \pm \frac{1}{2z^2}\sqrt{(z^2 - C^2)(z^2 - D^2)}\right)^{1/2}$$

is the lemniscatic map of E, and the corresponding lemniscatic domain is

$$\mathcal{L} = \left\{w \in \widehat{\mathbb{C}} : |w - \tfrac{D+C}{2}|^{1/2}|w + \tfrac{D+C}{2}|^{1/2} > \tfrac{\sqrt{D^2-C^2}}{2}\right\}. \tag{4.2}$$

Moreover, the inverse of Φ is given by

$$z = \psi(w) = w\sqrt{1 + \left(\frac{D-C}{2}\right)^2 \frac{1}{w^2 - (\frac{D+C}{2})^2}},$$

where we take the principal branch of the square root. Its Laurent series at infinity is

$$\psi(w) = w + \sum_{k=0}^{\infty} \frac{c_{2k+1}}{w^{2k+1}}, \tag{4.3}$$

where the coefficients are given by $c_{2k} = 0$, $k \geq 0$, *and*

$$c_{2k+1} = \frac{1}{2}\left(\frac{D-C}{2}\right)^2 \left(\frac{D+C}{2}\right)^{2k} - \frac{1}{2}\sum_{j=1}^{k} c_{2j-1}c_{2(k-j)+1}, \quad k \geq 0. \tag{4.4}$$

In particular, $c_1 = \frac{1}{2}\left(\frac{D-C}{2}\right)^2$.

Proof. The construction of Φ and ψ is given in [39, Corollary 3.3]. It thus remains to show the series expansion (4.3)–(4.4).

The function $w \mapsto \sqrt{1 + \left(\frac{D-C}{2}\right)^2 \frac{1}{w^2 - (\frac{D+C}{2})^2}}$ is analytic and even in $\mathcal{L}$, and thus has a uniformly convergent Laurent series at infinity of the form

$$\sqrt{1 + \left(\frac{D-C}{2}\right)^2 \frac{1}{w^2 - (\frac{D+C}{2})^2}} = \sum_{k=0}^{\infty} \frac{d_k}{w^{2k}}. \tag{4.5}$$

Setting $w = \infty$ shows $d_0 = 1$. Squaring (4.5) and expanding the left-hand side into a Laurent series yields

$$1 + \sum_{k=1}^{\infty} \left(\frac{D-C}{2}\right)^2 \left(\frac{D+C}{2}\right)^{2(k-1)} \frac{1}{w^{2k}} = \left(\sum_{k=0}^{\infty} \frac{d_k}{w^{2k}}\right)^2 = \sum_{k=0}^{\infty}\sum_{j=0}^{k} d_j d_{k-j} \frac{1}{w^{2k}}.$$

For $k \geq 1$ we see that

$$\left(\frac{D-C}{2}\right)^2 \left(\frac{D+C}{2}\right)^{2(k-1)} = \sum_{j=0}^{k} d_j d_{k-j} = 2d_0 d_k + \sum_{j=1}^{k-1} d_j d_{k-j},$$

and thus

$$d_k = \frac{1}{2}\left(\frac{D-C}{2}\right)^2 \left(\frac{D+C}{2}\right)^{2(k-1)} - \frac{1}{2}\sum_{j=1}^{k-1} d_j d_{k-j}.$$

Since $\psi(w) = w + \sum_{k=0}^{\infty} \frac{d_{k+1}}{w^{2k+1}}$, we find that $c_{2k} = 0$ and

$$\begin{aligned} c_{2k+1} = d_{k+1} &= \frac{1}{2}\left(\frac{D-C}{2}\right)^2 \left(\frac{D+C}{2}\right)^{2k} - \frac{1}{2}\sum_{j=1}^{k} d_j d_{k+1-j} \\ &= \frac{1}{2}\left(\frac{D-C}{2}\right)^2 \left(\frac{D+C}{2}\right)^{2k} - \frac{1}{2}\sum_{j=1}^{k} c_{2j-1}c_{2(k-j)+1} \end{aligned}$$

for $k \geq 0$. □

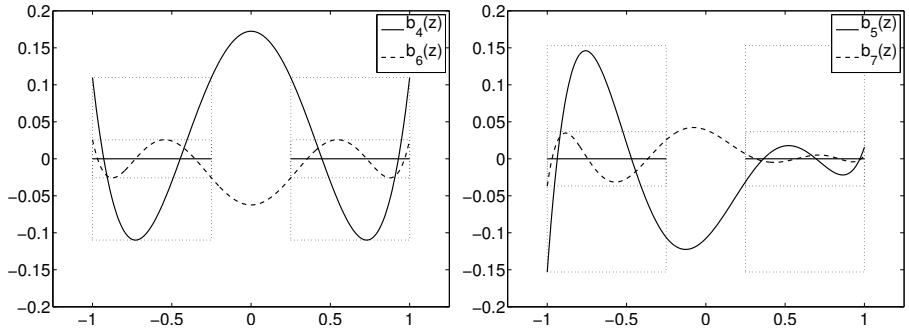

Figure 1: Faber–Walsh polynomials b_k for $E = [-1, -\frac{1}{4}] \cup [\frac{1}{4}, 1]$.

The definition of the lemniscatic domain in (4.2) shows the well-known fact that the logarithmic capacity of E is given by $\frac{1}{2}\sqrt{D^2 - C^2}$; cf. e.g. [1, p. 288] or [18].

Using the series expansion (4.3)–(4.4) and the recurrence stated in Proposition 2.4, we can compute the Faber–Walsh polynomials for E and the sequence $(\frac{D+C}{2}, -\frac{D+C}{2}, \frac{D+C}{2}, -\frac{D+C}{2}, \ldots)$, were $\frac{D+C}{2}$ and $-\frac{D+C}{2}$ are the two centers of the lemniscatic domain $\mathcal{L}$ in (4.2). In Figure 1 we plot the polynomials b_k for the set $E = [-1, -\frac{1}{4}] \cup [\frac{1}{4}, 1]$ and $k = 4, 6$ (left), $k = 5, 7$ (right). We observe that the polynomials of even degrees $k = 4, 6$ have $k + 2$ extremal points on E. This suggests that they are the Chebyshev polynomials for E, i.e., that $b_{2k}(z) = T_{2k}(z; E)$, where, for all $j \geq 0$,

$$T_j(z; E) := \operatorname{argmin}\{\|p\|_E : p \text{ monic and } \deg(p) = j\}$$

is the (uniquely determined) jth Chebyshev polynomial for the compact set E. We prove the following more general result, which for $n = 2$ gives the result for two intervals.

Theorem 4.2. *Let $E = \cup_{j=1}^{n} e^{i2\pi j/n}[C, D]$ with $0 < C < D$. Then the Faber–Walsh polynomials b_{nk} for E and $(\alpha_j)_{j=1}^{\infty} = \left(e^{i2\pi(j-1)/n}\left(\frac{D^{n/2}+C^{n/2}}{2}\right)^{n/2}\right)_{j=1}^{\infty}$ are the Chebyshev polynomials for E, i.e.,*

$$b_{nk}(z) = T_{nk}(z; E), \quad k \geq 0.$$

Proof. The result is trivial for $k = 0$, so we may consider $k \geq 1$. The idea of the proof is to consider E as a polynomial pre-image of $[-1, 1]$ and to relate both the Faber–Walsh polynomial and the Chebyshev polynomial for E to the Chebyshev polynomials of the first kind.

The polynomial

$$P(z) = \frac{2}{D^n - C^n} z^n - \frac{D^n + C^n}{D^n - C^n} = \frac{2z^n - C^n - D^n}{D^n - C^n},$$

satisfies $E = P^{-1}([-1,1])$, and the exterior Riemann map $\widetilde{\Phi}$ for $[-1,1]$ satisfies $\widetilde{\Phi}'(\infty) = 2$. Therefore, Theorem 3.3 shows that

$$b_{nk}(z) = \left(\frac{D^n - C^n}{4}\right)^k F_k(P(z)), \quad k \geq 0,$$

where F_k is the kth Faber polynomial for $[-1,1]$. On the other hand, we have

$$T_{nk}(z;E) = \left(\frac{D^n - C^n}{2}\right)^k T_k(P(z);[-1,1])$$

from [14, Corollary 2.2]. For $k \geq 1$, the kth Chebyshev polynomial for $[-1,1]$ is

$$T_k(z;[-1,1]) = \frac{1}{2^{k-1}} T_k(z),$$

where $T_k(z)$ is the kth Chebyshev polynomial of the first kind; see e.g. [13, Theorem 3.2.2]. Moreover, the kth Faber polynomial for $[-1,1]$ is given by $F_k(z) = 2T_k(z)$ for $k \geq 1$; see [42, p. 37]. Thus

$$T_{nk}(z;E) = \left(\frac{D^2 - C^2}{4}\right)^k 2T_k(P(z)) = \left(\frac{D^2 - C^2}{4}\right)^k F_k(P(z)) = b_{nk}(z),$$

which completes the proof. □

This theorem generalizes the classical relation of Faber and Chebyshev polynomials on the interval $[-1,1]$; see [42, p. 37]. For $n = 2$ the statement of the theorem also holds for any two real intervals of equal length, which can be seen as follows. Let $E = [A,B] \cup [C,D]$ with $B - A = D - C > 0$, and let $P(z) = z - \frac{B+C}{2}$. Then $\widetilde{E} = P(E)$ consists of two intervals of equal length which are symmetric with respect to the origin. If we denote the Faber–Walsh polynomials for $\widetilde{E}$ by $\widetilde{b}_n$, we find

$$b_{2k}(z) = \widetilde{b}_{2k}(P(z)) = T_{2k}(P(z);\widetilde{E}) = T_{2k}(z;E),$$

where we used Proposition 3.4, Theorem 4.2 and [14, Corollary 2.2].

In Proposition 3.7 we have shown that the normalized Faber–Walsh polynomials are asymptotically optimal. For sets E of the form (4.1) this result can be strengthened as follows.

Corollary 4.3. *Let $E = [-D,-C] \cup [C,D]$ with $0 < C < D$ and $z_0 \in \mathbb{R}\backslash E$. Then the normalized Faber–Walsh polynomials for E and $(\alpha_j)_{j=1}^{\infty} = (\frac{D+C}{2}, -\frac{D+C}{2}, \frac{D+C}{2}, -\frac{D+C}{2}, \ldots)$ of even degree are optimal in the sense that*

$$\frac{\|b_{2k}\|_E}{|b_{2k}(z_0)|} = \min_{p \in \mathcal{P}_{2k}(z_0)} \|p\|_E, \quad k \geq 0.$$

Proof. By Theorem 4.2, the Faber–Walsh polynomials of even degree are the Chebyshev polynomials for E. For $z_0 \in \mathbb{R}\backslash[-D, D]$, Corollary 3.3.8 in [13] shows that the optimal polynomial is the normalized Chebyshev polynomial. For $z_0 \in]-C, C[$, a little more work is required. First, it is not difficult to show that $T_2(z; E) = z^2 - \frac{D^2+C^2}{2}$ with $\|T_2(z; E)\|_E = \frac{D^2-C^2}{2}$, and that $T_2(z; E)$ has the four extremal points $\pm C, \pm D$. Therefore, the optimal polynomial is the normalized Chebyshev polynomial; see [13, Corollary 3.3.6]. □

We point out that the argument in the previous proof is restricted to *real* z_0, since the proofs in [13] are based on the alternation property of the Chebyshev polynomials for subsets of the real line.

Note that the normalized Faber–Walsh polynomials $b_k(z)/b_k(z_0)$ of odd degrees are not optimal: If $z_0 \in]-C, C[$, it is known that the optimal polynomial is "defective", i.e., the optimal polynomial for degree $2k+1$ is the same as for degree $2k$; see [13, Corollary 3.3.6]. If $z_0 \in \mathbb{R}\backslash[-D, D]$, the optimal polynomial is the normalized Chebyshev polynomial ([13, Corollary 3.3.8]), while in general the Faber–Walsh polynomials of odd degree are not the Chebyshev polynomials, since they do not have $k+1$ extremal points on E [13, Corollary 3.1.4]; see the example in Figure 1.

Let us continue with a numerical study of the maximum norm of the normalized Faber–Walsh polynomials, where we focus on the constraint point $z_0 = 0$. We compute the Faber–Walsh polynomials $b_{k,j}$, $k = 1, 2, \ldots$, for the sets

$$E_j := [-1, -2^{-j}] \cup [2^{-j}, 1], \quad j = 1, 2, 3, 4, \tag{4.6}$$

and the sequence $(\frac{D+C}{2}, -\frac{D+C}{2}, \frac{D+C}{2}, -\frac{D+C}{2}, \ldots)$ using the coefficients of the Laurent series (4.3)–(4.4) and Proposition 2.4. Figure 2 (left) shows the values $\frac{\|b_{k,j}\|_{E_j}}{|b_{k,j}(0)|}$ of the normalized Faber–Walsh polynomials for the sets E_j. A comparison with the values $R_0(E_j)^k$ shows that the actual convergence speed of $\frac{\|b_{k,j}\|_{E_j}}{|b_{k,j}(0)|}$ to zero almost exactly matches the rate predicted by the asymptotic analysis even for small values of k. Recall from Proposition 3.6 that $R_{z_0}(E)^k$ is a lower bound on $\|p\|_E$ for any $p \in \mathcal{P}_k(z_0)$. The "zigzags" in the curves are due to the fact that for even degrees $b_{k,j}(z)/b_{k,j}(0)$ is the optimal polynomial (as shown in Corollary 4.3), while for odd degrees it is not.

From Proposition 3.6 and Proposition 4.1 we have

$$R_{z_0}(E) = \frac{\mu}{|U(\Phi(z_0))|} = \frac{1}{\sqrt{\frac{2}{D^2-C^2}\left|z_0^2 - \frac{D^2+C^2}{2} \pm \sqrt{(z_0^2-C^2)(z_0^2-D^2)}\right|}}$$

for $z_0 \in \mathbb{C}\backslash E$, where the sign of the square root is chosen to maximize the absolute value of the denominator. We thus obtain $R_{z_0}(E)$ in terms of elementary functions and for all complex $z_0 \notin E$. Compare this with the expression of the asymptotic convergence factor in terms of Jacobi's elliptic and theta functions [2], see also [13], and the estimates of the asymptotic convergence factor in

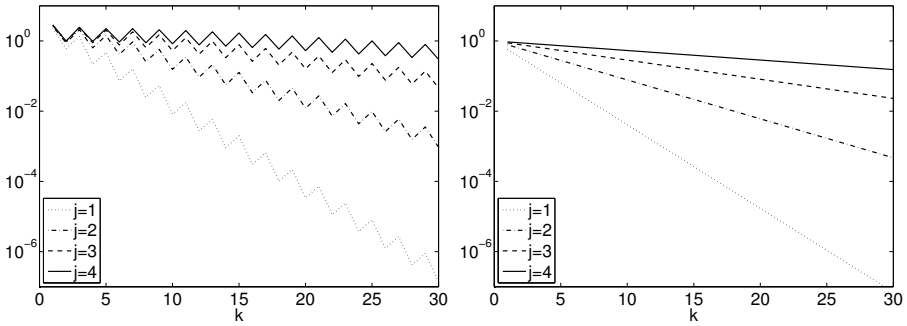

Figure 2: The values $\frac{\|b_{k,j}\|_{E_j}}{|b_{k,j}(0)|}$ (left) and $R_0(E_j)^k$ (right) for the sets E_j from (4.6).

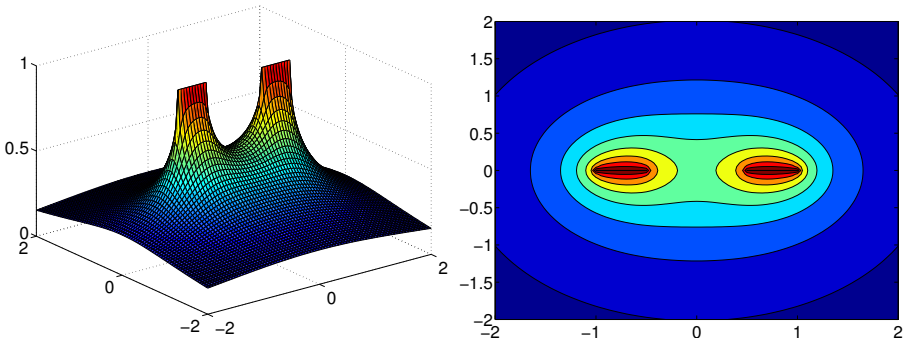

Figure 3: Asymptotic convergence factor $R_{z_0}([-1,-\frac{1}{2}]\cup[\frac{1}{2},1])$ as a function of $z_0 \in \mathbb{C}$.

terms elementary functions in [36]. For the special case $z_0 = 0$ we have $\Phi(0) = 0$ and hence

$$R_0(E) = \sqrt{\frac{D-C}{D+C}}.$$

In Figure 3 we plot the asymptotic convergence factor $R_{z_0}([-1,-\frac{1}{2}]\cup[\frac{1}{2},1])$ as a function of $z_0 \in \mathbb{C}$.

In Figure 4 we plot the asymptotic convergence factors $R_{z_0}(E_j)$ for the sets E_j of the form (4.6) and real z_0 ranging from -2 to 2. Note that when z_0 is to the left or the right of the two intervals (i.e. $|z_0| > 1$) the asymptotic convergence factors $R_{z_0}(E_j)$ are almost identical for all j, and they decrease quickly with increasing $|z_0|$. On the other hand, when z_0 is between the two intervals the asymptotic convergence factors $R_{z_0}(E_j)$ strongly depend on j, and for a fixed z_0 they increase quickly with increasing j. Moreover, $R_{z_0}(E_j)$ for $|z_0| < 2^{-j}$ is minimal when $z_0 = 0$, i.e., when z_0 is the midpoint between the two intervals.

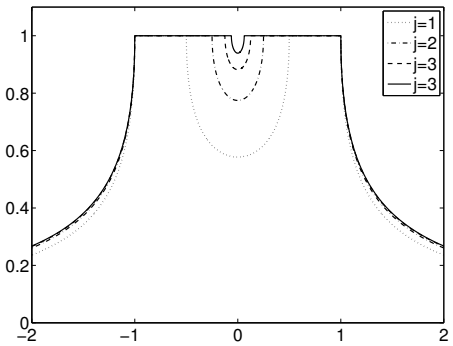

Figure 4: Asymptotic convergence factors $R_{z_0}(E_j)$ for E_j from (4.6) and $z_0 \in [-2, 2]$.

4.2 Two arbitrary real intervals

In this section we consider the general case of two disjoint real intervals, i.e.,

$$E = [A, B] \cup [C, D] \quad \text{with } A < B < C < D. \tag{4.7}$$

For such sets, the lemniscatic map and lemniscatic domain are not known analytically. We therefore compute the map and the domain numerically using the method introduced in [31]. This methods needs as its input a discretization of the boundary of the set E, which is assumed to consist of Jordan curves. For N-times connected domains, the method then requires to solve N boundary integral equations with the Neumann kernel. This costs $\mathcal{O}(N^2 n \log(n))$ operations, where n is the number of nodes in the discretization of each boundary component of E. The numerical examples in [31] show that the method is efficient and works accurately even for domains with close-to-touching boundaries, non-convex boundaries, piecewise smooth boundaries, and of high connectivity.

We will apply two preliminary conformal maps in order to map $\widehat{\mathbb{C}}\backslash E$ for the set E in (4.7) onto a domain bounded by Jordan curves. The prelimary maps are basically (inverse) Joukowski maps, as stated in the following lemma, which can be proven by elementary means.

Lemma 4.4. *Let $\alpha, \beta \in \mathbb{R}$ with $\alpha < \beta$. Then*

$$\Phi : \widehat{\mathbb{C}}\backslash[\alpha, \beta] \to \left\{ w \in \widehat{\mathbb{C}} : \left| w - \frac{\beta + \alpha}{2} \right| > \frac{\beta - \alpha}{4} \right\},$$
$$w = \Phi(z) = \frac{1}{2}\left(z + \frac{\beta + \alpha}{2} \pm \sqrt{(z - \alpha)(z - \beta)} \right),$$

where we take the branch of the square root such that $|\Phi(z) - \frac{\beta+\alpha}{2}| > \frac{\beta-\alpha}{4}$, is a bijective conformal map which is normalized at infinity by $\Phi(z) = z + \mathcal{O}(1/z)$.

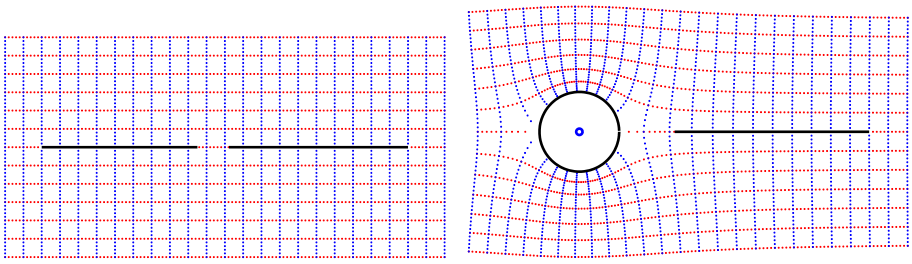

(a) Original domain $\mathcal{K} = \widehat{\mathbb{C}} \backslash E$ (b) $\mathcal{K}_1 = \Phi_1(\mathcal{K})$

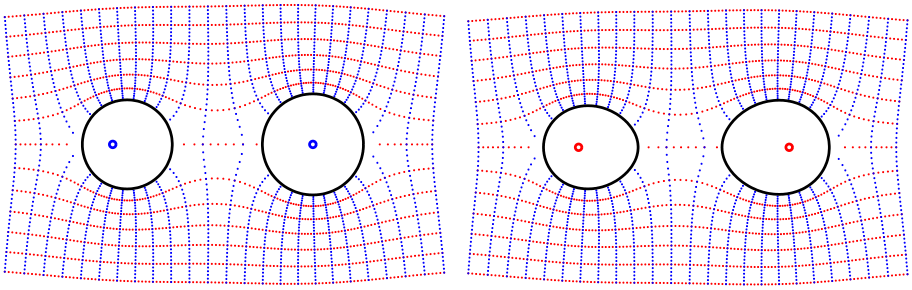

(c) $\mathcal{K}_2 = \Phi_2(\mathcal{K}_1)$ (d) Lemniscatic domain $\mathcal{L} = \Phi_3(\mathcal{K}_2)$

Figure 5: Construction of the lemniscatic map of $[-1, -h] \cup [h^2, 1]$ with $h = 0.15$.

We now construct the lemniscatic map of $E = [A, B] \cup [C, D]$. The construction is illustrated in Figure 5 for the set $E = [-1, -h] \cup [h^2, 1]$ with $h = 0.15$. First we apply Lemma 4.4 to the interval $[A, B]$ to obtain the conformal map Φ_1, mapping $\mathcal{K}$ onto $\mathcal{K}_1 = \Phi_1(\mathcal{K})$, which is the exterior of

$$\{z_1 : |z_1 - w_1| = r_1\} \cup [\widetilde{C}, \widetilde{D}],$$

with $w_1 = \frac{B+A}{2}$, $r_1 = \frac{B-A}{4}$, $\widetilde{C} = \Phi_1(C)$, and $\widetilde{D} = \Phi_1(D)$; see Figure 5(b). In a second step, let Φ_2 be given by Lemma 4.4 for the interval $[\widetilde{C}, \widetilde{D}]$. Then Φ_2 maps $\mathcal{K}_1$ onto the exterior of

$$\Phi_2(\{z_1 : |z_1 - w_1| = r_1\}) \cup \{z_2 : |z_2 - w_2| = r_2\},$$

where $w_2 = \frac{\widetilde{D}+\widetilde{C}}{2}$ and $r_2 = \frac{\widetilde{D}-\widetilde{C}}{4}$; see Figure 5(c). This domain is bounded by two analytic Jordan curves, which we parametrize by

$$\eta_1(t) = \Phi_2(w_1 + r_1 e^{-it}) \quad \text{and} \quad \eta_2(t) = w_2 + r_2 e^{-it}, \quad t \in [0, 2\pi]. \tag{4.8}$$

We then apply the numerical method from [31] to compute the lemniscatic domain $\mathcal{L}$ and lemniscatic map Φ_3 of $\mathcal{K}_2 = \Phi_2(\mathcal{K}_1)$. As mentioned above, the input of this method is a discretization of the boundary, which is easily computable using the parameterization (4.8). The result is the lemniscatic map

$$\Phi := \Phi_3 \circ \Phi_2 \circ \Phi_1 : \widehat{\mathbb{C}} \backslash E \to \mathcal{L},$$

where Φ_1 and Φ_2 are given analytically as above, and Φ_3 is computed numerically. The output of the numerical method from [31] are the parameters of $\mathcal{L}$ and the boundary values of Φ_3 at the discretization points on the boundary. The values of Φ_3 at other points can be computed by Cauchy's integral formula for domains with infinity as interior point, applied to the function $\Phi_3(z) - z$, which is analytic in $\mathcal{K}_2$ and vanishes at infinity. We thus have

$$\Phi_3(z) = z + \frac{1}{2\pi i} \int_{\partial \mathcal{K}_2} \frac{\Phi_3(\zeta) - \zeta}{\zeta - z} \, d\zeta,$$

where the boundary is parametrized such that $\mathcal{K}_2$ is to the left of the contour; see [31] for details on the practical computation of this integral. Note that this numerical method extends to any finite number of intervals.

With the lemniscatic map Φ and lemniscatic domain $\mathcal{L}$ available, we can compute the Faber–Walsh polynomials by

$$b_k(z) = \frac{1}{2\pi i} \int_\gamma \frac{u_k(\Phi(\zeta))}{\zeta - z} \, d\zeta = \frac{1}{2\pi i} \int_\gamma \frac{\prod_{j=1}^k (\Phi(\zeta) - \alpha_j)}{\zeta - z} \, d\zeta,$$

see (2.6), where γ is any positively oriented contour containing E and z in its interior, and where the sequence $(\alpha_j)_{j=1}^\infty$ is chosen from the centers of the lemniscatic domain as indicated in the discussion below Lemma 2.2.

Figure 6 shows some computed Faber–Walsh polynomials of even (left) and odd (right) degrees for the set $E = [-1, -\frac{1}{4}] \cup [\frac{1}{3}, 1]$. Unlike in the case of two equal intervals, the Faber–Walsh polynomials for two unequal intervals are in general not Chebyshev polynomials, nor are the normalized Faber–Walsh polynomials the optimal polynomials. We numerically compute the Faber–Walsh polynomials $b_{k,j}$ for the sets

$$E_j := [-1, -2^{-j}] \cup [3^{-1}, 1], \quad j = 1, 2, 3, 4. \tag{4.9}$$

Figure 7 (left) shows the corresponding values $\|b_{k,j}\|_E / |b_{k,j}(0)|$ for $k = 1, \ldots, 30$. As for the equal intervals, a comparison with the values $R_0(E_j)^k$ shows that the convergence speed to zero of the norms matches closely the predicted asymptotic rate, already for small values of k. Unlike in the case of two equal intervals, the sequence of norms has a few irregular jumps, which are due to the lack of symmetry in the problem. More precisely, all jumps happen when one of the centers a_1, a_2 of the lemniscatic domain appears twice in a row in the sequence $(\alpha_j)_{j=1}^\infty$. This happens in the construction of the sequence as described below Lemma 2.2, since for two intervals of different lengths the exponents m_1 and m_2 of the lemniscatic domain are different.

Finally, the numerical method from [31] yields the lemniscatic map Φ, as well as the parameters of the lemniscatic domain $\mathcal{L}$. Therefore, the asymptotic convergence factor can be numerically computed by its characterization from Proposition 3.6. In Figure 8 we plot the asymptotic convergence factor $R_{z_0}([-1, -\frac{1}{2}] \cup [\frac{1}{3}, 1])$ as a function of $z_0 \in \mathbb{C}$.

In Figure 9 we plot the asymptotic convergence factors $R_{z_0}(E_j)$ for the sets E_j from (4.9) and real z_0 ranging from -2 to 2. Similar remarks as in the case of

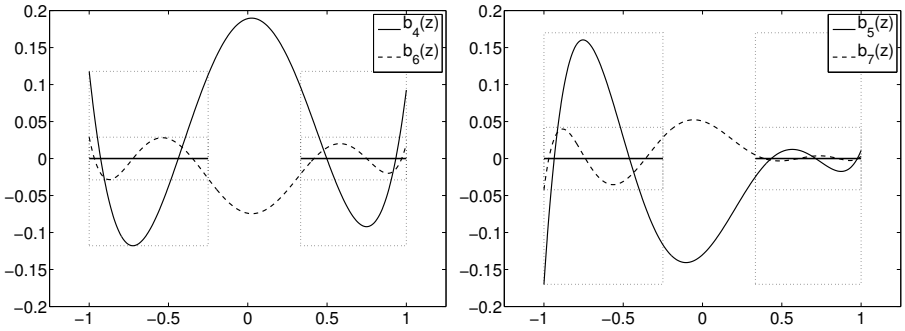

Figure 6: Faber–Walsh polynomials b_k for $E = [-1, -\frac{1}{4}] \cup [\frac{1}{3}, 1]$.

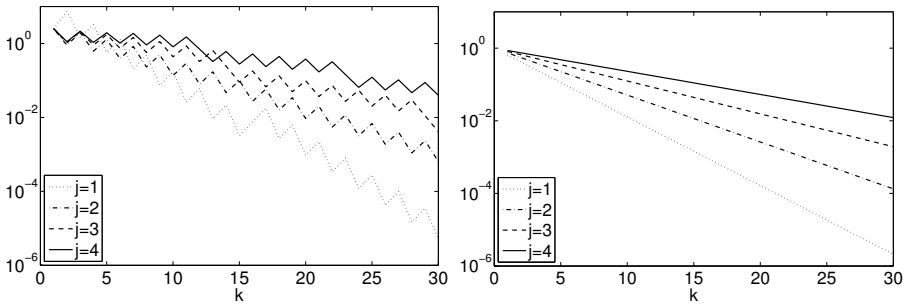

Figure 7: The values $\frac{\|b_{k,j}\|_{E_j}}{|b_{k,j}(0)|}$ (left) and $R_0(E_j)^k$ (right) for the sets E_j from (4.9).

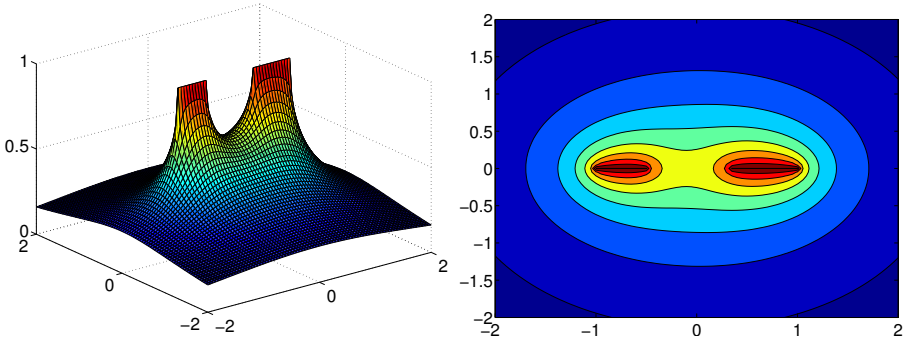

Figure 8: Asymptotic convergence factor $R_{z_0}([-1, -\frac{1}{2}] \cup [\frac{1}{3}, 1])$ as a function of $z_0 \in \mathbb{C}$.

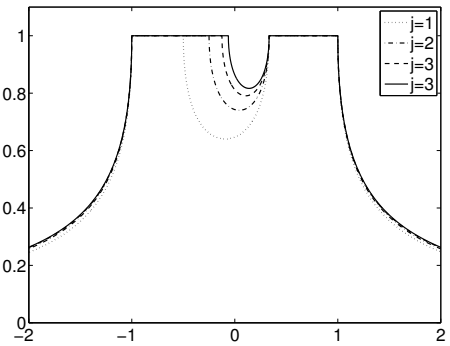

Figure 9: Asymptotic convergence factors $R_{z_0}(E_j)$ for E_j from (4.9) and $z_0 \in [-2, 2]$.

two equal intervals apply, with one exception: Here the computation shows that $R_{z_0}(E_j)$ for $z_0 \in [-2^{-j}, 3^{-1}]$ attains its minimum not in the midpoint between the two intervals, but slightly to its left for $j = 1$, and to its right for $j = 2, 3, 4$. A similar observation has already been made by Fischer [13, Example 3.4.5].

5 Two non-real examples

In this section we give examples of Faber–Walsh polynomials for sets E that are not subsets of the real line.

5.1 Two disks

We consider sets E consisting of two equal disks, i.e.,

$$E = E(z_0, r) := \{z \in \mathbb{C} : |z - z_0| \le r\} \cup \{z \in \mathbb{C} : |z + z_0| \le r\},$$

where we take $z_0, r \in \mathbb{R}$ with $0 < r < z_0$. The lemniscatic map of $E(z_0, r)$ is known analytically from [39, Theorem 4.2], and the lemniscatic domain is of the form

$$\mathcal{L} = \mathcal{L}(z_0, r) = \{w \in \widehat{\mathbb{C}} : |w - a_1|^{1/2}|w + a_1|^{1/2} > \mu\}$$

for some $a_1 > 0$ and $\mu > 0$. With these $\mathcal{L}$ and Φ we obtain the Faber–Walsh polynomials for $E(z_0, r)$ and $(a_1, -a_1, a_1, -a_1, \ldots)$ by their integral representation; see also the discussion in Section 4.2.

In Figure 10 we plot the phase portraits of several Faber–Walsh polynomials for $E(1, 0.8)$; see [45, 46] for details on phase portraits. The figure shows that the k roots of b_k are all contained in E. We further compute the Faber–Walsh polynomials $b_{k,r}$ for the sets

$$E_r = E(1, r) \quad \text{for } r = 0.5, 0.7, 0.9, \tag{5.1}$$

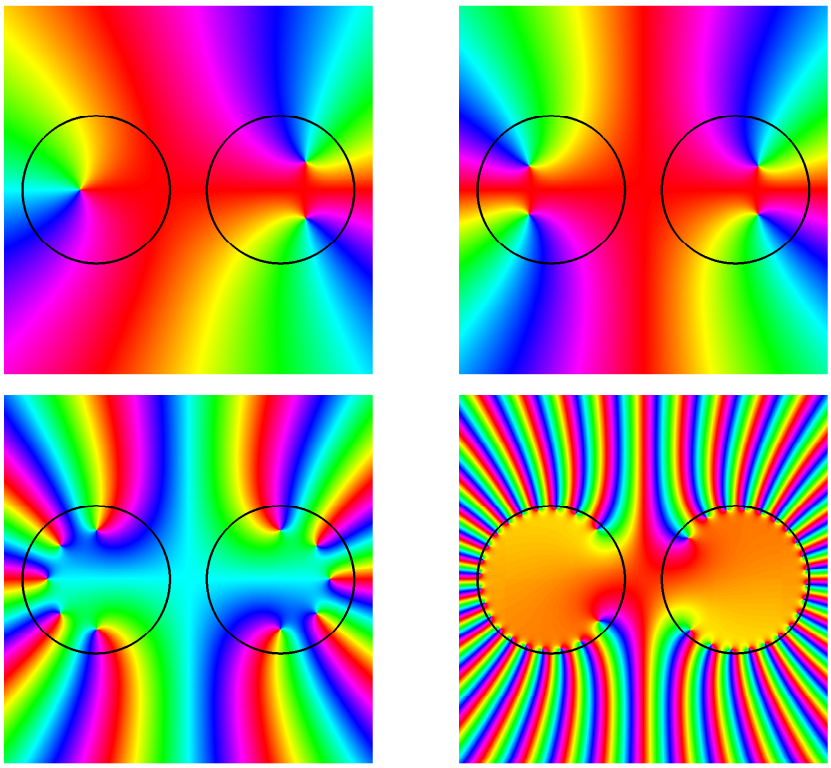

Figure 10: Phase portraits of Faber–Walsh polynomials b_k for $E(1, 0.8)$ for $k = 3, 4, 10, 40$.

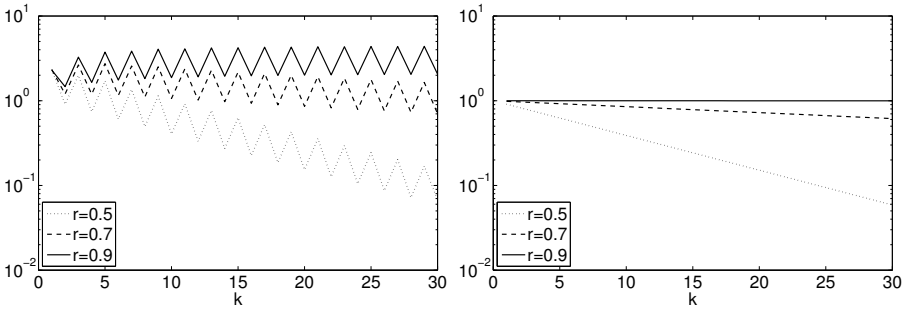

Figure 11: The values $\frac{\|b_{k,r}\|_{E_r}}{|b_{k,r}(0)|}$ (left) and $R_0(E_r)^k$ (right) for the sets E_r from (5.1).

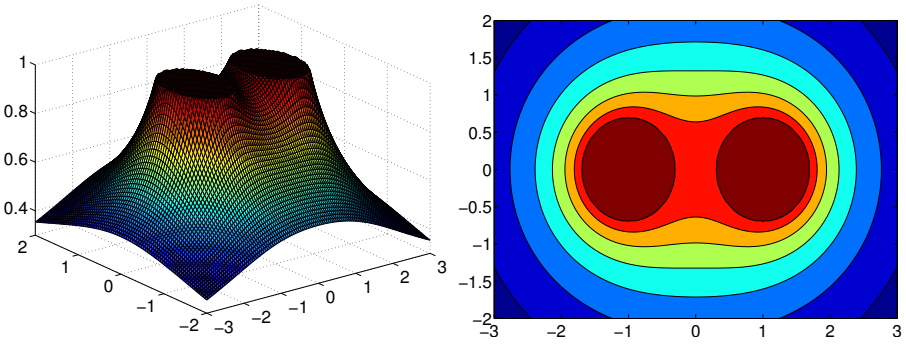

Figure 12: Asymptotic convergence factor $R_{z_0}(E(1, 0.7))$ as a function of $z_0 \in \mathbb{C}$.

and the sequence $(a_1, -a_1, a_1, -a_1, \ldots)$. In Figure 11 (left) we plot the values $\frac{\|b_{k,r}\|_{E_r}}{|b_{k,r}(0)|}$ for $k = 1, \ldots, 30$. As in the case of two intervals, we observe that the convergence speed to zero of the norms almost exactly matches the rate predicted by the asymptotic analysis, already for small k. The numerically computed asymptotic convergence factors (rounded to five digits) for the three sets E_r are $R_0(E_{0.5}) = 0.9099$, $R_0(E_{0.7}) = 0.9839$ and $R_0(E_{0.9}) = 0.9999$, which in particular explains the slow convergence to zero for $r = 0.7$ and the (almost) stagnation for $r = 0.9$.

Figure 12 shows the numerically computed asymptotic convergence factor $R_{z_0}(E(1, 0.7))$ as a function of $z_0 \in \mathbb{C}$.

5.2 A set with more components

In this section we will give another illustration of Theorem 3.3, starting from a simply connected set of the form introduced in [23, Theorem 3.1]; see Figure 13(a) for an illustration.

Theorem 5.1 ([23, Theorem 3.1]). *Let $\lambda \in \mathbb{C}$ with $|\lambda| = 1$, $\phi \in]0, 2\pi[$ and $R \in [1, P[$, where*

$$P := \tan(\phi/4) + \frac{1}{\cos(\phi/4)}.$$

Then $\Omega = \Omega(\lambda, \phi, R)$ is the compact set bounded by $\widetilde{\psi}(\{w \in \mathbb{C} : |w| = 1\})$, where

$$\widetilde{\psi}(w) = \frac{(w - \lambda N)(w - \lambda M)}{(N - M)w + \lambda(NM - 1)}, \text{ with } N = \frac{1}{2}\left(\frac{P}{R} + \frac{R}{P}\right), M = \frac{R^2 - 1}{2R\tan(\phi/4)},$$

is a bijective conformal map from the exterior of the unit circle onto $\widehat{\mathbb{C}}\backslash\Omega$ and satisfies $\widetilde{\psi}(\infty) = \infty$ and $\widetilde{\psi}'(\infty) = t = 1/(N - M) > 0$. We further have $\lambda \notin \Omega$ and $\{\lambda e^{i\beta} : \phi/2 \le \beta \le 2\pi - \phi/2\} \subseteq \Omega$.

Let us consider polynomial pre-images of such sets. As an example we consider the set $\Omega = \Omega(-1, 2\pi/3, 1.1)$, which satisfies $\Omega = \Omega^*$. Let $E = P^{-1}(\Omega)$ with $P(z) = z^n$; see Figure 13(a) and 13(b) for an illustration with $n = 5$. By Theorem 3.2, the lemniscatic domain corresponding to E is

$$\mathcal{L} = \{w \in \widehat{\mathbb{C}} : |U(w)| = |w^n - tN|^{1/n} > t^{1/n}\},$$

where the logarithmic capacicty t of Ω is given as in Theorem 5.1. Since $tN > 0$, the centers of the lemniscate are $a_j = e^{2\pi i \frac{j-1}{n}}(tN)^{1/n}$ for $j = 1, 2, \ldots, n$. By Theorem 3.3, the (kn)th Faber–Walsh polynomials for E and

$$(a_1, a_2, \ldots, a_n, a_1, a_2, \ldots, a_n, \ldots)$$

are given by

$$b_{nk}(z) = t^k F_k(z^n), \tag{5.2}$$

where the F_k are the Faber polynomials for Ω, which are explicitly known from [23, Lemma 4.1]. There, the Faber polynomials are computed by a recursion involving all previous Faber polynomials. The Faber polynomials for Ω can also be computed by a short (three term) recursion; see [26]. The "missing" Faber–Walsh polynomials can be computed numerically using their definition (2.6), where we obtain the lemniscatic map Φ of E from $\widetilde{\psi}^{-1}$ by Theorem 3.2. Note that $\widetilde{\psi}$ is a composition of two Möbius transformations and the Joukowski map, so that its inverse is easily computable; see [23, Theorem 3.1].

We plot the phase portraits of the Faber–Walsh polynomials b_{5k} for $k = 1, 2, 3, 4$ in Figure 13. For degrees 5 and 10 we observe that not all zeros of the Faber–Walsh polynomial are in E, in contrast to the case of the two disks. This follows from the relation (5.2) and the fact that the zeros of the Faber polynomials F_1 and F_2 for Ω do not lie in Ω; see [25] for details on these Faber polynomials. This also shows that the lower bound in (2.7) cannot, in general, hold for all k. In Figure 14 we plot the values $\|b_{5k}\|_E/|b_{5k}(0)|$ and, for comparison, the values $R_0(E)^k$, where $R_0(E) = 0.9803$ (rounded to five digits).

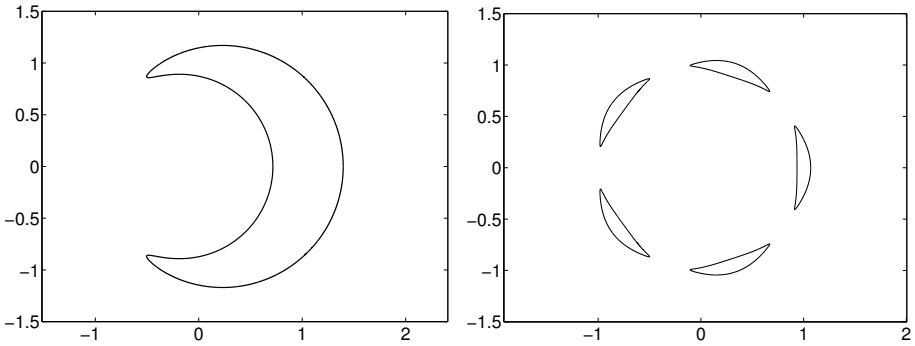

(a) Set $\Omega = \Omega(-1, 2\pi/3, 1.1)$ (b) $E = P^{-1}(\Omega)$ with $P(z) = z^5$.

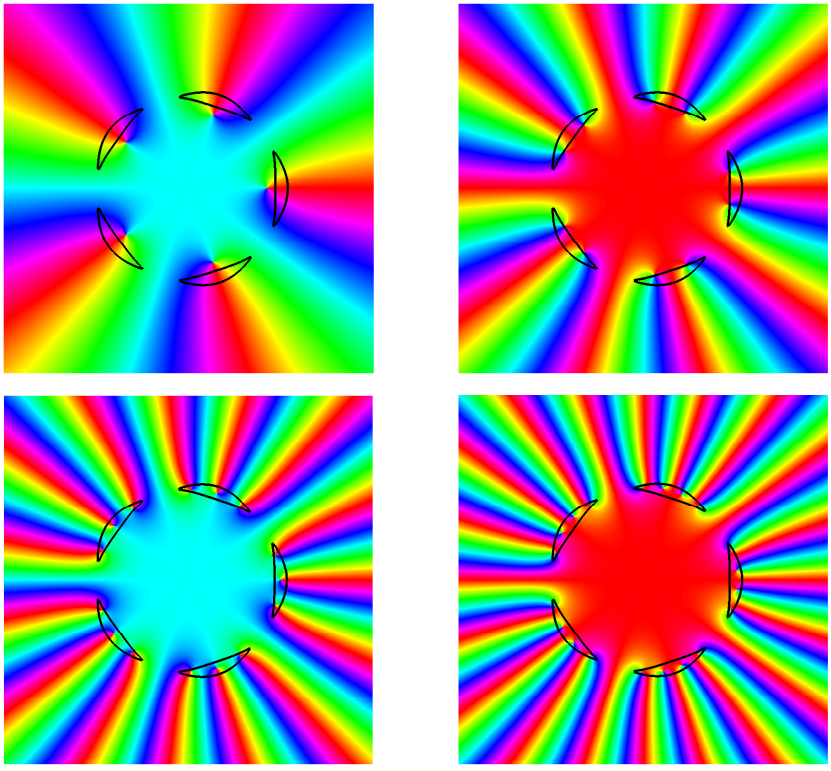

Figure 13: Set $\Omega = \Omega(-1, 2\pi/3, 1.1)$, its pre-image E, and phase portraits of Faber–Walsh polynomials for E of degrees $k = 5, 10, 15, 20$.

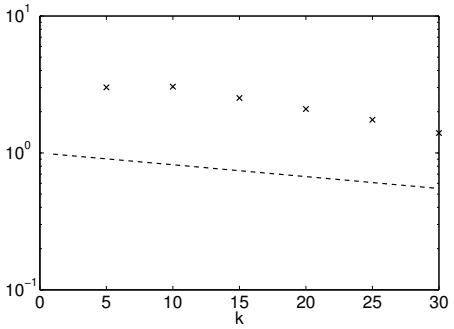

Figure 14: The values $\frac{\|b_k\|_E}{|b_k(0)|}$ and $R_0(E)^k$.

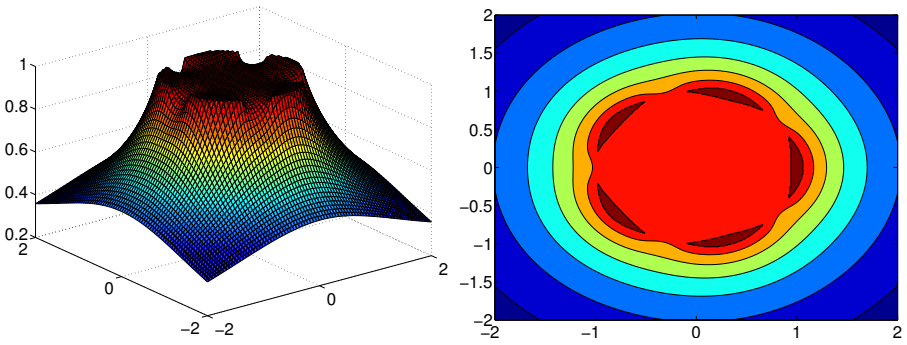

Figure 15: Asymptotic convergence factor $R_{z_0}(P^{-1}(\Omega))$ as a function of $z_0 \in \mathbb{C}$, where $P(z) = z^5$ and $\Omega = \Omega(-1, 2\pi/3, 1.1)$.

From Proposition 3.6 and Theorem 3.2 we find for the asymptotic convergence factor for E and $z_0 \in \mathbb{C}\backslash E$

$$R_{z_0}(E) = \frac{\mu}{|U(\Phi(z_0))|} = \frac{1}{|\widetilde{\Phi}(z_0^n)|^{1/n}}.$$

Figure 15 shows the asymptotic convergence factor for E as a function of $z_0 \in \mathbb{C}$.

References

[1] N. I. Achieser, *Theory of approximation*, Translated by Charles J. Hyman, Frederick Ungar Publishing Co., New York, 1956.

[2] N. Akhiezer, *Über einige Funktionen, welche in zwei gegebenen Intervallen am wenigsten von Null abweichen. I.*, Bull. Acad. Sci. URSS, 1932 (1932), pp. 1163–1202.

[3] ———, *Über einige Funktionen, welche in zwei gegebenen Intervallen am wenigsten von Null abweichen. II.*, Bull. Acad. Sci. URSS, 1933 (1933), pp. 309–344.

[4] B. Beckermann and L. Reichel, *Error estimates and evaluation of matrix functions via the Faber transform*, SIAM J. Numer. Anal., 47 (2009), pp. 3849–3883.

[5] J. H. Curtiss, *Faber polynomials and the Faber series*, Amer. Math. Monthly, 78 (1971), pp. 577–596.

[6] M. Eiermann, *On semiiterative methods generated by Faber polynomials*, Numer. Math., 56 (1989), pp. 139–156.

[7] M. Eiermann, X. Li, and R. S. Varga, *On hybrid semi-iterative methods*, SIAM J. Numer. Anal., 26 (1989), pp. 152–168.

[8] M. Eiermann and W. Niethammer, *On the construction of semi-iterative methods*, SIAM J. Numer. Anal., 20 (1983), pp. 1153–1160.

[9] M. Eiermann, W. Niethammer, and R. S. Varga, *A study of semi-iterative methods for nonsymmetric systems of linear equations*, Numer. Math., 47 (1985), pp. 505–533.

[10] S. W. Ellacott, *Computation of Faber series with application to numerical polynomial approximation in the complex plane*, Math. Comp., 40 (1983), pp. 575–587.

[11] ———, *A survey of Faber methods in numerical approximation*, Comput. Math. Appl. Part B, 12 (1986), pp. 1103–1107.

[12] G. Faber, *Über polynomische Entwickelungen*, Math. Ann., 57 (1903), pp. 389–408.

[13] B. Fischer, *Polynomial based iteration methods for symmetric linear systems*, Wiley-Teubner Series Advances in Numerical Mathematics, John Wiley & Sons, Ltd., Chichester; B. G. Teubner, Stuttgart, 1996.

[14] B. Fischer and F. Peherstorfer, *Chebyshev approximation via polynomial mappings and the convergence behaviour of Krylov subspace methods*, Electron. Trans. Numer. Anal., 12 (2001), pp. 205–215 (electronic).

[15] H. Grunsky, *Über konforme Abbildungen, die gewisse Gebietsfunktionen in elementare Funktionen transformieren. I*, Math. Z., 67 (1957), pp. 129–132.

[16] ———, *Über konforme Abbildungen, die gewisse Gebietsfunktionen in elementare Funktionen transformieren. II*, Math. Z., 67 (1957), pp. 223–228.

[17] ———, *Lectures on theory of functions in multiply connected domains*, Vandenhoeck & Ruprecht, Göttingen, 1978.

[18] M. Hasson, *The capacity of some sets in the complex plane*, Bull. Belg. Math. Soc. Simon Stevin, 10 (2003), pp. 421–436.

[19] ———, *The degree of approximation by polynomials on some disjoint intervals in the complex plane*, J. Approx. Theory, 144 (2007), pp. 119–132.

[20] V. Heuveline and M. Sadkane, *Arnoldi-Faber method for large non-Hermitian eigenvalue problems*, Electron. Trans. Numer. Anal., 5 (1997), pp. 62–76 (electronic).

[21] J. A. Jenkins, *On a canonical conformal mapping of J. L. Walsh*, Trans. Amer. Math. Soc., 88 (1958), pp. 207–213.

[22] S. O. Kamo and P. A. Borodin, *Chebyshev polynomials for Julia sets*, Vestnik Moskov. Univ. Ser. I Mat. Mekh., (1994), pp. 65–67.

[23] T. Koch and J. Liesen, *The conformal "bratwurst" maps and associated Faber polynomials*, Numer. Math., 86 (2000), pp. 173–191.

[24] H. J. Landau, *On canonical conformal maps of multiply connected domains*, Trans. Amer. Math. Soc., 99 (1961), pp. 1–20.

[25] J. Liesen, *On the location of the zeros of Faber polynomials*, Analysis (Munich), 20 (2000), pp. 157–162.

[26] ———, *Faber polynomials corresponding to rational exterior mapping functions*, Constr. Approx., 17 (2001), pp. 267–274.

[27] A. I. Markushevich, *Theory of functions of a complex variable. Vol. I*, Translated and edited by Richard A. Silverman, Prentice-Hall Inc., Englewood Cliffs, N.J., 1965.

[28] ———, *Theory of functions of a complex variable. Vol. III*, Revised English edition, translated and edited by Richard A. Silverman, Prentice-Hall, Inc., Englewood Cliffs, N.J., 1967.

[29] I. Moret and P. Novati, *The computation of functions of matrices by truncated Faber series*, Numer. Funct. Anal. Optim., 22 (2001), pp. 697–719.

[30] ———, *An interpolatory approximation of the matrix exponential based on Faber polynomials*, J. Comput. Appl. Math., 131 (2001), pp. 361–380.

[31] M. M. S. Nasser, J. Liesen, and O. Sète, *Numerical computation of the conformal map onto lemniscatic domains*, ArXiv e-prints: 1505.04916, (2015).

[32] F. Peherstorfer, *Inverse images of polynomial mappings and polynomials orthogonal on them*, in Proceedings of the Sixth International Symposium on Orthogonal Polynomials, Special Functions and their Applications (Rome, 2001), vol. 153, 2003, pp. 371–385.

[33] F. Peherstorfer and K. Schiefermayr, *Description of extremal polynomials on several intervals and their computation. I, II*, Acta Math. Hungar., 83 (1999), pp. 27–58, 59–83.

[34] F. Peherstorfer and R. Steinbauer, *Orthogonal and L_q-extremal polynomials on inverse images of polynomial mappings*, J. Comput. Appl. Math., 127 (2001), pp. 297–315.

[35] K. Schiefermayr, *A lower bound for the minimum deviation of the Chebyshev polynomial on a compact real set*, East J. Approx., 14 (2008), pp. 223–233.

[36] ———, *Estimates for the asymptotic convergence factor of two intervals*, J. Comput. Appl. Math., 236 (2011), pp. 28–38.

[37] ———, *A lower bound for the norm of the minimal residual polynomial*, Constr. Approx., 33 (2011), pp. 425–432.

[38] O. Sète, *Some properties of Faber–Walsh polynomials*, ArXiv e-prints: 1306.1347v1, (2013).

[39] O. Sète and J. Liesen, *On conformal maps from multiply connected domains onto lemniscatic domains*, ArXiv e-prints: 1501.01812, (2015).

[40] V. I. Smirnov and N. A. Lebedev, *Functions of a complex variable: Constructive theory*, Translated from the Russian by Scripta Technica Ltd, The M.I.T. Press, Cambridge, Mass., 1968.

[41] G. Starke and R. S. Varga, *A hybrid Arnoldi-Faber iterative method for nonsymmetric systems of linear equations*, Numer. Math., 64 (1993), pp. 213–240.

[42] P. K. Suetin, *Series of Faber polynomials*, vol. 1 of Analytical Methods and Special Functions, Gordon and Breach Science Publishers, Amsterdam, 1998.

[43] J. L. Walsh, *On the conformal mapping of multiply connected regions*, Trans. Amer. Math. Soc., 82 (1956), pp. 128–146.

[44] ———, *A generalization of Faber's polynomials*, Math. Ann., 136 (1958), pp. 23–33.

[45] E. Wegert, *Visual Complex Functions*, Birkhäuser/Springer Basel AG, Basel,

2012.
[46] E. Wegert and G. Semmler, *Phase plots of complex functions: a journey in illustration*, Notices Am. Math. Soc., 58 (2011), pp. 768–780.

Zusammenfassung

Die vorliegende Dissertationsschrift behandelt Themen der Interpolations- und Approximationstheorie, welche durch Fragestellungen aus der Numerischen Linearen Algebra motiviert sind. Im ersten Teil dieser Arbeit werden die Nullstellen von rationalen harmonischen Funktionen der Form $r(z) - \overline{z}$ untersucht. Wir verbessern eine bekannte obere Schranke für die Anzahl der Nullstellen dieser Funktionen und beheben eine Ungenauigkeit im ursprünglichen Beweis. Weiter zeigen wir, dass extremale rationale harmonische Funktionen, d.h. Funktionen, die die maximal mögliche Anzahl an Nullstellen besitzen, keine singulären Nullstellen besitzen. Des weiteren untersuchen wir, wie sich die Anzahl der Nullstellen einer rationalen harmonischen Funktion ändert, wenn man zu dieser einen Pol addiert. Dies verallgemeinert eine Konstruktion von Rhie (arXiv:astro-ph/0305166v1, 2003), die die ersten Beispiele extremaler Funktionen gegeben hat. Ihre Beispiele besitzen starke Rotationssymmetrie. Unsere Analyse liefert ein Konstruktionsverfahren für unsymmetrische extremale Funktionen. Dieses Ergebnis wenden wir auf Gravitationslinsen in der Astrophysik an und erhalten ein Konstruktionsverfahren für unsymmetrische Gravitationslinsen, die die maximal mögliche Anzahl Bilder erzeugen.

Der zweite Teil der vorliegenden Arbeit behandelt die Approximation von analytischen Funktionen durch Reihen nach Faber–Walsh-Polynomen. Letztere verallgemeinern Faber-Polynome auf Mengen, die aus mehreren einfach zusammenhängenden und kompakten Komponenten bestehen, und sind durch eine konforme Abbildung vom äußeren der kompakten Menge auf Lemniskatengebiete definiert. Zunächst leiten wir ein Konstruktionsprinzip für diese Lemniskatenabbildungen für eine Klassen von Urbildern von einfach zusammenhängenden kompakten Mengen unter Polynomen her. Zudem konstruieren wir explizit zwei Beispiele. Sodann leiten wir allgemeine Eigenschaften der Faber–Walsh-Polynome her. Insbesondere untersuchen wir ihre Beziehung zu den klassischen Faber und Tschebyscheff-Polynomen. Des weiteren untersuchen und berechnen wir die Faber–Walsh-Polynome auf zwei reellen Intervallen sowie auf komplexen Mengen mit mehreren Komponenten.